Investigating neurodegeneration after traumatic brain injury: a longitudinal study of axonal injury

Dr Neil Graham

Imperial College London

Department of Brain Sciences, Faculty of Medicine

Computational, Cognitive and Clinical Neuroimaging Laboratory

Degree: PhD

Abstract

Traumatic brain injury (TBI) is associated with neurodegeneration and dementia, with Alzheimer's disease (AD) reported to be more prevalent post-injury. Traumatic axonal injury (TAI) is suspected to trigger progressive neurodegeneration, with axonal damage leading to proteinopathies of tau and amyloid, also features of AD. However, while axonal injury has been difficult to assess clinically, advances in biomarkers now make this more amenable to quantification.

This thesis uses advanced fluid and imaging biomarkers to investigate TAI longitudinally and assess how this relates to neurodegeneration post-TBI. I assess biomarkers in plasma and cerebral microdialysate after acute moderate-severe injuries, relating changes to diffusion tensor imaging (DTI) MRI measures of TAI, brain volumetric change and clinical outcomes. In a separate cohort in the chronic phase I assess how DTI measures predict neurodegeneration in comparison with other possible predictors, and characterise the neurodegenerative consequences of injury in comparison with AD and atrophy in healthy ageing.

I found that axonal markers neurofilament light (NfL) and tau were markedly increased in concentration within brain extracellular fluid early post-TBI, correlating closely with plasma levels. Subacute plasma NfL related to DTI measures of TAI, predicted clinical outcomes and white matter neurodegeneration, with peak tau predicting grey matter atrophy. In the chronic phase, I found that DTI predicts the extent and pattern of brain atrophy and explains substantially more variance than clinical severity measures. Comparing post-traumatic atrophy with AD and ageing, I show that post-traumatic atrophy patterns are distinctive and reminiscent of axonal injury spatially.

These findings provide evidence of axonal injury as a trigger of progressive neurodegeneration and show this can be sensitively measured with fluid and neuroimaging tools both early and late after single moderate-severe injury. These approaches have the potential to improve clinical diagnosis of TAI and its sequelae, prognostication, and facilitate trials of anti-neurodegeneration treatments.

Acknowledgements

Foremost I would like to thank my supervisor Professor David Sharp who supported me academically and clinically throughout. He provided vital support in applying for a research training fellowship and provided an environment in which to train and perform the investigations set out in this thesis. The work would not have been possible without the further support of Professor Jonathan Schott and Dr James Cole, my co-supervisors. All of these individuals provided invaluable guidance.

My clinical research fellowship was funded by Alzheimer's Research UK to whom I am very grateful. At the start of my programme, I was supported by the Imperial Health Charity who provided a pre-doctoral fellowship. The BIO-AX-TBI study which comprises a substantial part of my programme of work within this thesis was funded by the ERANET-neuron programme.

I thank our patients, healthy volunteers and their families who gave so freely of their time to support this research. I am pleased to share these results and hope that an improved understanding of neurodegeneration after TBI will be of benefit to patients in future.

Statement of publications

A proportion of the material within Chapter 1 has been published in JNNP. The study protocol relating to Chapters 3 and 4 is published in BMJ Open, and material within Chapter 5 is published in Brain:

Graham NS, Sharp DJ. Understanding neurodegeneration after traumatic brain injury: from mechanisms to clinical trials in dementia. J Neurol Neurosurg Psychiatry. 2019 Nov;90(11):1221-1233. doi: 10.1136/jnnp-2017-317557. Epub 2019 Sep 21. PMID: 31542723; PMCID: PMC6860906.

Graham NSN*, Zimmerman KA*, Bertolini G, Magnoni S, Oddo M, Zetterberg H, Moro F, Novelli D, Heslegrave A, Chieregato A, Fainardi E, Fleming JM, Garbero E, Abed-Maillard S, Gradisek P, Bernini A, Sharp DJ. Multicentre longitudinal study of fluid and neuroimaging BIOmarkers of AXonal injury after traumatic brain injury: the BIO-AX-TBI study protocol. BMJ Open. 2020 Nov 10;10(11):e042093. doi: 10.1136/bmjopen-2020-042093. PMID: 33172948; PMCID: PMC7656955. *Joint first author.

Graham NSN, Jolly A, Zimmerman K, Bourke NJ, Scott G, Cole JH, Schott JM, Sharp DJ. Diffuse axonal injury predicts neurodegeneration after moderate-severe traumatic brain injury. Brain. 2020 Oct 25:awaa316. doi: 10.1093/brain/awaa316. Epub ahead of print. PMID: 33099608.

Data within Chapters 3 and 4 are in revision at Science Translational Medicine and material within Chapter 6 is being submitted to Alzheimer's and Dementia.

Copyright declaration

Statement of originality

The prospective cohort study of acute TBI reported in Chapters 3 and 4 is a multi-centre study conducted with multiple collaborators at different centres within Europe. I worked closely with research technician and PhD candidate Karl Zimmerman in London to collect the UK data and analyse the data across all centres. We have jointly prepared a manuscript reporting these data and this is in revision. In addition, I was assisted by the Imperial College Healthcare NHS Trust research nurses who aided with recruitment and blood sampling in London. Specific analyses performed by Zimmerman are highlighted within the relevant chapter. Chapter 4 reports my analyses on data in the chronic phase after TBI. Patients in this chapter were assessed by Professor Sharp's team prior to my PhD and I am grateful to him for sharing the data. Furthermore, much of the neuroimaging data analysed in Chapter 5 was collected prior to my arrival, at Imperial and within the UCL MIRIAD dataset of Alzheimer's disease imaging.

I confirm the work presented within this thesis is my own and conforms with Imperial College London's rules and guidelines. All work of others is appropriately referenced.

Contents

Tables

Abbreviations

AD – Alzheimer's disease

AUC – area under the receiver operating characteristic curve

CI – confidence interval

DAI – diffuse axonal injury

DCE – dynamic contrast enhanced

DWI – diffusion weighted imaging

EDH – extradural haematoma

FA – fractional anisotropy

FDR – false discovery rate

FLAIR – fluid-attenuated inversion recovery

FSL – fMRIB software library

FTD – frontotemporal dementia

GCS – Glasgow coma scale

GOSE – Glasgow outcome scale extended

GFAP – glial fibrillary acidic protein

GLM – general linear model

GM – grey matter

HC – healthy control

HR – hazard ratio

ICD – International classification of diseases

IQR – interquartile range

JD – Jacobian determinant rate of volume change

LOC – loss of consciousness

MD – microdialysate

MNI – Montreal Neurological Institute

MRI – magnetic resonance imaging

MPRAGE – magnetisation-prepared rapid gradient echo

NfL – neurofilament light

NTT – non-TBI trauma

OR – odds ratio

PD – Parkinson's disease

PTA – post-traumatic amnesia

RR – relative risk

SD – standard deviation

SDH – subdural haematoma

S100B – S100 calcium binding protein B

SWI – susceptibility weighted imaging

TAI – traumatic axonal injury

TBI – traumatic brain injury

TFCE – threshold-free cluster enhancement

UCH-L1 – ubiquitin carboxyl-terminal hydrolase L1

WASI – Wechsler Abbreviated Scale of Intelligence

WM – white matter

1 Introduction

In this chapter I describe the aims of this programme of investigation. I critically assess the human epidemiological data linking head injuries, axonal damage and neurodegenerative disease and review the neuropathological mechanisms by which neurodegeneration may be triggered by axonal injury in particular. I describe the role of biomarkers, including fluid and neuroimaging tools, in assessing axonal damage and degenerative neuropathologies post-injury, and discuss how such tools could be used in the design of clinical trials to prevent dementia. Material within this Chapter has been published in JNNP (Graham and Sharp, 2019).

1.1 Aim, Objectives and Chapter Summaries

1.1.1 Aim

To characterise the relationship between TBI, axonal injury and progressive neurodegeneration.

1.1.2 Objectives

- To assess axonal injury longitudinally using advanced biomarkers including diffusion tensor MRI, neurofilament light (NfL) and tau after moderate-severe TBI, cross-validating these measures;
- To establish how fluid/imaging biomarkers of injury relate to outcomes including neurodegeneration after TBI;
- To characterise chronic post-traumatic neurodegeneration in comparison to Alzheimer's disease, a possible consequence of injury.

1.1.3 Hypotheses

I aim to test the following hypotheses throughout this thesis:

i) Moderate-severe traumatic brain injury will be associated with axonal damage, causing significant elevations in NfL concentrations;

ii) Levels of neurofilament light will be highly correlated in plasma and brain extracellular fluid tested using invasive cerebral microdialysis, and will relate to DTI axonal measures, validating the peripheral NfL sampling approach;

iii) Plasma NfL early post-injury will predict functional outcomes and post-traumatic brain atrophy;

iv) Plasma NfL and brain atrophy rates on serial T1 MRI will be increased after TBI indicating progressive neurodegeneration;

v) Axonal injury markers will predict the extent and distribution of subsequent progressive brain atrophy;

vi) Patterns of atrophy after TBI will reflect the degenerative sequelae of axonal damage and differ from Alzheimer's disease and healthy ageing.

1.1.4 Summary of Chapters

An overview of the experimental design for each Chapter is provided in Table 1. In Chapter 2 I describe the general methods used throughout this thesis, with additional detail provided within each chapter's methods section as needed. Chapter 3 reports a longitudinal evaluation of fluid biomarkers over a year after moderate-severe TBI in the BIO-AX-TBI study. Chapter 4 describes the neuroimaging correlates of axonal injury in this cohort and relationships between imaging and fluid markers of injury. Chapter 5 investigates the relationship in the chronic phase after injury between axonal damage, defined using diffusion tensor MRI, and progressive brain atrophy. Chapter 6 investigates the patterns of neurodegeneration seen after injury, contrasting post-traumatic longitudinal atrophy with patients who have Alzheimer's disease. Lastly, in Chapter 7, I discuss the findings of this programme of work and set out future steps for this field of research. The biomarker assessment types and timeline in relation to injury within this thesis are summarised Table 2 and Figure 1.

Chapters	Groups	Measure	Assessment frequency
3,4	Acute TBI patients (n=197)	Fluid biomarkers (NfL, tau, UCH-L1, GFAP, S100B)	Sampled twice in first ten days post injury, once subacutely (ten days-six weeks), at six months and at 12 months
		Neuroimaging (including DWI and volumetric sequences, in a subset)	Subacutely (ten days-six weeks), at six and twelve months
		Invasive cerebral microdialysis biomarkers (NfL, tau, UCH-L1, GFAP, in a separate group of patients)	Upto 4 hourly during first ten days post-injury with aligned 12 hourly plasma sampling
	Acute non-TBI trauma patients (n=25)	Fluid biomarkers (NfL, tau, UCH-L1, GFAP, S100B)	Twice within ten days of trauma
	Healthy controls (n=128 cross sectional, 30 longitudinal)	Fluid biomarkers (NfL, tau, UCH-L1, GFAP, S100B)	Single timepoint
		Neuroimaging (including DWI and volumetric sequences)	Single timepoint; Longitudinally in a subgroup
5	Chronic TBI patients (n=55), 3.3 years post-injury Healthy controls (n=19)	Neuroimaging (DWI and volumetric T1)	At baseline and one year later
6	Chronic TBI patients (n=48), 1.9 years post-injury Alzheimer's patients (n=45), mild-moderate disease Healthy controls (n=23 age-matched to AD group, n=23 age matched to TBI group, n=15 older controls scanned on same scanner as TBI patients but age-matched to AD group)	Neuroimaging (volumetric T1) assessment at baseline and 1.5 years later	At baseline and 1.5 years later

Table 1. Chapter-by-chapter overview of experimental design

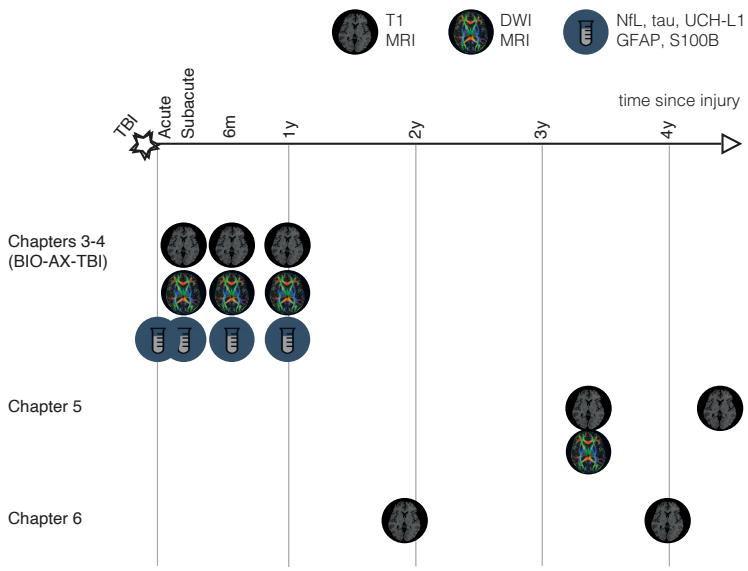

Figure 1. Biomarker assessment timeline in thesis experimental chapters

Schematic overview of fluid and neuroimaging biomarker assessments performed within this thesis. Assessment timepoints are indicated by x-axis position.

Measure	Abbreviation	Target	Description
Fractional anisotropy	FA	White matter organisation	Diffusion tensor imaging measure. Reductions in FA associated with disrupted WM organisation.
Jacobian determinant rate	JD	Rate of brain volume change	Tensor based morphometry measure of brain volume change over time. Negative values represent atrophy over time, and positive values expansion.
Neurofilament light	NfL	Axonal damage	Type IV intermediate filament particularly expressed in large myelinated axons. Sensitive marker of TBI and progressive neurodegeneration.
Microtubule associated protein tau	Tau	Axonal damage	Axonal protein associated with microtubule apparatus, with preferential cortical exprssion, and implicated in proteopathic seeding, toxicitity and neurodegeneration after injury.
Ubiquitin C terminal hydrolase L1	UCH-L1	Neuronal damage	Neuronal protein nvolved in protein turnover with somal-predominant expression.
Glial fibrillary acidic protein	GFAP	Glial damage	Type III intermediate filament prominently expressed in astrocytes
S100 calcium binding protein B	S100B	Glial damage	Astrocytic protein involved in calcium regulation

Table 2. Biomarker overview

1.2 Background abstract

TBI is associated with increased rates of dementia, including Alzheimer's disease and is considered to be a risk factor for progressive neurodegeneration. The mechanisms by which trauma can trigger neurodegeneration are increasingly understood. For example, diffuse axonal injury disrupts microtubule functioning, providing the context for tau and amyloid pathology to develop. The neuropathology of post-traumatic dementias is also well characterised, with recent work focusing on chronic traumatic encephalopathy (CTE). However, the clinical diagnosis of post-traumatic dementias is problematic. It is often difficult to disentangle the direct effects of TBI from those produced by progressive neurodegeneration or other post-traumatic sequelae such as psychiatric impairment. CTE can only be confidently identified at post-mortem and patients are often confused and anxious about the most likely cause of their post-traumatic problems. A new approach to the assessment of the long-term effects of TBI is needed. Accurate methods are available for the investigation of other neurodegenerative conditions. These should be systematically employed in TBI. For example, MRI and fluid biomarkers can quantify both axonal injury and post-traumatic neurodegeneration. Brain atrophy is a potentially useful measure of disease progression and can be used to quantify neuronal loss. Fluid biomarkers such as neurofilament light (NfL) complement neuroimaging, as together they provide sensitive methods to track neurodegenerative processes that develop after TBI. These biomarkers, alongside molecular-specific tools such as PET could be used to characterise endophenotypes associated with distinct types of post-traumatic neurodegeneration. In addition, they might profitably be used in clinical trials of neuroprotective and disease modifying treatments, improving trial design by providing precise and sensitive measures of neuronal loss.

1.3 Defining traumatic brain injury

TBI has been defined as "an alteration in brain function, or other evidence of brain pathology, caused by an external force" (Menon et al., 2010). This definition however captures an extremely wide range of events and requires some refinement for practical use in the clinical or research settings. Notably, it does not imply that there need be any structural damage related to head injury for a TBI to have occurred, only a

disturbance of *function*. This can cause confusion as the phrase 'brain injury' may be misinterpreted by patients or clinicians as implying the presence of underlying structural damage (Sharp and Jenkins, 2015).

To navigate these definitional issues, in this thesis wherever possible I have used the Mayo Classification of injury (Malec et al., 2007). This provides an indication both of the likelihood of underlying brain damage being present following a head injury, as well as the severity of such damage. It proposes three main categories: symptomatic possible injury, mild probable injury and moderate-severe TBI. Patients described in each of the experimental chapters are individuals who have a history of moderate-severe TBI. This is indicated by either the presence of an acute intracranial abnormality on neuroimaging (e.g. contusion, subdural, extradural haematoma, penetrating injury, brainstem injury, but not including skull fractures), post-traumatic amnesia lasting over 24 hours, loss of consciousness for more than 30 minutes or death due to TBI.

1.4 The epidemiology of dementia after head injury

1.4.1 All-subtype dementia

Motivating this investigation of the relationship between TBI and dementia is a large body of epidemiological evidence linking head injuries with increased rates of all-subtype dementia (Table 3). A recent meta-analysis of more than two million individuals showed ~1.6 times the risk of dementia after head injury (Li et al., 2017). Several large register studies have since arrived at similar conclusions. The Finnish Care Register captured 0.5 million person-years and showed a dose-response relationship between TBI and neurodegenerative disease: moderate-severe TBI had 1.8 times the risk of dementia compared to mild TBI (Raj et al., 2017). Mild TBI is also associated with an increased dementia risk, with a recent large study showing a doubling of the risk of dementia following severe injuries, but also a 1.6 times increase after mild TBI (Nordstrom and Nordstrom, 2018). Risk continues to be elevated for long periods, with increases reported after 14 and 30 years on two large studies (Fann et al., 2018, Nordstrom and Nordstrom, 2018). These findings have been replicated in

a military study of almost 200,000 US veterans with TBI where TBIs of varying severity were associated with an increased risk of subsequent dementia (Barnes et al., 2018).

1.4.2 Alzheimer's disease

The relative risk of AD after TBI has been estimated in a large meta-analysis to be increased by about 1.5 times (Li et al., 2017), similar to earlier estimates (Fleminger et al., 2003, Mortimer et al., 1991). A marginally higher risk was seen in patients who lost consciousness after TBI. A limitation of many studies is the absence of post-mortem confirmation of the diagnosis of AD. However, the Kentucky BRAiNS study used post-mortem data for 238 TBI patients and reported higher rates of AD neuropathology in men but not women with dementia after head injury. This mirrors a general trend towards greater post-TBI dementia risk in men in observational studies (Abner et al., 2014). A further study of autopsy-confirmed AD cases reported an earlier symptom onset and dementia diagnosis of 3.6 years in patients with prior TBI (Schaffert et al., 2018). However, the neuropathology data are inconsistent. One large study (N=525) showed no increase in AD pathology in patients who had suffered a TBI, although Lewy body pathology was increased (Crane et al., 2016). This study relied on self-reported head injury. This may have resulted in an unusual clinical sample, as the larger clinical element of the study (N=7130) also found no increase in clinically diagnosed all-type dementia or AD, but did find an increased risk of PD.

1.4.3 Parkinson's disease

Parkinson's disease (PD) risk is increased after single TBI (Jafari et al., 2013). This may be the case for mild as well as moderate to severe TBI as PD risk was increased in a recent military study of outcomes after injuries of varying severities (N=320,000) (Gardner et al., 2018). Repeated mild TBI has historically been associated with Parkinsonism in the context of sporting injuries such as in boxing, attracting labels such as 'Punch Drunk' or 'Dementia Pugilistica'. The syndrome is not typical of idiopathic Parkinson's disease as extrapyramidal signs were frequently accompanied by prominent pyramidal, cerebellar and neuropsychiatric problems. Very few contemporary studies of PD have systematically investigated the relationship with repeated mild TBI. One recent study of ~ 700 Thai traditional boxers, of whom only

five developed PD, did report increased risk but only in those with the highest number of professional fights (>100) during a career (Lolekha et al., 2010).

1.4.4 Amyotrophic lateral sclerosis

The risk of amyotrophic lateral sclerosis (ALS) has been reported to be modestly increased after single TBI (Watanabe and Watanabe, 2017). However, several large register studies have not replicated this finding (Chen et al., 2007, Armon and Nelson, 2012). In relation to repeated injuries, one meta-analysis showed no increased risk of ALS (Watanabe and Watanabe, 2017). Several smaller studies have reported a connection in the context of sports-related head injuries. For example, elevated ALS rates are reported in former soccer players, where risk was proportional to the duration of participation (Woods, 1911, Chio et al., 2005, Chio et al., 2009, Armon, 2007). This association has not consistently been reported in National Football League players (Lehman et al., 2012, Savica et al., 2012).

1.4.5 Frontotemporal dementia

No recent meta-analysis describes the relationship between TBI and frontotemporal dementia (FTD). A small number of studies have assessed this outcome after single injuries and report increased hazard ratios ranging from ~ 1.5 - 4.5 times depending on injury severity. There is no good evidence of a relationship between mild, or repeated mild TBI and FTD (Deutsch et al., 2015, Wang et al., 2015, Rosso et al., 2003, Kalkonde et al., 2012, LoBue et al., 2016).

1.4.6 Chronic traumatic encephalopathy

Although CTE has clear neuropathological features, and clinical diagnostic criteria for the clinical syndrome (‘traumatic encephalopathy syndrome’) are preliminary and unvalidated. Hence, the prevalence of the condition is unknown. Neuropathological studies suggest a heterogenous clinical phenotype, overlapping considerably with cognitive and psychiatric problems produced directly by TBI (McKee et al., 2013, Katz et al., 2021). Conversely, many reported cases of CTE are asymptomatic at the time of death (Bieniek et al., 2015, Iverson et al., 2018, McKee et al., 2013). The lack of a

distinct clinical phenotype associated with neuropathologically proven cases of CTE makes it particularly difficult to disentangle the direct effects of TBI from those due to progressive neurodegeneration with cross-sectional studies. This motivates the used of detailed longitudinal evaluation of patients at risk of developing CTE using the neurodegenerative approaches described below (Stern et al., 2013, Perry et al., 2016).

Study	n	Design	TBI exposure	Outcome	Conclusion
(Barnes et al., 2018)	357,558	Cohort study (US Veterans Health Administration) Mean follow-up 4.2 years	Moderate-severe TBI (≥1) Mild TBI (≥1) with LOC Mild TBI (≥1) without LOC	Dementia	HR 3.77 [3.63 – 3.91] HR 2.52 [2.29 – 2.76] HR 2.36 [2.10 – 2.66]
(Fann et al., 2018)	2,794,852	Cohort study (Danish National Patient Register) Mean follow-up 9.89 years	Severe TBI (single) Mild TBI (single)	Dementia	HR 1.35 [1.26 – 1.45] HR 1.17 [1.13 – 1.20]
(Gardner et al., 2018)	325,870	Cohort study (US Veterans Health Administration) Mean follow-up 4.6 years	Moderate-severe TBI (≥1) Mild TBI (≥1)	PD	HR 1.83 [1.61 – 2.07] HR 1.56 [1.35 – 1.80]
(Schaffert et al., 2018)	2133	Autopsy-confirmed cases from cohort studies (from US National Alzheimer's Coordinating Center)	TBI with LOC (≥1)	AD (neuropathologically confirmed)	3.6 years earlier onset & diagnosis
(Nordstrom and Nordstrom, 2018)	3,329,360	Cohort study (Swedish National Patient Register) Mean follow-up 15.3 years	Severe TBI (single) Mild TBI (single)	Dementia	OR 2.06 [1.95 – 2.19] OR 1.63 [1.57 – 1.70]
(Li et al., 2017)	2,013,197	Meta-analysis of 21 case-control and 11 cohort studies	All severities (≥1)	Dementia AD	RR 1.63 [1.34 – 1.99] RR 1.51 [1.26 – 1.80]
(Raj et al., 2017)	40,639	Cohort study (Finnish Care Register) Median follow-up 10 years. Used mild TBI controls.	Moderate-severe TBI (≥1)	Dementia PD ALS	HR 1.9 [1.6 – 2.2] HR 1.3 [0.9 – 1.9] (NS) HR 1.3 [0.5 – 3.2] (NS)
(Watanabe and Watanabe, 2017)	511,016	Meta-analysis of 13 case-control and 3 cohort studies	All severity TBI (single) All severity TBI (repeated)	ALS	OR 1.23 [1.08 – 1.42] OR 1.17 [0.73 – 1.89] (NS)
(Crane et al., 2016)	7130	Multiple US cohort studies (Memory and Aging Project, Adult Changes in Thought Study and Religious Orders Study)	TBI with LOC > 1 hour (single)	PD PD neuropathology Dementia AD or AD neuropathology	HR 3.56 [1.52 – 8.28] HR 2.64 [1.40 – 4.99] NS NS
(Abner et al., 2014)	649	Cohort study (Kentucky BRAiNS) Median follow-up 10.8 years	All severities (≥1)	AD neuropathology (men) AD neuropathology (women)	OR 1.47 [1.03 – 2.09] OR 1.18 [0.83 – 1.68] (NS)
(Jafari et al., 2013)	97,372	Meta-analysis of 19 case-control, 2 nested case-control studies and 1 cohort study	Symptomatic TBI (single)	PD	OR = 1.57 [1.35 – 1.83]
(Fleminger et al., 2003)	346	Meta-analysis of 15 case-control studies	TBI with LOC (single)	AD	OR = 1.58 [1.21 – 2.06]
(Mortimer et al., 1991)	137	Meta-analysis of 7 case-control studies	Head injury (single) with LOC	AD	RR = 1.82 [1.26 – 2.67]

Table 3. Key epidemiological evidence relating TBI to dementia

1.5 Complexities interpreting the epidemiological evidence

Although the link between TBI and all-subtype dementia is robust, there are complexities in interpreting many of the studies. A central issue is how dementia is defined. Neurologists typically use the term dementia to refer to progressive cognitive syndromes, assuming a progressive underlying neurodegenerative pathology. However, many diagnostic manuals including the World Health Organisation's International Classification of Diseases, ICD, the American Psychiatric Association's Diagnostic and Statistical Manual of Mental Disorders, DSM accommodate both progressive, or static cognitive deficits under a 'dementia' label (American Psychiatric Association, 2013, World Health Organisation, 2018). In the context of TBI, this means that a patient left with a fixed cognitive deficit could be classified as having post-traumatic dementia. Indeed, the ICD contains a specific code for 'dementia due to injury to the head' (6D85) which refers to cognitive problems due to TBI which "must arise immediately following trauma…" and does not require the cognitive impairment to progress.

This is an important issue, as patients often have significant cognitive impairment as a direct result of their injuries (Wilson et al., 2020). There is also a wide range of trajectories for cognitive function after TBI and most patients show spontaneous improvement in the initial months after injury (Figure 2). This heterogeneity potentially confounds interpretation of epidemiological studies of TBI. For example, the recent Nordstrom study of dementia after TBI in Sweden used a generic ICD code (F03.9, 'unspecified dementia') which includes both static and progressive cognitive impairment. An early peak of dementia diagnosis soon after TBI was reported (hazard ratios ~3.5x), with a long tail of persistently elevated risk (1.25x thirty years after TBI). The early peak is most likely to represent the direct effects of TBI without a contribution from underlying neurodegeneration (Figure 2A, green trajectory). In contrast, the persistent elevation in risk years after injury is more likely to correspond to a true increase in dementia risk due to progressive underlying neurodegeneration (Figure 2A, yellow trajectory) (Nordstrom and Nordstrom, 2018). Similar possible confounds arise when considering repeated mild TBIs, where each injury has varying spontaneous recovery as well as the possibility of triggering long-term decline related

to neurodegeneration (Figure 2B). Ideally, the term post-traumatic dementia should be reserved for progressive neuropathology/clinical deterioration that is either suspected or confirmed, such as in CTE, AD or PD.

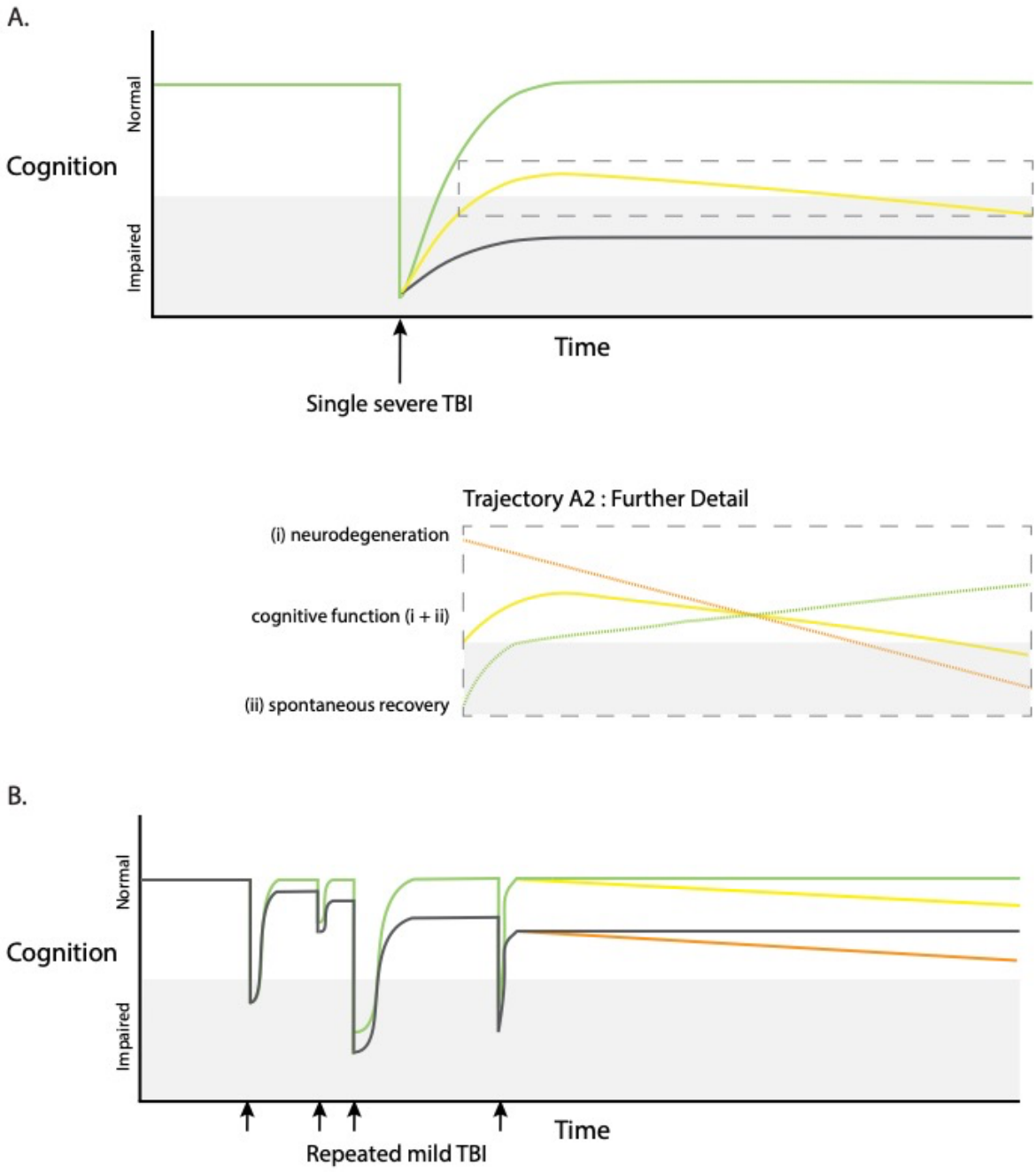

Figure 2. Possible cognitive trajectories after injury

(A) Cognitive function in relation to single severe TBI (black arrow). Marked early deterioration in cognition which may recover fully (green colour), recover partially but subsequently deteriorate (progressive neurodegeneration, yellow colour), or recover

partially leaving persistent non-progressive cognitive impairment (black colour). Further detail of trajectory A2 (dashed box) illustrating that overall cognitive function (yellow colour) may be influenced by a spontaneous recovery (green colour) and neurodegeneration (orange colour). (B) Cognitive function in relation to repeated mild TBI or 'concussions' (small black arrows). Possible trajectories include transient impairment in cognition associated with good recoveries and no progression (green colour), or late progressive neurodegeneration (yellow colour). TBI may be followed by incomplete recovery, without late progression (grey colour) or with late progressive deterioration (orange colour).

A further limitation of many epidemiological studies is the paucity of clinical information that is often available. This is problematic given the heterogeneity of TBI, as it makes judgements about the severity or associated clinical features of injury impossible. Studies relying on self-reported TBI are particularly prone to confounds in this respect, as recall bias with respect to injury exposure is a significant problem (Malec et al., 2007).

1.6 Mechanisms relating TAI and progressive neurodegeneration

The neurodegenerative pathology produced by TBI is increasingly well understood. Injuries of varying severity produce early proteinopathy, which can persist into the chronic phase. Hyperphosphorylated tau (P-tau), amyloid beta (β) or TAR DNA-binding protein 43 (TDP-43) abnormalities are seen. In the chronic phase they are associated with progressive neuronal loss, brain atrophy and ventriculomegaly.

These proteinopathies have similarities to other dementias, in particular AD (Smith et al., 2013). Neurofibrillary tangle tau pathology in CTE has a similar biochemical composition to AD (and primary age-related tauopathy), comprising 3R and 4R tau (Schmidt et al., 2001, Arena et al., 2020). However, the appearance of NFT tau in CTE is distinctive in comparison with AD when imaged at very high resolution, with a typical fold pattern (Falcon et al., 2019). Astroglial tau in CTE is even more distinct from AD, being typically 4 repeat, and present in immunoreactive thorn shaped astrocytes, reminiscent of ageing related tau astrogliopathy. A further notable difference is the perivascular distribution of astroglial tau at the base of brain sulci in CTE (Tagge et

al., 2018, Bieniek et al., 2015). This sulcal location is predicted by the distribution of biomechanical forces seen at the time of injury, as strain produced injury is focused at anatomical inflection points (Ghajari et al., 2017).

Traumatic axonal injury (TAI) is a possible trigger of this neurodegenerative pathology (Figure 3A). Axonal injury triggers slow neuronal loss in the form of Wallerian degeneration, which is a direct cause for progressive white matter atrophy seen after TBI (Maxwell et al., 2015, Hill et al., 2016). In addition, axonal injury can also lead to the production of highly pathogenic species of tau and amyloid β in the damaged axon (Goldstein et al., 2012, Tagge et al., 2018, Kondo et al., 2015). Shearing forces applied to the cytoskeleton at the time of injury cause microstructural damage and impair axonal transport (Figure 3B) (Tagge et al., 2018). Within hours of an injury, amyloid precursor protein and the cleaving enzymes beta secretase 1 and presenilin 1 accumulate in axonal varicosities. Intraneuronal amyloid β is produced with later accumulation of extracellular plaques (Gentleman et al., 1993, Johnson et al., 2013b, Uryu et al., 2007, Jucker and Walker, 2013). Similar shearing forces lead to tau dissociating from microtubules, leading to hyperphosphorylation, aggregation, and aberrant processing (Figure 3C) (Tagge et al., 2018). This can produce a highly pathogenic tau proteoform (*cis* P-tau) which contributes to apoptosis, mitochondrial damage and abnormal long-term potentiation early after TBI (Kondo et al., 2015, Nakamura et al., 2012, Zanier et al., 2018).

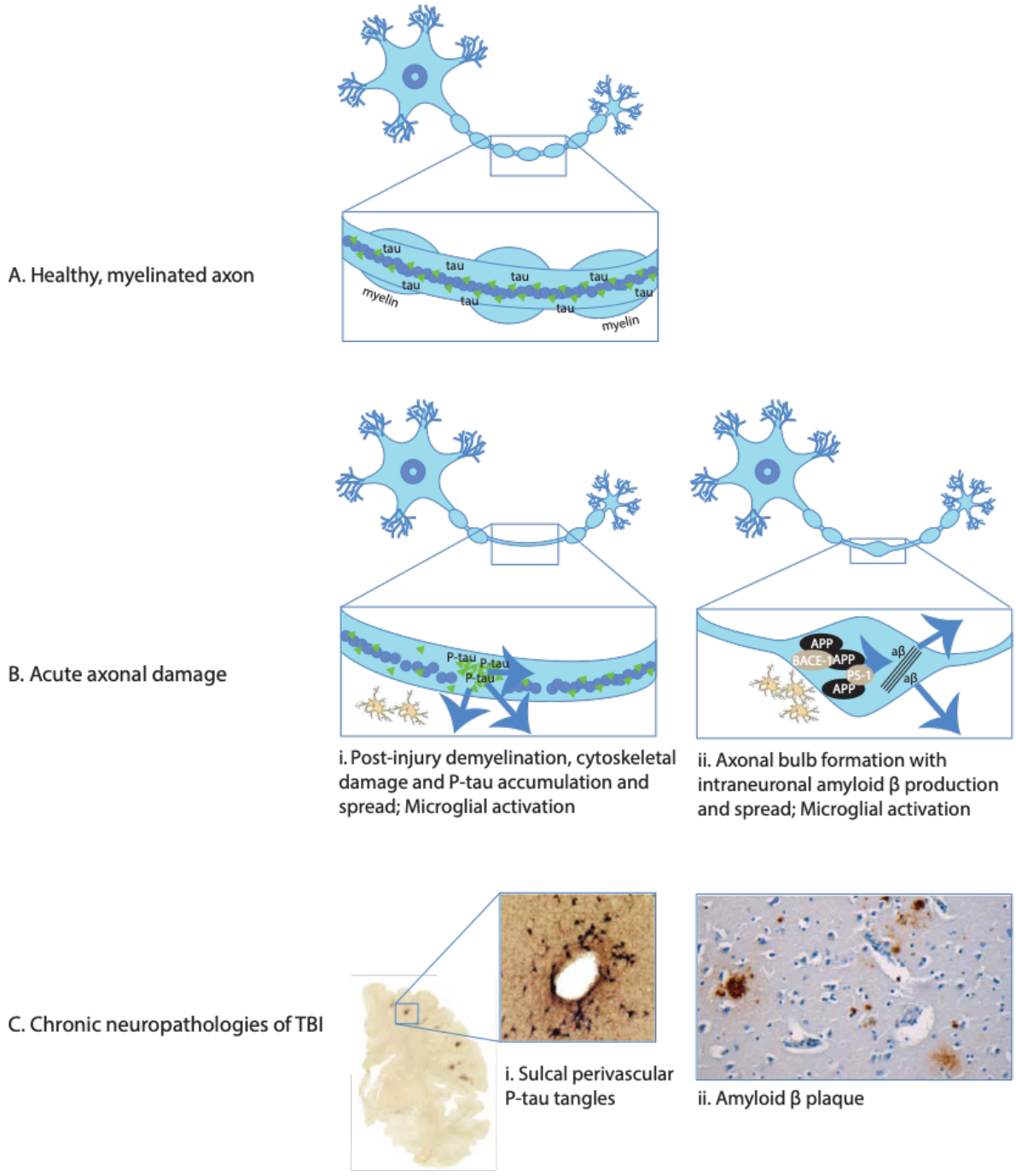

Figure 3. Acute neuropathologies and chronic neurodegeneration

(A) Healthy, myelinated axon prior to TBI. The box shows detail of the mid-segment of axon with central microtubules surrounded by tau with intact myelin sheath present. (B) Acute axonal damage with demyelination of the axon (panels i and ii). Tau pathology and demyelination of axon: (i) axonal injury causes cytoskeletal disruption, tau dissociation from microtubules and accumulation. Tau is aberrantly phosphorylated and may spread through extracellular, paracellular, transcellular and

glymphatic mechanisms (Tagge et al., 2018). Amyloid pathology: (ii) axonal damage causes formation of axonal bulbs/varicosities. Amyloid precursor protein accumulates with cleavage enzymes beta-site APP cleaving enzyme 1 and presenilin 1. This produces amyloid beta which may spread to the surrounding structures following lysis of damaged neurons (Johnson et al., 2013b). Traumatic axonal damage stimulates local inflammatory response including microglial activation (panels i and ii) (C) Chronic neuropathologies. (i) Tau pathology: shearing forces during head injury localise to cortical sulcal depths causing microstructural damage, blood brain barrier disruption, axonopathy, astrogliopathy and inflammation. Sulcal perivascular localisation of P-tau neurofibrillary tangles is pathognomonic of chronic traumatic encephalopathy, visible on CP13 immunostaining (McKee et al., 2013). (ii) Amyloid pathology: amyloid beta plaques in a middle-aged woman who died many decades after TBI evident on immunohistochemical and thioflavine-S stains (Johnson et al., 2012).

The perivascular location of tau pathology suggests that damage to the neurovascular unit may be an important causative factor in post-traumatic neurodegeneration (Tagge et al., 2018, McKee et al., 2013). The blood brain barrier (BBB) is disrupted in the first minutes after injury, producing a complex inflammatory response in the hours and days after TBI (Csuka et al., 1999, Shapira et al., 1993, Nagamoto-Combs et al., 2007, Koshinaga et al., 2000, Smith et al., 1997). Microglia and astrocytes activate in response to the extravasation of pro-inflammatory molecules and infiltrating monocytes contribute to the subsequent inflammatory response (Tagge et al., 2018). Microglia remain activated at the site of axonal injury for many years after TBI, and are associated with the long-term effects of diffuse axonal injury (Johnson et al., 2013a). The functional impact of these microglia remains uncertain, as it is unclear when they exhibit neuroinflammatory or restorative phenotypes (Tagge et al., 2018, Johnson et al., 2013a, Koshinaga et al., 2000, Ramlackhansingh et al., 2011, Ransohoff, 2016, Scott et al., 2018). Reduced clearance of neurodegenerative precursors may also increase late neurodegeneration, potentially caused by disruption to the normal functioning of the glymphatic system. Misfolded amyloid β and P-tau is cleared through the glymphatic system in a process dependent on the aquaporin-4 water channel located in astrocytic end-feet (Iliff et al., 2012, Iliff et al., 2014). Early reactive

astrogliosis following experimental TBI is associated with loss of aquaporin channels, reduced CSF flow and impaired protein clearance suggesting a role in the subsequent accumulation of neurotoxic proteins (Iliff et al., 2014).

A key challenge is to understand the links between the earliest stages of neurodegeneration produced at the time of injury and widespread pathological changes seen at post-mortem in many cases of CTE and other types of dementia. It is proposed that CTE progresses over time in an individual to involve increasingly large parts of the brain (McKee et al., 2013). The staging of CTE reflects this progression, but it is important to note that this staging is based on cross-sectional data, as it has not yet been possible to study the progression the disease *in vivo*. Hence, an important goal for future clinical research is to distinguish in individuals the direct effects of TBI from a truly progressive neurodegenerative process that spreads to involve neurons not necessarily affected at the time of the initial injury. An important recent observation is that TBI can produce a prion-like spread of self-seeding proteinopathy. In animal models of TBI, P-tau, initially present at the site of injury, becomes detectable in the contralateral hemisphere six months after injury (Clavaguera et al., 2015, Kondo et al., 2015, Johnson et al., 2013a, Tagge et al., 2018). In addition, local inoculation of healthy animals with contused brain homogenate induces progressive tauopathy, suggesting that brain trauma produces a transmissible self-propagating tau pathology (Jucker and Walker, 2013, Zanier et al., 2018).

1.7 Clinical features of neurodegeneration after TBI

A major clinical challenge is to improve our approach to the diagnosis of post-traumatic neurodegenerative conditions. This is a difficult problem, in part because the clinical features of CTE and other post-traumatic dementias overlap with the direct cognitive and psychiatric effects of the brain injury (McKee et al., 2013). For example, McKee and colleagues propose CTE staging based on neuropathological disease progression and highlight clinical features that are characteristic of each pathological stage (McKee et al., 2013, Stern et al., 2013). Symptoms of CTE include headache, memory loss, word finding difficulty and aggression, all of which are common as direct sequelae of TBI (Katz et al., 2021).

Without prolonged longitudinal clinical observation, it is not usually possible to disentangle the direct effects of TBI from those resulting from the neurodegenerative processes on the grounds of clinical presentation. However, a wide range of investigations have been developed in other neurodegenerative conditions, which can usefully be applied to the study of post-traumatic neurodegeneration, perhaps revealing distinct and informative endophenotypes of the process (Iacono, 2018). It is proposed that the systematic use of clinical assessment in combination with multi-modal biomarkers will allow the development of accurate diagnostic criteria for post-traumatic dementias, as well as accurate ways of measuring disease progression and prognostication.

1.8 Investigating acute axonal injury and neurodegeneration after TBI

1.8.1 Brain atrophy and axonal injury

Brain atrophy provides a key measure of disease progression in neurodegenerative conditions. Neuronal loss results from diverse neurodegenerative processes produces atrophy, which can be measured using serial MRI (Cole et al., 2018a, Sidaros et al., 2009). This is a sensitive albeit non-specific way to assess progressive neurodegeneration. A standard approach in other neurodegenerative conditions is to use repeated volumetric T1 MRI. Refined analysis pipelines are available, providing precise and sensitive measures of how an individual's brain changes over time (Worker et al., 2018). MRI is already used widely in the assessment of TBI. It is sensitive to contusions, haemorrhage and features associated with diffuse axonal injury such as microhaemorrhages (Maas et al., 2017). Atrophy is a particularly important neurodegenerative biomarker as it provides an integrated measure of neuronal loss seen months to years after injuries and spatial information about the pattern of this loss. Atrophy is often obvious on standard neuroimaging as ventricular enlargement and cavum septum pellucidum (Smith et al., 2013) and can be quantified using serial volumetric T1 MRI (Cole et al., 2018a).

Progressive brain atrophy is very common after TBI and can be obvious when scans are compared over time (Cole et al., 2018a). Quantifying these changes using serial volumetric MRI shows strikingly elevated rates of atrophy, which continue for many

years after a moderate-severe TBI (Sidaros et al., 2009, Cole et al., 2018a). A yearly loss of ~ 1.5% in the grey and white matter has been described (Figure 3). These atrophy rates approach those seen in established AD and contrast with the absence of atrophy in healthy subjects of similar ages (Smith et al., 2007).

Different tissue classes appear to atrophy at different rates over time after injury: grey matter atrophy is seen early post-injury and white matter atrophy is seen more in the chronic phase (Brezova et al., 2014, Tomaiuolo et al., 2012, Farbota et al., 2012). Higher rates are seen with greater TBI severity: lower GCS, loss of consciousness, coma and post-traumatic amnesia are all associated with atrophy (Cole et al., 2018a, Brezova et al., 2014, Bendlin et al., 2008, MacKenzie et al., 2002, Trivedi et al., 2007, Sidaros et al., 2009). Higher rates have been reported in cortical sulci relative to gyri, reflecting strain levels produced by many injuries in the sulci and the characteristic location of CTE neuropathology (Ghajari et al., 2017, McKee et al., 2016). The extent of brain atrophy also relates to cognitive and functional outcomes after TBI (Zhou et al., 2013, Cole et al., 2018a, Warner et al., 2010, Sidaros et al., 2009, Ross et al., 2012), with high atrophy rates associated with declining memory performance (Cole et al., 2018a).

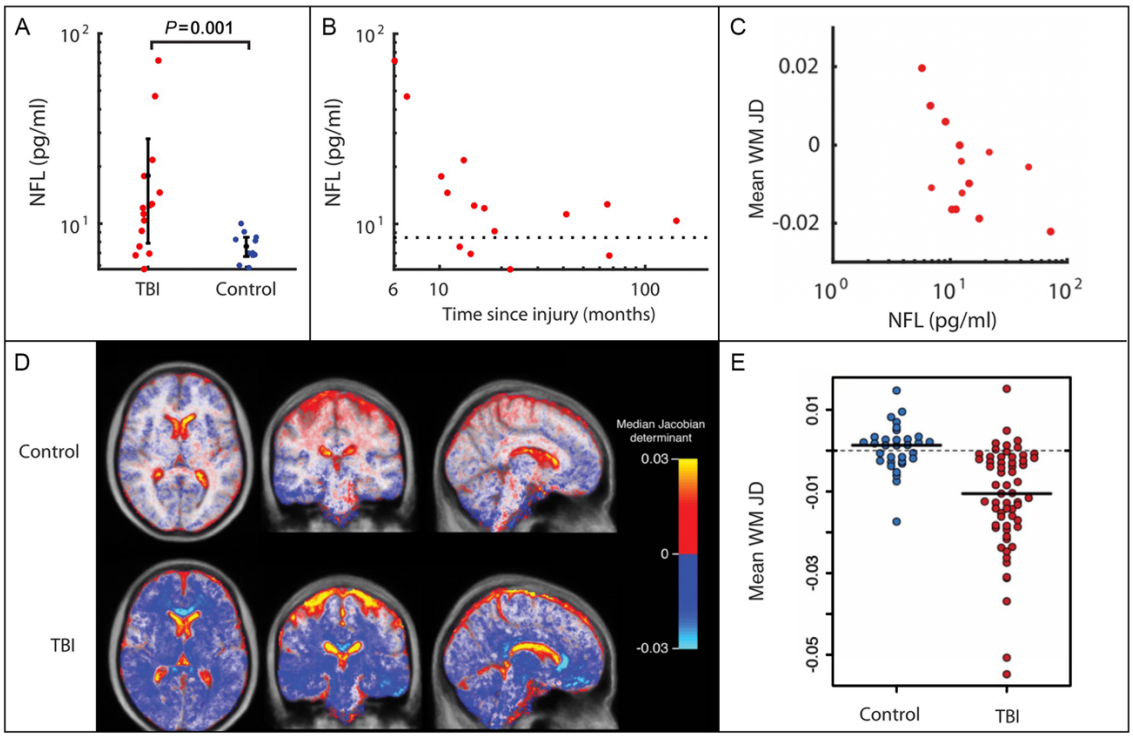

Figure 4. Biomarker quantification of neurodegeneration

A. Plasma neurofilament light (NfL) levels plotted for moderate-severe TBI in the chronic phase and controls. Levels are significantly higher in patients with TBI than in controls (Cole et al., 2018a). B. NfL levels for moderate-severe TBI in the chronic phase plotted against time since injury (months). C. Mean white matter (WM) Jacobian determinant (annualised JD rate) calculated over a 6-month scan–rescan interval in patients in the chronic phase after moderate-severe TBI, plotted against baseline plasma NfL level (Scott et al., 2018). D. Spatial maps of average JD values in healthy controls and TBI patient groups. Marked progressive white matter atrophy is present after moderate-severe TBI (blue-white areas) with expansion of cerebrospinal fluid spaces (red-yellow areas) in comparison with minimal change in healthy controls (Cole et al., 2018a). E. Progressive atrophy of white matter following moderate-severe TBI. Scatter plot of JD rates of brain volume change in TBI compared with age-matched healthy volunteers, in white matter. A JD of 0 indicates no change in brain volume over the follow-up period (Scott et al., 2018).

Brain structure can also provide information about ageing (Cole et al., 2019). Variations in brain volume can be used to estimate chronological age in healthy individuals. In disease states, the discrepancy between a 'Brain Age' estimated from neuroimaging and a patients chronological age can be informative. Older than expected brain age has been reported in settings such as mild cognitive impairment and Alzheimer's disease patients and significantly, when the measure was tested in the Lothian Birth Cohort, individuals with older appearing brains were likely to survive for a shorter duration (Cole et al., 2018b). It has previously been shown that moderate-severe TBI adds around five years to measured brain age, relative to chronological age, and that this difference predicts cognitive impairment and increases with time after injury (Cole et al., 2015). Hence, brains appear 'older' after a significant head injury, an effect that accentuates with time since injury and that correlates with post-traumatic cognitive impairments.

Diffusion MRI provides complementary information about the location and extent of diffuse axonal injury (Mac Donald et al., 2007a). This is relevant to post-traumatic neurodegeneration as axonal injury is linked to the production of amyloid β and P-tau

proteinopathies (Tagge et al., 2018, Johnson et al., 2010). Diffusion tensor imaging (DTI) has been widely used to investigate quantifying white matter damage produce by DAI. Subtle abnormalities in the organisation of white matter can be detected, even when the gross scan appearances are normal. The location and severity of these changes correlate well with post-injury cognitive problems such as poor speed, executive dysfunction, memory issues, and functional outcomes (Hellyer et al., 2013) Hence DTI can be used to identify the presence of an important potential trigger for neurodegeneration and also provides a way to test the hypothesis that proteinopathies initiated by TBI spread in a way that is constrained by the structure of the white matter connectome (Warren et al., 2012).

1.8.2 Fluid biomarkers of neurodegeneration

Neuroimaging can be complemented by blood, cerebrospinal fluid (CSF) and microdialysate biomarkers of neurodegeneration to better understand the chronic consequences of injury. Dramatic improvements in assay sensitivity have resulted from the transfer of standard enzyme linked immunosorbent assays onto the single molecule assay (Simoa) platform. This allows ultrasensitive measurement of biomarkers such as neurofilament light (NfL) and tau (Kuhle et al., 2016), dramatically improving sensitivity for neurodegenerative conditions.

NfL is a particularly promising biomarker of both acute injury and the chronic sequelae of TBI. It is found in high concentrations within myelinated axons, and animal models of neurodegeneration show NfL to be a sensitive measure of the onset of a range of proteopathic lesions in the brain. Changes in NfL levels can be used to track disease progression and treatment response in neurodegenerative disease, (Bacioglu et al., 2016) and in humans, increased levels are observed in a variety of processes, including AD and motor neuron disease (Gaiottino et al., 2013, Lu et al., 2015, Gisslén et al., 2016, Bacioglu et al., 2016) as well as long after TBI (Shahim et al., 2020a). Serial NfL sampling in individuals at risk of AD predicts brain atrophy rates, cognitive impairment and disease progression (Preische et al., 2019). As plasma NfL levels are highly correlated with CSF NfL, blood testing of NfL appears to be informative (Hansson et al., 2017, Shahim et al., 2016a, Gisslén et al., 2016, Lu et al., 2015).

NfL and tau have also been used to assess TBI, particularly in the acute setting (Zetterberg et al., 2013). Blood and CSF levels increase acutely after brain injury, and relate to the severity of injury (Shahim et al., 2017, Shahim et al., 2016a). Concentrations in blood and CSF rise briskly after even mild injuries, such as following a bout of contact in boxers, or head injury in ice hockey (Neselius et al., 2013, Shahim et al., 2018).

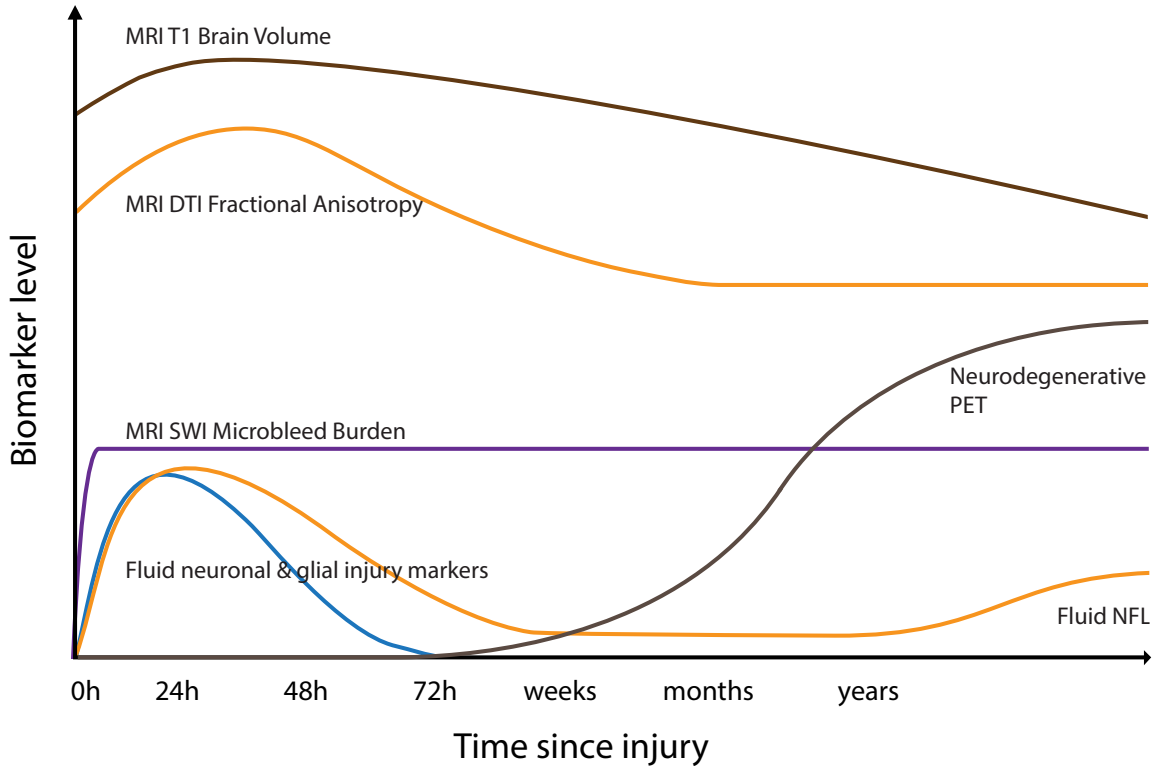

Figure 5. Potential longitudinal biomarker trajectories post-TBI

Potential longitudinal biomarker trajectories following TBI. Hypothecated trajectories of biomarkers after moderate-severe TBI. Brain volumes measured by volumetric MRI may initially increase due to oedema before progressively reducing and continuing to decline as a result of progressive neurodegeneration after injury. Fractional anisotropy, a measure of white matter organisation derived from diffusion tensor imaging (DTI), initially increases due to acute oedema, with a subacute reduction days to weeks later reflecting axonal damage. Cerebral microbleeds, a marker of diffuse vascular injury, appear rapidly after TBI and do not resolve. They are identified most sensitively with susceptibility weighted imaging (SWI) (Maas et al., 2017). Indicative biomarker trends after injury (possible trajectories). Acute injury markers ubiquitin carboxy-terminal hydrolase L1 (UCH-L1), S100B, neuron specific enolase (NSE), glial fibrillary acidic protein (GFAP), amyloid and tau are briskly elevated after TBI. Neurofilament light levels peak later and may be elevated in the chronic phase, correlating with progressive brain atrophy (Thelin et al., 2017, Bogoslovsky et al., 2017) on PET.

Levels of NfL but not tau remain elevated in the chronic phase after TBI in some individuals and levels correlate with measures of diffuse axonal injury and progressive brain atrophy (Figure 4C) (Scott et al., 2018, Ljungqvist et al., 2017, Shahim et al., 2020a). This suggests that NfL levels reflect the extent of traumatic injury, particularly to large, myelinated axons. In the chronic phase after injury, persistently increased blood NfL may reflect the presence of progressive post-traumatic neurodegeneration. If this is confirmed in larger studies, plasma NfL could prove diagnostically useful in identifying patients at risk of developing post-traumatic dementias of various types and for stratifying patient recruitment into clinical trials.

1.8.3 Molecular imaging: amyloid, tau and microglial activation

MRI measures of brain atrophy and NfL levels provide sensitive but non-specific measures of post-traumatic neurodegeneration, with differing longitudinal trajectories (Figure 5). In contrast, molecular imaging techniques such as positron emission tomography (PET) allow specific types of proteinopathy to be identified. PET tracers sensitive to P-tau in neurofibrillary tangles and amyloid-β aggregates have been developed. The application of these in TBI promise to dramatically improve the investigation of post-traumatic neurodegeneration and should facilitate the diagnosis of CTE and other types of post-traumatic dementia *in vivo*.

Amyloid PET tracers such as ^{11}C-Pittsburgh compound-B (^{11}C-PIB) have been used widely to identify fibrillar amyloid β pathology. ^{11}C-PIB binding is increased in AD in a similar pattern to amyloid pathology (Quigley et al., 2011, Rowe et al., 2007). In the first year after TBI, ^{11}C-PIB binding is also increased in cortical grey matter and striatum (Hong et al., 2014), remaining high many years after injury in some patients (Scott et al., 2016). There are similarities between ^{11}C-PIB binding in TBI and AD, although binding is typically much higher in AD. However, after TBI, ^{11}C-PIB binding is also seen in the cerebellum where increased amyloid is not typically observed in AD, which may suggest a distinct mechanism for the production of amyloid pathology after TBI.

There has been particular focus on developing tracers which are sensitive and specific to tau pathology in neurodegenerative disease. There is PET evidence of increased

tau signal after moderate-severe TBI (Gorgoraptis et al., 2019), and some studies have used tau PET to investigate patients with repetitive TBI produced by sports injury. However, these studies have been very small, have often lacked controls and have usually lacked neuropathological confirmation of CTE (Dickstein et al., 2016, Small et al., 2013, Barrio et al., 2015). One case report of an American Football player with a history of repetitive TBI and progressive neuropsychiatric symptoms described increased Flortaucipir binding (Dickstein et al., 2016). A second case study reported increased ^{18}F-FDDNP binding in an American Football player with history of repeated mild TBI who was later diagnosed with CTE post-mortem. In this case, the spatial pattern of abnormal PET findings correlated to some extent with the spatial pattern of P-tau post-mortem (Omalu et al., 2018, James et al., 2015). If tau PET is to make a significant contribution to the diagnosis of post-traumatic neurodegeneration, convincing evidence of binding to the range of post-traumatic tau pathologies is necessary. For example, Flortaucipir, while performing well for AD tau conformations on autoradiography had very poor binding to CTE tau (Marquié et al., 2019). This is a major limitation at present.

Chronic inflammation is a feature of neurodegenerative disease. TSPO PET ligands bind to a translocator protein expressed on the mitochondria of activated microglia (Owen et al., 2014). These have been widely used in AD, generally showing increased binding that tracks progression of the disease (Lagarde et al., 2018). In neuropathological studies of TBI, chronic microglial activation is associated with evidence of persistent axonal injury (Johnson et al., 2013a). In keeping with these observations, TSPO PET binding is increased many years after TBI, predominantly in subcortical white matter and thalamic locations (Ramlackhansingh et al., 2011, Scott et al., 2018). High binding is seen in areas of diffuse axonal injury that also show progressive brain atrophy (Scott et al., 2018). Hence, microglial activation persists in areas of axonal injury for years after TBI and progressive neurodegeneration occurs at these locations.

1.8.4 Vascular damage

Neurodegenerative abnormalities are particularly seen in a perivascular location suggesting that TBI may trigger a neurodegenerative cascade through an effect on BBB permeability (Tagge et al., 2018, McKee et al., 2013). Hence, investigating neurovascular structures could provide insights into the triggers for neurodegeneration. Blood vessels are often directly damaged by TBI. Large intracerebral haemorrhages are common at extradural, subdural and parenchymal locations. These are often the focus for initial management. However, their relationship to long-term dementia risk is unclear. In other contexts, such as intraparenchymal or non-traumatic subarachnoid haemorrhage, long-term dementia risk is elevated independent of vascular risk factors: dementia risk is significantly greater following haemorrhagic compared with ischaemic stroke (Corraini et al., 2017). More subtle peri-vascular haemorrhage is also common and can be sensitively assessed using gradient echo or susceptibility weighted imaging (SWI) (Scheid et al., 2003). These MRI sequences are now routinely used in the assessment of TBI, and microhaemorrhages provide evidence of diffuse vascular injury, which may not be apparent using conventional imaging approaches. Diffuse vascular injury is often associated, but is not synonymous with, diffuse axonal injury (Griffin et al., 2019). Hence the location and extent of microhaemorrhages may be another way to investigate the link between initial injury severity and post-traumatic neurodegeneration.

1.9 Clinical trials and outcome measures of post-traumatic neurodegeneration

Establishing clear relationships between biomarkers and disease states can facilitate the development of new treatments, as well as improving patient assessment. For example, treatment advances have been accelerated by establishing the links between intraocular pressure and visual function in glaucoma; bone mineral density and osteoporotic fractures; and CD4 lymphocyte count and HIV infection (Yu et al., 2015). This consideration is relevant for TBI because there is a pressing need to develop new approaches to evaluating new treatments. The heterogeneity of TBI leads to significant challenges in powering clinical trials (Narayan et al., 2002). Previous studies of neuroprotection and disease modification have largely produced

negative results. It is often unclear if these trials were underpowered to detect treatment effects, which were usually measured using noisy clinical end-points. Hence, there is a significant risk that we have failed to properly evaluate promising new treatments because of suboptimal trial design.

Incorporating biomarkers of neurodegeneration as primary or secondary outcome measures in phase II and III clinical trials will improve the ability to detect neuroprotective and disease modifying treatment by providing precise and sensitive measures of neuronal loss (Figure 6). Fluid biomarkers such as NfL provide one potential surrogate marker of neurodegeneration.

For example, changes in blood or CSF levels of NfL provide a dynamic measure of treatment effects that have been validated in animal studies (Bacioglu et al., 2016) and show promising results as a read out of active neurodegeneration in one experimental medicine study of minocycline use (Scott et al., 2018). MRI measurements of brain atrophy provide a second option with strong face validity as an integrated measure of neuronal loss and benefit from an established link with neuropathology in other contexts such as AD (Bobinski et al., 2000). This approach has been already established as a surrogate end-point for disease progression (Cash et al., 2014).

MRI measurements of atrophy typically have high test-retest reliability in healthy subjects, allowing the impact of TBI to be sensitively detected. The effect of TBI on brain atrophy is substantial in comparison to a number of potential confounds. For example, TBI explained ~20% of the variance in atrophy rates compared to ~0.5% due to either age or sex one recent study in the chronic phase after moderate-severe TBI (Cole et al., 2018a). Hence, relatively small treatment effects on atrophy rate could be sensitively identified using this approach (Cole et al., 2018a, Maclaren et al., 2014).

Sample size could be reduced by enriching for high rates of neurodegeneration using complementary biomarkers, an approach routinely taken in AD trials (Schott et al., 2010).

In TBI, this type of enrichment might involve inclusion criteria such as positive tau PET, the presence of diffuse axonal injury indicated by DTI and high levels of plasma NfL. The primary goal of this approach would be to facilitate cost-effective and feasible phase II clinical trials that provide robust evidence about the effect of neuroprotective or disease modifying treatments on neuronal loss after TBI.

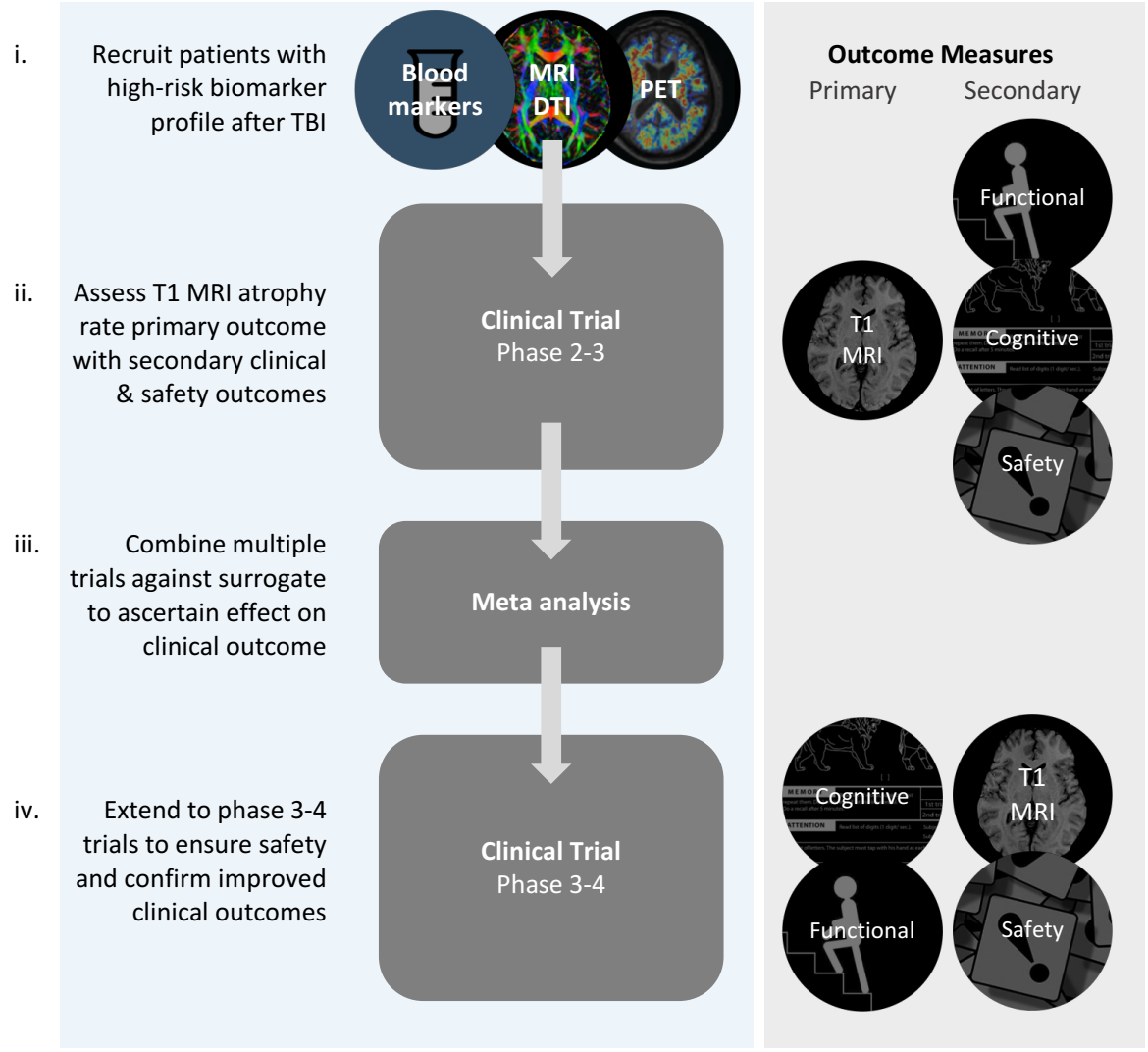

Figure 6. Biomarkers and clinical trial design

Stages for the evaluation of disease modifying/neuroprotective treatment after TBI. (i) Recruitment of patients at high risk for neurodegeneration using baseline blood NfL, diffusion-weighted MRI and PET abnormality. (ii) Phase 2–3 trials powered to primary outcome measure of change in atrophy rate (using repeated T1 MRI) with secondary functional/cognitive/safety outcomes. (iii) Meta-analysis of phase 2–3 trials to clarify the relationship between the surrogate (T1 atrophy rate) and patient-centred outcomes. (iv) Late-stage phase 3–4 trials using primary functional or cognitive outcome. This may be a composite measure.

In AD drug trials a 25% reduction in atrophy rate is considered to be clinically meaningful (Hua et al., 2009). This represents a pragmatic starting point for the modelling of potential trial designs in TBI. In the chronic phase after TBI, a sample size of around 200 patients per group has been shown to be adequate to assess white matter volume change in a trial designed with 80% power to detect a 25% reduction in atrophy rate using a two-sided test (α = 0.05) (Cole et al., 2018a).

$$Subjects\ per\ arm = \left[\frac{1.96 + 0.842}{0.25\ \times\ effect\ size}\right]^2$$

$$effect\ size = \frac{mean\ atrophy\ rate_{patients} - mean\ atrophy\ rate_{controls}}{variance\ of\ atrophy\ rate_{patients}}$$

Adapted from (Cash et al., 2015)

Sample sizes might be reduced by limiting variability in the outcome measure. This could be achieved by optimising the accuracy of T1 MRI volume assessment, for example by using tensor-based morphometry (the 'Jacobian determinant' method). Between-subject variability can be reduced, further limiting sample sizes, through techniques such as enriching the trial population by selecting individuals at high risk of neurodegeneration for a more homogeneous group (Cole et al., 2018a). Biomarkers such as blood NfL, genetic risk, PET imaging or baseline atrophy status or rate could perform this role. Other approaches such as adjusting for baseline covariates may yield further reductions in sample size (Schott et al., 2010).

However, there are several complexities that need to be considered when using MRI measures of brain atrophy following TBI. Injury-related oedema produced in the acute phase may spuriously elevate atrophy rates as it resolves. A similar issue is recognised in multiple sclerosis following the initiation of treatments which reduce neuroinflammation ('pseudo-atrophy') (Arnold and De Stefano, 2013). Studies that accurately characterise the time course of atrophy using repeated MRI in the acute and subacute period after TBI are necessary and should clarify how best to precisely measure neuronal loss and distinguish this from resolving oedema and any treatment related effects (Zhang et al., 2012, Whittall et al., 1997). A simpler approach is to

measure atrophy in the subacute-to-chronic phase, following the resolution of acute oedema. Brain atrophy progresses months to years after injuries and so can provide an integrative measure of neuronal loss over time. This may prove to be a sensitive measure of treatment effects that were administered in the acute phase prior to MRI assessment. Regardless of the timing of assessment, focal lesions need to be controlled for in the estimation of atrophy rates. This could be achieved by delineating focal lesions and then incorporating this information into the calculation of atrophy rates. Separate rates of atrophy are likely to be needed for brain regions close or remote to focal injury (Kamnitsas et al., 2017, Ledig et al., 2017). Other non-TBI specific factors that need to be considered include hydrations status, motion, scanner variability and harmonisation of analysis technique (Kempton et al., 2009, Reuter et al., 2015, Cash et al., 2015).

Another important issue is to understand how atrophy rates relate to clinical outcomes after TBI. Whilst clinical outcomes such as quality of life and disability are ultimately key to evaluating new treatments, there is likely to be a complex relationship between progressive brain atrophy and these clinical measures. Although there is already evidence that patients with high rates of atrophy show worse functional outcomes and cognitive impairment, much more work is necessary to understand these relationships (Sidaros et al., 2009, Ross et al., 2012, Cole et al., 2018a). One issue is that spontaneous recovery early after TBI is likely to be the major driver of clinical outcome and so early neurodegeneration will not show a simple relationship to these outcomes. For example, cognitive impairment generally improves over the first few months after TBI at the same time as high rates of brain atrophy are seen. However, it would be wrong to conclude that progressive atrophy is causally related to clinical recovery. A second issue is that the effects of accelerated neurodegeneration may take years if not decades to become apparent. A young person with accelerated neurodegeneration after TBI may have a large neural and cognitive reserve to protect against the impact of neuronal loss. Hence the cumulative effects of progressive neuronal loss may not be immediately apparent.

Similar complexities have been discussed in the context of early stage neurodegenerative studies, where pre-clinical effects of drugs may be disease

modifying but would not be expected to have immediate clinical effects (Rafii and Aisen, 2019). In early 2018, the US Food and Drug Administration (FDA) released draft guidance for the assessment of early Alzheimer's disease treatments (US Food and Drug Administration, 2018). This recognises the challenges of assessing treatments in high risk people without cognitive or functional impairments, a pre-clinical period they term 'stage 1' of the disease. Significantly, both for Alzheimer's disease and by extension, the potential to intervene before post-traumatic neurodegeneration, it is accepted that biomarker changes may be sufficient grounds for initial approval, with post-marketing surveillance: "In Stage 1 patients, an effect on the characteristic pathophysiologic changes of AD, as demonstrated by an effect on various biomarkers, may be measured. Such an effect, analysed as a primary efficacy measure, may, in principle, serve as the basis for an accelerated approval (i.e., the biomarker effects would be found to be reasonably likely to predict clinical benefit, with a post-approval requirement for a study to confirm the predicted clinical benefit). As with the use of neuropsychological tests, a pattern of treatment effects seen across multiple individual biomarker measures would increase the persuasiveness of the putative effect" (US Food and Drug Administration, 2018).

These considerations have important implications for the design of clinical trials in TBI and the choice of the endpoints selected. One pragmatic option, considering the FDA's draft guidance for AD may be to apply brain atrophy measures of neuronal loss as a primary endpoint for the initial evaluation of neuroprotective treatment, making later use of highly sensitive, likely compound functional and cognitive outcome scores in post-marketing studies. This approach would recognise the protection of brain volume as a legitimate post-traumatic treatment goal, in the first instance.

1.10 Conclusions

The relationship of TBI to chronic neurodegeneration and dementia is increasingly well characterised at epidemiological and mechanistic levels. Post-traumatic neurodegeneration warrants urgent attention as contributor to the growing worldwide burden of dementia, with special importance as a therapeutic opportunity following a timed, identifiable insult.

Axonal injury has been implicated as a mechanistic driver of chronic pathologies and biomarker techniques are available which promise to quantify this clinically, if successfully validated. Likewise, markers of subsequent neurodegeneration are available, which would help to both clarify the nature of post-traumatic change and expedite trials of treatments to prevent progressive disease. An experimental medicine approach to assessing treatments using biomarkers to identify those at risk for neurodegeneration and measure outcomes is very promising and feasible, drawing on key lessons from conditions such as Alzheimer's disease.

2 General methods

In this chapter I review the methods involved in blood biomarker assessment, neuroimaging acquisition and analysis pipelines used in several of the investigations within this thesis. Investigation-specific detail, where needed in addition, is provided within each chapter.

2.1 Fluid biomarkers

Previous data suggesting that the axonal marker NfL could be reliably quantified in blood and related to clinical outcomes after TBI motivated a central focus on this biomarker given the importance of white matter pathologies after TBI (Shahim et al., 2016a). Assessment of the axonal marker tau was supported by evidence of brisk increases after injury when quantified centrally (Magnoni et al., 2012) and its potential role in proteopathic seeding. Exploratory analyses of neuronal (somal) marker UCH-L1 and glial markers S100-B and GFAP were included to contextualise axonal biomarker change, markers related to traumatic injuries in previous work (Zetterberg et al., 2013).

Blood biomarker assessment was performed in the BIO-AX-TBI study (Chapters 3,4) in the following way: blood was sampled via peripheral venepuncture or a central venous line if available. Two K3 EDTA (6 ml) samples were taken for analysis of plasma biomarkers and two serum z-clot activator (5ml) samples were taken for serum analyses.

The Lausanne and Ljubljana research sites within the BIO-AX-TBI research study also performed invasive cerebral microdialysis facilitating biomarker assessment on brain extracellular fluid sampled from the deep white matter. These assessments were performed in patients where an existing clinical indication for microdialysis was already present (Oddo and Hutchinson, 2018). 100kD MDialysis AB catheters are surgically implanted via burr hole in normal-appearing white matter regions defined by CT. Typically this is the right frontal lobe but may be left sided if contusions are present. Standard dextran solutions are added to perfusion fluid to aid recovery of proteins using a standard sampling rate of 0.3 microlitres per minute (Giorgi-Coll et al., 2020).

Samples are taken and frozen for biomarker assessment upto 4 hourly. In patients undergoing invasive cerebral microdialysis, a 6ml K3 EDTA sample is taken up to 12 hourly. After a 30 minute window, plasma and serum for fluid biomarker analysis are centrifuged at 2000-2500g and frozen at -80C.

Neuro-glial injury biomarker assessment was performed on fluid samples by the UK Dementia Research Institute biomarker laboratory at UCL where the Quanterix Simoa digital ELISA platform is used. Assessments described in this thesis were performed using the Neuro 4plex B chip to quantify plasma NfL, total tau, glial fibrillary acidic protein (GFAP), and ubiquitin carboxyl hydrolase L1 (UCH-L1) in plasma and microdialysate. S100 calcium binding protein B (S100B) was measured in a separate assay (Millipore Merck ELISA kit) in serum. Microdialysate samples were assessed as per plasma using the 4plex B but with a 200:1 dilution. Any samples with results lower than the lower limit of quantification were re-recorded at 50% of the lower limit. In this set of experiments the lower limit of quantification for the various markers were: NfL 0.5 pg/ml; tau 0.125 pg/ml; UCH-L1 9.38 pg/ml; GFAP: 9.38 pg/ml; S100B 2.7 pg/ml.

2.2 MRI acquisition

In this thesis all longitudinal neuroimaging reported represents scans on the same scanner system. At Imperial College London, there are two scanner systems: a Philips and a Siemens scanner. Chapters 4 and 6 report neuroimaging data collected on the Siemens scanner alone at Imperial College London whereas Chapter 5 data were collected on a combination of the Philips and Siemens systems.

The Siemens Verio 3T system (Siemens Healthineers AG, Erlangen, Germany), used a volumetric MPRAGE sequence used the following parameters: slice thickness of 1mm, with 160 slices and a matrix of 256x240, with a repetition time of 2300ms, echo time of 2.98ms, flip angle 9°, field of view of 25.6cm x 24cm, with a voxel size of 1.0 x 1.0 x 1.0 mm. DWI was acquired on the Siemens scanner with the following parameters: Echo time = 103ms, repetition time = 9500ms, 64 contiguous slices, FOV 256mm, voxel size $2mm^3$, b = 1000 s/mm^3, four images with b = 0 s/mm^2.

The following parameters were used on the Philips 3 Achieva system: T1-TFE slice thickness = 1.2mm, 150 slices, matrix = 208x208, repetition time = 9.60ms, echo time

= 4.60ms, flip angle = 8 degrees, FOV = 24x24cm. The following DWI parameters were used: voxel size = 1.75 x 1.75 x 2mm, b = 1000 s/mm^3, four images b = 0 s/mm^2, slice thickness = 2mm, 73 contiguous slices, FOV 224mm. On the Philips scanner, diffusion weighted images were in four runs of 16 non-colinear directions to give a total of 64 directions.

2.3 Volumetric MRI analyses

Volumetric analyses throughout this thesis were performed according to well established approaches (Cole et al., 2018a), using SPM 12 (UCL). T1 images were segmented into grey matter, white matter and CSF, and volumes of these tissue classes were calculated at baseline and follow-up scanning timepoints.

Voxelwise longitudinal analysis was performed using the SPM 12 longitudinal registration tool, in which baseline and follow-up images are iteratively registered to produce a mid-point temporal average image (Cole et al., 2018a, Ashburner and Ridgway, 2012). The transformation necessary to move from the baseline to follow-up scan image is encoded by the Jacobian determinant (JD) representing the contraction or expansion necessary to warp each voxel to the temporal average. The JD is weighted by the interval between the two scans to give an annualised rate of change (the 'JD atrophy rate'). Since there is a JD for each voxel, a map of the brain can be readily visualised and further analysed. Annualised atrophy rates were calculated voxelwise, by taking an average of the JD values for each tissue class, such as grey or white matter.

To facilitate group comparisons, registration to standard space such as Montreal Neurological Institute 152 was performed. Specifically, tissue specific JD maps were multiplied by the temporal average space T1 images for each subject. A study-specific template was then generated using the temporal average images of 20 randomly selected patients and controls using the SPM DARTEL non-linear registration (Diffeomorphic Anatomical Registration using Exponentiated Lie algebra) (Ashburner, 2007). Baseline, follow-up and individual average space JD rate images were normalised to group space using DARTEL before affine registration to MNI space, with normalisation of volume and smoothing using an 8mm gaussian kernel.

Scans were reported by experienced neuroradiologists with the aid of susceptibility weighted imaging (SWI) and fluid-attenuated inversion recovery (FLAIR) sequences. Individualised scan-specific lesion 'masks' were constructed in the ImSeg software comprehensively for patients whose data is reported in Chapters 4 and 5 (BioMedIA, Imperial College London).

2.4 Diffusion MRI analyses

Visual inspection of diffusion weighted images was performed prior to processing. And any scans with uncorrectable artefacts were excluded. Scans were then processed using the FMRIB software library (version 5.0.8) standard tract base spatial statistics (TBSS) pipeline including distortion and eddy correction (Kinnunen et al., 2011). Brain extraction was performed using either HD-BET (BIOAXTBI, Heidelberg University Hospital & Division of Medical Image Computing, German Cancer Research Center) (Isensee et al., 2019) or FSL BET. Tensor-based registration was performed using DTI-TK (Zhang et al., 2007). Tensor images were normalised by bootstrapping volumes to the IXI aging template and then refining a group template using affine followed by non-linear diffeomorphic registration (Zhang et al., 2007). Diffusion data were then registered to this template (group DTI-TK-space).

BIOAXTBI imaging data was processed in DTI-TK space, whereas in Chapter 4 data, an affine registration was performed to register the DTI-TK-space data to Montreal Neurological Institute (MNI) space using the FMRIB58 FA atlas where later analyses were performed. The mean fractional anisotropy (FA) images were thresholded at 0.2 to generate a white matter skeleton, and subject FA data projected onto the mean FA skeleton (FSL) (Smith et al., 2006). Tract level data, where used, were generated using the Johns Hopkins University white matter atlas. The cingulum, fornices and tapetum were not included in region of interest analyses due to poor sensitivity in these regions. Images were repeatedly inspected at the brain extraction, eddy current correction and tensor registration stages.

2.5 Statistics

Data were assessed for normality. Where appropriate, mean averages were used and ranges expressed using standard deviations, and parametric tests were performed for

group differences. Where the normality assumption was violated, data were described as median (IQR) and non-parametric tests performed. Standard t-tests were used for comparisons of normally distributed continuous data, and the non-parametric Wilcoxon test for non-normally distributed continuous variables. Paired t-tests, repeated measures ANOVA designs or linear mixed effects models, were used for longitudinal within-subject data, as appropriate. Owing to the data distribution, linear regressions on fluid biomarker concentrations were performed on $\log_{10}$ transformed data. Bonferroni multiple comparison corrections were performed to correct for the number of timepoints and groups assessed other than in analysis of plasma NfL where an a-priori hypothesis existed in Chapters 3 and 4.

Voxelwise tests were performed using threshold-free cluster enhancement (TFCE) multiple comparisons correction and are reported at a threshold significance level of $P<0.05$. Tests were two-sided unless otherwise stated. Tests are conducted using the general linear model with non-parametric permutation testing (n=10,000) in FSL Randomise (Winkler et al., 2014) and age, sex and head size included as a nuisance covariate unless otherwise stated. Where appropriate, focal lesions were incorporated voxelwise at the individual level into these tests to exclude the effect of focal damage.

3 Fluid biomarkers of axonal injury and neurodegeneration after acute moderate-severe TBI

Here I describe results of the BIO-AX-TBI prospective study of axonal injury after acute moderate-severe TBI. Fluid biomarker results, including blood biomarkers and invasive cerebral microdialysis are included within this Chapter, while neuroimaging results, cross-validation of axonal injury makers and outcome data are combined within Chapter 4. These data have been collected and prepared for publication with Mr Karl Zimmerman (KZ) who assisted with the study. KZ performed the diffusion analyses and comparison of marker concentrations relating to focal lesions. Dr Eyal Soreq assisted with modelling of fluid biomarker relationships between plasma and microdialysate. Content within these Chapters has been jointly written-up with KZ and submitted for publication in Science Translational Medicine.

3.1 Abstract

Fluid biomarker assays can now sensitively measure concentrations of neuroaxonal proteins in blood, with components such as NfL potentially providing a new diagnostic measure of injury. Patients after moderate-severe TBI were assessed in eight major trauma centres across Europe within the BIO-AX-TBI prospective study of axonal injury markers. Blood biomarkers were assessed twice within ten days post-TBI, and again subacutely at ten days to six weeks, and at six and twelve months. Invasive cerebral microdialysis was used to sample biomarker concentrations acutely post-injury aligned to frequent plasma sampling twelve hourly.

197 patients were recruited and assessed longitudinally. Axonal marker plasma NfL increased markedly after TBI, peaking subacutely, whereas plasma tau, UCH-L1, GFAP and S100B all peaked within a day of injury. Plasma NfL and GFAP remained elevated at one year. Eighteen patients underwent invasive cerebral microdialysis revealing highly elevated concentrations of NfL, tau, UCH-L1 and GFAP in brain extracellular fluid. Levels in microdialysate and plasma were highly correlated for NfL,

tau and UCH-L1, validating the peripheral sampling approach. Biomarker levels were significantly higher after TBI than in controls with extracranial injuries only.

In conclusion, axonal injury markers plasma NfL and tau were markedly raised post-injury. These related to biomarker changes within damaged white matter on microdialysis and were specific to head, rather than extracranial injuries. It is notable that at one year post-injury NfL and GFAP remained chronically elevated, suggesting the presence of chronic neurodegeneration after TBI.

3.2 Introduction

Long-term outcomes of TBI are frequently poor, with neurological problems common in survivors and increased risk of neurodegenerative disease and dementia (Maas et al., 2017, Livingston et al., 2020). Axonal injury is a potentially important contributor (Smith et al., 2003, Sidaros et al., 2008) but has been difficult to quantify clinically. Several proteins are potential biomarkers of axonal injury after TBI, such as the cytoskeletal proteins NfL, microtubule associated protein tau (tau), and more the more widely expressed ubiquitinating enzyme ubiquitin carboxyl-terminal hydrolase L1 (UCH-L1) (Wilkinson et al., 1989). Proteins whose expression is predominantly astroglial rather than neuronal, such as calcium binding protein S100 B (S100B), or glial fibrillary acidic protein (GFAP) may provide a surrogate readout of axonal damage by quantifying the inflammatory response and non-neuronal tissue damage.

NfL has shown considerable utility in the diagnosis, assessment of treatment response and prognosis across several neurological diseases (Gaetani et al., 2019). Advanced immunoassay techniques such as single molecule array (SiMoA) mean that ultra-low concentrations in venous blood can be accurately quantified, with evidence that such levels reliably reflect CSF concentration (Shahim et al., 2020a, Gisslén et al., 2016, Shahim et al., 2016a). Following moderate-severe TBI, NfL is elevated in blood and remains elevated for several years after injury in some patients (Scott et al., 2018, Shahim et al., 2020a). Given the mechanistic importance of traumatic axonal injury (TAI) in TBI, NfL assessment may be a particularly predictive of long-term outcome. However, its performance in this setting has so far been modest: for instance, serum levels within two weeks of injury predicted 12-month outcome, but with poorer

performance than GFAP, UCH-L1, tau, and S100B (Thelin et al., 2019). Likewise, NfL sampled within 1-15 days related to 6 to 12-month outcome but with limited accuracy (Shahim et al., 2016a, Al Nimer et al., 2015). Later measurement at a month post-injury predicted three-month outcomes but did not do so at later timepoints (Shahim et al., 2020a).

The optimal time to sample NfL after TBI is currently unclear, and its longitudinal dynamics have not been characterised in detail particularly in the subacute period. Levels appear to rise for in blood for at least several weeks post-injury, in contrast to other markers which typically peak within days (Thelin et al., 2017, Shahim et al., 2016a). There is a need to ascertain the time course of plasma NfL after moderate-severe TBI with a high temporal resolution. It may be that sampling which covers the peak captures more variance and realises maximal predictive performance in relation to outcomes.

Brain specificity is an important attribute of any proposed axonal injury biomarker given the occurrence of extracranial injuries in TBI patients. For example, it is known that S100B has substantial expression in adipose tissue as well as astrocytes which may limit its clinical use in the trauma setting (Anderson et al., 2001). NfL is expressed within axons of the peripheral, as well as central nervous system, motivating its consideration as a potential marker of disease activity in peripheral neuropathy (Sandelius et al., 2018). Comparison of NfL levels between patients with extracranial injuries only and TBI, is needed.

Invasive cerebral microdialysis using catheters permeable to neuroaxonal breakdown products provides a way to measure biomarker levels at the site of injury. In the context of axonal injury, this approach has previously been used to investigate tau changes post-TBI, and correlated with imaging evidence of damage. Indeed, high levels of tau on microdialysis early post-injury correlate with the extent of local axonal injury defined using DTI (Magnoni et al., 2015). It is also possible to quantify NfL using invasive microdialysis (Magnoni et al., 2012). Early work after severe injury has shown elevations in both peri-contusional and apparently normal-appearing white matter regions defined by CT scanning, which correlated with extracellular tau levels. However, NfL concentrations in microdialysate and peripheral venous samples have

not yet been compared. This is important for clinical interpretation of peripherally sampled concentrations, as a direct link between NfL levels in white matter tissue and blood has not been established.

In this analysis of the multicentre prospective BIO-AX-TBI study (NCT03534154) (Graham et al., 2020a), I investigate the temporal trajectories of fluid biomarkers of axonal injury following single moderate-severe TBI and compare plasma biomarker levels against brain extracellular fluid in human. The following specific hypotheses are assessed relation to NfL: (a) levels will increase significantly after TBI and this will be detectable in plasma; (b) changes in NfL will be specific to head injury versus extracranial injuries; (c) plasma NfL will correlate with levels in interstitial fluid on invasive cerebral microdialysis and (d) levels will be chronically raised late post-injury suggesting chronic neurodegeneration after TBI. **Secondary hypotheses were that: (f) Acute post-traumatic increases would be seen in related injury biomarkers tau, UCH-L1, GFAP and S100B; (g) these markers would normalise more rapidly than NfL; and (h) relate to clinical outcomes after injury.**

3.3 Methods

Inclusion criteria were patients aged 18-80 with moderate-severe TBI, defined by the Mayo classification (Malec et al., 2007) attending trauma wards in eight trauma centres across Europe (Careggi University Hospital, Lausanne University Hospital, Niguarda Hospital, Policlinico of Milan, Santa Chiara Hospital, St. Mary's Hospital, St George's University Hospital and the University Medical Centre Ljubljana). Exclusion criteria included pre-existing neurological disease, previous TBI requiring hospitalisation, significant drug or alcohol abuse, pregnancy and, for the MRI component, the presence of typical MRI contraindications such as ferrous implants.

Patients after TBI were approached and invited to take part. Individuals lacking capacity entered the study via an assent process involving the next of kin or personal/nominated consultee. If mental capacity was later re-gained, for example following extubation or resolution of post-traumatic amnesia, these participants were re-consented when able.

Common data elements were used to capture clinical and demographic information at the time of entry into the study, which were recorded in a standard electronic case report form. Blood biomarkers were assessed at all research sites on two occasions in the first ten days following injury. This timing was chosen to provide flexibility for recruitment across different participating sites (eg. while assent procedures were followed), while providing good temporal coverage of biomarker changes early post-injury. Patients were then followed-up at a subacute testing timepoint at 10 days to six weeks post-injury at seven study sites (patients from St Marys Hospital and St Georges University Hospital were followed-up at a single site – 'London'). Follow-up assessment at 10 days to six weeks (subacute) included blood, MRI and clinical assessment (Figure 7). Additional follow-up visits were performed at six months and 12 months post-injury with a functional assessment using the Glasgow Outcome Scale Extended (GOSE) (Wilson et al., 1998) alongside a universally collected outcome dataset. In a subgroup of study sites (Lausanne, Policlinico and London), the 6- and 12-month assessments included additional blood biomarker and neuroimaging assessment. Cerebral microdialysis was performed acutely at two study sites. In patients undergoing cerebral microdialysis, blood biomarker assessment was performed up to twice per 24 hours.

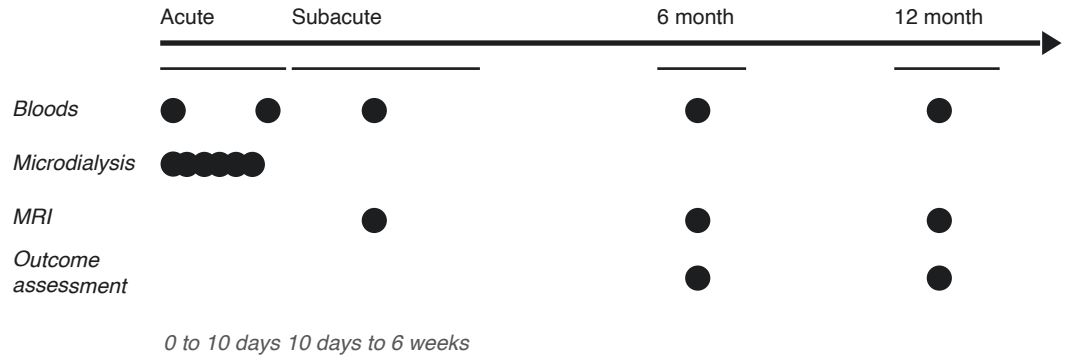

Figure 7. Assessment timepoints in BIO-AX-TBI

Clinical and demographic data are collected on enrolment to the study acutely after TBI. Blood samples were taken on two occasions within the first 10 days after injury. Invasive cerebral microdialysis is performed within the first two weeks of injury at Lausanne and Ljubljana research sites, with samples taken every four hours at most, with aligned plasma sampling a maximum of twice daily. At the subacute visit (10 days

to six weeks post-injury), patients undergo MRI scanning and blood biomarker assessment. In London, Policlinico and Lausanne MRI and blood biomarker assessments were performed at six and 12 months. Outcome data were collected at six and 12 months in all sites.

A group of patients with extracranial injuries requiring admission to the major trauma ward was recruited. These patients with non-TBI trauma (NTT) were screened to exclude any symptomatic possible TBI (as per Mayo classification of injury) or any known spinal injury. This group underwent blood biomarker assessment on two occasions within the first ten days post-injury. All NTT patients were assessed at the London site.

Healthy volunteers were recruited and underwent assessment at each of the study sites. The same exclusion criteria applied as per TBI patients, i.e. no history of significant previous head injury / major neurological or psychological problems. A single MRI brain was performed, and blood biomarker assessment undertaken, using the same protocols per TBI patients.

The sample size (minimum n=140) was determined based on an assessment of the contribution of DTI to prognostic modelling (type 1 error=0.05, power=0.95). Patient data were curated once the required number of patients with baseline DTI had been followed-up at 6 months (Graham et al., 2020a).

3.3.1 Statistical analyses

A linear mixed effects model was used to clarify the relationship between fluid biomarker concentrations in plasma and brain extracellular fluid. This required complete data sampled at aligned timepoints. Two values were identified missing in two patients (a GFAP result and UCH-L1 result). Using the markers surrounding the concentration and the time since injury as features vectors, these were imputed independently using a sklearn distance-based k nearest neighbours imputer (k=2). Brain extracellular fluid markers were up-sampled using a time-weighted interpolation model. Any missing paired observations in either the beginning or the end of the matching sequence were then removed. Finally, redundant brain observations were omitted to match the sampling frequency in the blood. In the model for each biomarker,

subject was a fixed effect, with main effects of log-transformed brain concentration, and an interaction of log-transformed brain concentration and time since injury, to predict log-transformed plasma concentration.

Multiple comparisons correction was performed using the Bonferroni method. Correction was performed for the number of groups (eg. patient/control/non-TBI trauma), the number of testing timepoints and number of biomarkers analysed. This was the case except for analyses relating to NfL specifically. This was the core focus of the experiment, with strong prior hypotheses, and was therefore not corrected for the number of biomarkers in the study (but was corrected for groups/timepoints).

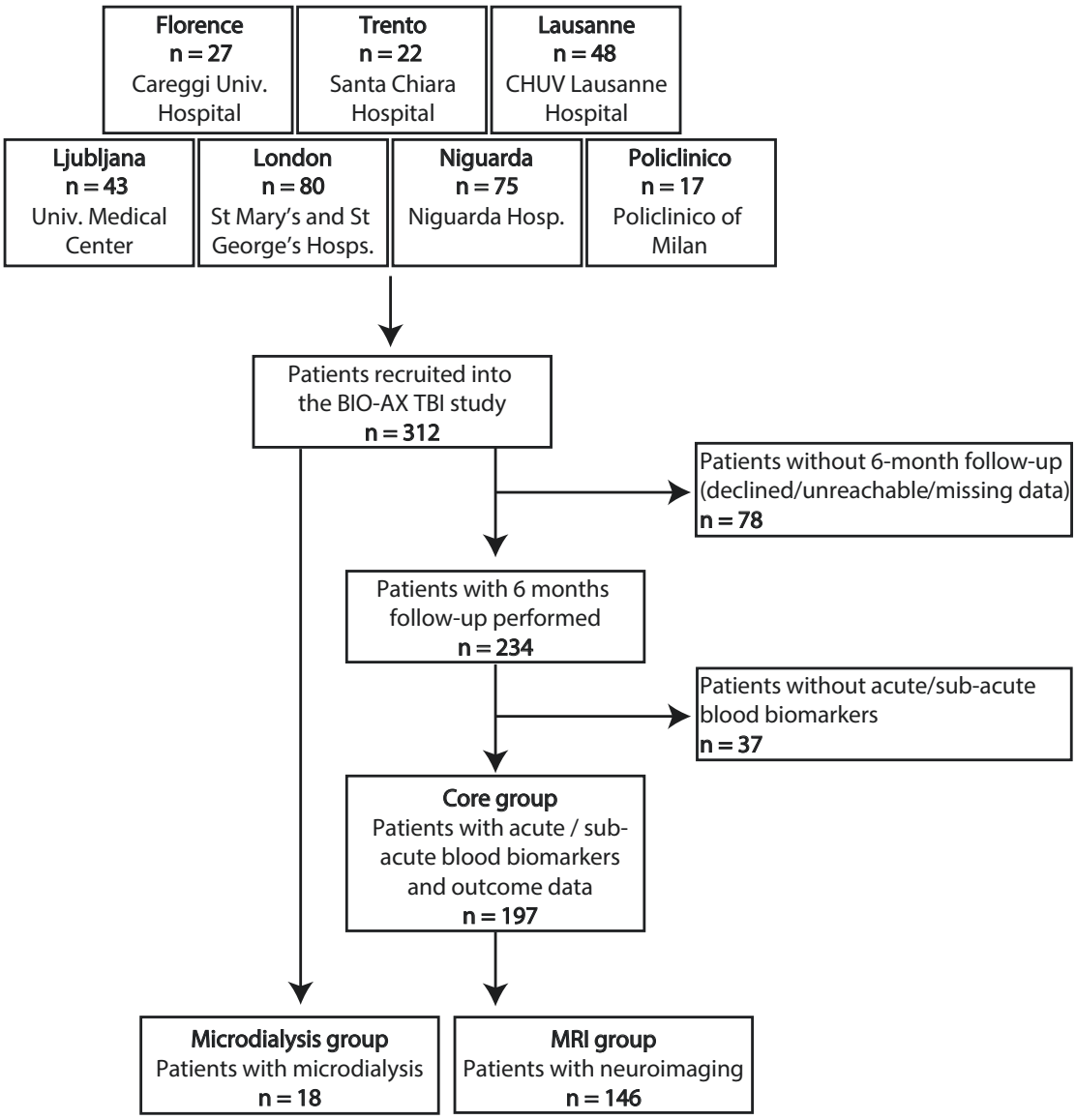

Figure 8. Study recruitment

Recruitment from different BIO-AX-TBI research sites and flow of patients through study, accounting for exclusions/loss to follow-up. Univ.=university; Hosp.=hospital

3.4 Results

3.4.1 Clinical features and outcomes

One hundred ninety-seven patients were recruited after moderate-severe TBI across eight European major trauma centres (Figure 8). Across the group, the median age at injury was 47 years (IQR 30) with 77% (152) male (Figure 9A, Table 4). 74% (146) of patients underwent MRI assessment, with a median age of 44 (IQR 30) of whom 80% (116) were male.

	TBI			**NTT**	**Healthy controls**	
	All	Imaging	Microdialysis	All	Cross sectional	Longitudinal
Total, N	197	146	18	25	128	30
Age, median (IQR)	47 (30)	44 (29.5)	34 (27.5)	41 (29)	39 (27)	39.9 (26.9)
Male, N (%)	152 (77.2)	116 (79.5)	14 (77.8)	23 (92.0)	78 (61)	21 (70)

Table 4. Demographics overview

TBI: traumatic brain injury; NTT: non-TBI trauma patients; HC: healthy controls. Of the eighteen participants in the microdialysis arm, five are also in the main group ('all').

Injuries were defined as high energy in 56% (110) of cases, comprising falls from more than three metres or collision at more than 30 km/h (Table 5). 91% (180) were accidental in cause, with 47% (93) road traffic collision related. Loss of consciousness at the time of injury was definite or suspected in 75% (147) of patients and 69% (136) experienced definite or suspected retrograde amnesia. The cohort included a range of severities within the moderate-severe classification, with pre-hospital Glasgow Coma Scale (GCS) 3 to 8 in 45% (89) (Figure 9C). Acute CT (Figure 9E) identified parenchymal contusions in 66% (130), subarachnoid haemorrhage in 60% (118), subdural haematoma in 57% (113) and extradural haematomas in 22% (44). Diffuse axonal injury was reported on CT in 18% (35). Raised intracranial pressure was present in 29% (58) of patients and was persistent or refractory to treatment in 16% (31). Neurosurgical evacuation of haematoma, or decompression was performed in 34% (66) of patients.

Clinical Characteristics		Injury details	
Initial GCS		Biophysics	
3 to 8	89 (45.2)	High energy TBI	110 (55.8)
9 to 13	55 (27.9)	Low energy TBI	68 (34.5)
14 to 15	51 (25.9)	Unknown	19 (9.6)
unknown	2 (1.0)	Injury cause	
Lowest GCS first 24h, median (IQR)	7.5 (8)	Accidental	180 (91.4)
Pupils in ED		Violence/assault	13 (6.6)
bilaterally reactive	138 (70.1)	Self-harm	1 (0.5)
unilaterally dilated/non-reactive	25 (12.7)	Other/unknown, N (%)	3 (1.5)
bilaterally dilated/nonreactive	1 (0.5)	Road traffic accident	93 (47)
unknown	34 (17.3)	Blunt weapon	4 (2.0)
Post-traumatic amnesia		Gunshot	1 (0.5)
definite/suspected	136 (69.0)	Crush	2 (1.0)
absent	14 (7.1)		
unknown	61 (31.0)		
Retrograde amnesia			
definite	57 (28.9)		
suspected	63 (32.0)		
absent	19 (9.6)		
unknown	58 (29.4)		

Table 5. Clinical and injury characteristics

GCS=Glasgow coma scale; High vs low energy cut-off: fall from more than three metres or collision at more than 30 km/h

During the study period, 7% (13) of patients died, at a median of 11 days post-injury. Functional outcomes were assessed over a year following injury (Figure 9F, Table 6). All 197 patients had a known outcome at six or 12 months post injury: specifically, the GOSE was available in 94% (185) at six months and 82% (161) at 12 months. At six months, 29% (58) of patients had made a good recovery, defined as a GOSE score of 7 or 8. Six individuals were in a vegetative state (GOSE 2) at six months, and were unchanged at 12 months. By 12 months post-injury 32% (62) of patients had a favourable outcome.

Glasgow Outcome Scale Extended			
6 months		12 months	
dead (1)	13 (6.6)	dead (1)	13 (6.6)
vegetative state (2)	6 (3.0)	vegetative state (2)	6 (3.0)
severe disability (3,4)	48 (24.4)	severe disability (3,4)	28 (14.2)
moderate disability (5,6)	60 (30.5)	moderate disability (5,6)	52 (26.4)
good recovery (7,8)	58 (29.4)	good recovery (7,8)	62 (31.5)
unknown	12 (6.1)	unknown	36 (18.3)

Table 6. Clinical outcomes at six and twelve months after TBI

Several different control populations were assessed. To measure the brain-specificity of blood biomarkers, 25 patients with non-TBI extracranial injuries requiring hospitalisation in a major trauma centre were recruited, with a median age at injury of 41 years (IQR 29) of whom 92% (23) were male. NTT patients had fluid biomarker assessment twice in the first ten days post-injury, aligned to the TBI group. The groups did not differ significantly in age or sex.

A cross-sectional healthy control group was recruited across all the sites, comprising 128 healthy individuals with a median age of 39 years (IQR 27) of whom 78% (61) were male. 95% (121) underwent MRI assessment and 75% (96) had a blood biomarker assessment. The cross-sectional healthy control group was slightly younger (W= 10784, P=0.028) and more female (X^2=9.10, df=1, P=0.003) than the TBI group. However, there was no significant age difference between TBI patients and healthy controls who underwent MRI. To contextualise MRI atrophy rate assessments after TBI within normal life-course change, 30 healthy controls with a median age of 40 years (IQR 27), of whom 70% (21) were male, were serially imaged twice. Neither sex nor age differed significantly between the main and longitudinal healthy control groups. Two longitudinal controls were also members of the cross-sectional control group.

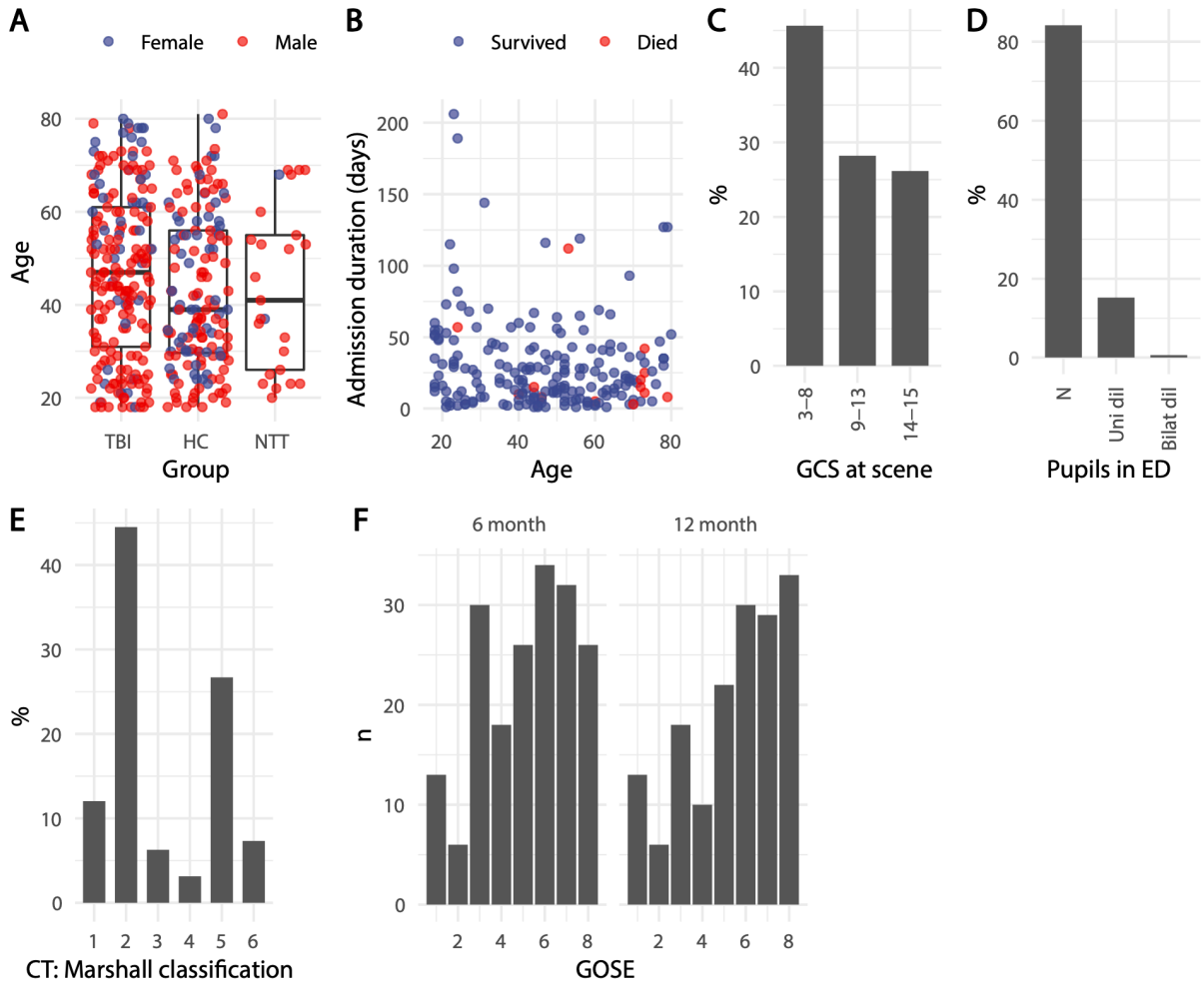

Figure 9. Demographics and clinical characteristics of patients after TBI

(A) Age and sex of patients after TBI, HCs and NTTs. (B) Relationship of age at injury to hospital admission duration following TBI, with outcome indicated by colour (red died, blue survived). (C) GCS at the scene of injury in TBI patients. (D) Pupillary assessment in emergency department (ED) in initial hospital: normal ('N'), unilaterally dilated ('uni dil') or bilaterally dilated ('bilat dil'). (E) Marshall classification of most severe CT scan in first day following injury. (F) Pathologies on MRI at subacute testing timepoint (ten days to six weeks post-injury. (G) GOSE outcome assessment in patients at six and twelve months after TBI.

3.4.2 NfL peaks subacutely and remains elevated in the chronic phase post-TBI

Plasma NfL was significantly elevated post-injury (Figure 10A, top, Table 7), increasing over time and peaking at the subacute timepoint (Figure 9B) median peak NfL 507.3 pg/ml, IQR 728.2). NfL remained elevated at six and 12 months post-injury compared with healthy controls (W=387/431 respectively, both P<0.001, Figure 10C). 85% (45/53) of TBI patients had abnormally high NfL at six months (i.e. > two standard deviations from the healthy control mean), as did 52% (13/25) at 12 months post-injury. Patients with raised NfL levels at six months post-injury had a higher preceding peak NfL than those with normal six-month NfL (W=19, P<0.001). However, no significant difference was seen in the magnitude of the peak NfL level in those with raised levels at 12 months. The rate of decline of NfL was assessed between the subacute visit and six months, and from the six to 12 month visit. Patients with raised NfL at six months had a significantly steeper decline in plasma concentration preceding, than those with normal six-month NfL (W=342,P<0.001); however, no significant difference was present across the six to 12 month interval. Age at injury was not a significant determinant of NfL level at six or 12 months on linear regression.

3.4.3 Early-phase biomarker peaks post-TBI

Furthermore, there were marked elevations in plasma total tau, serum S100B, plasma UCH-L1 and GFAP vs healthy controls. Maximal levels were reached within 24 hours (median peak for tau 7.0pg/ml; S100B 215.1pg/ml; UCH-L1 97.6pg/ml; GFAP 12,590.5 pg/ml). These biomarkers normalised following the subacute visit except for GFAP, which remained elevated at 12 months (W=691,P=0.041). 34% (18/53) of patients had raised GFAP at six months, as did 32% (8/25) at twelve months. The early peak was higher in patients with raised GFAP at six (W=173,P=0.007) but not at 12 months post-injury. The rate of reduction in plasma GFAP did not differ in patients with raised vs normal chronic levels, spanning either the subacute to six-month or six to 12 month intervals. Age at injury modestly contributed to the GFAP levels at six months (adjusted R^2 0.27, P<0.001) but not 12 months post-injury. Patients with raised plasma GFAP at six months were significantly older than those with normal levels (W=134, P=0.001).

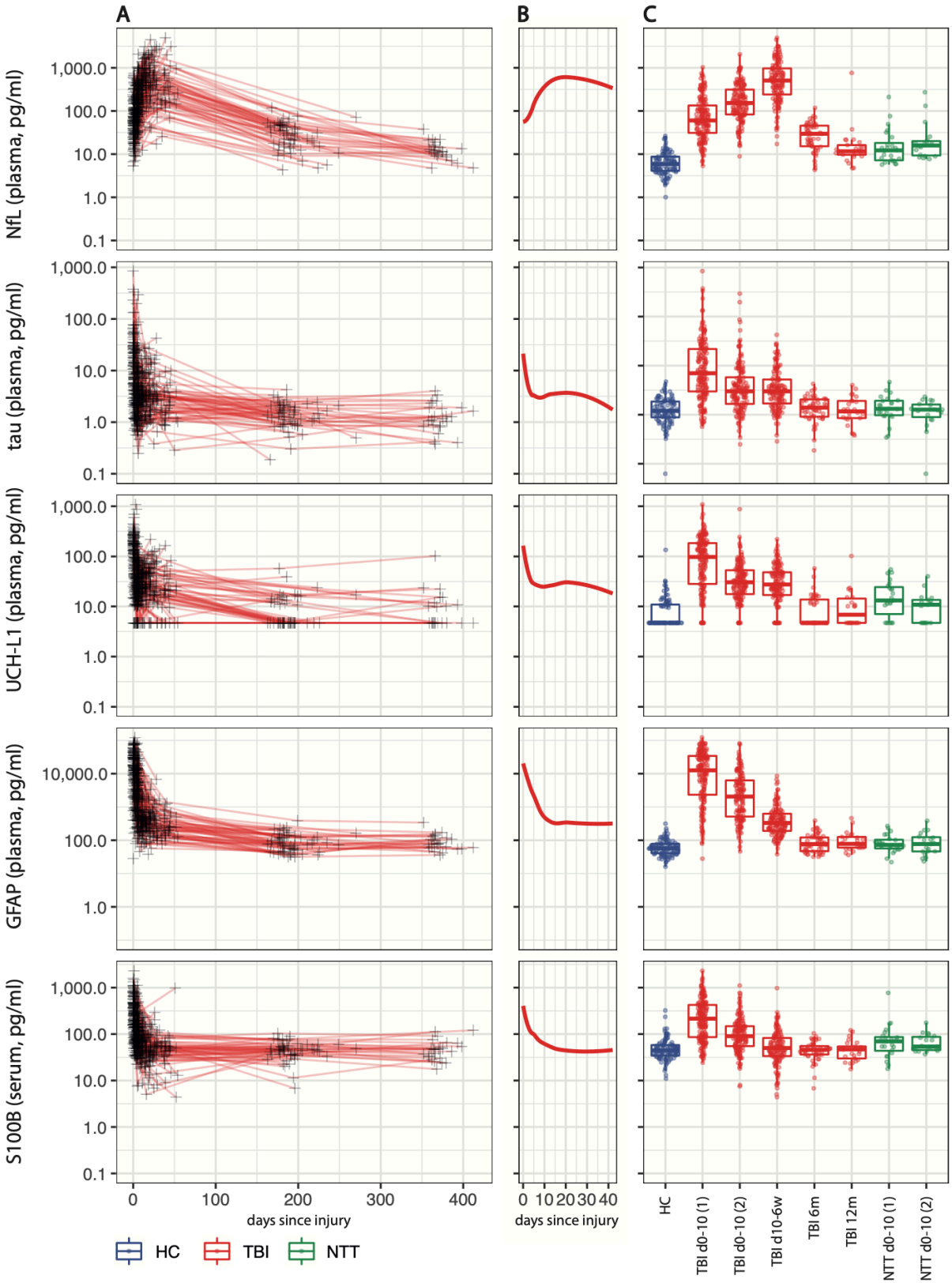

Figure 10. Blood biomarker trends in TBI, NTT and healthy controls

(A) Longitudinal biomarker trajectories. (B) Local polynomial (LOESS) regression curves modelling concentrations. (C) Group comparisons of biomarkers.

Biomarker		TBI					NTT		HC
		Acute 1	Acute 2	Subacute	6 m	12 m	V 1	V 2	Visit 1
	Days since TBI, md, (IQR)	1 (1)	5 (2)	20 (14)	188 (24)	376.5 (30.25)	2 (1.25)	4 (2)	-
NfL plasma	n	167	149	141	53	25	24	19	96
	conc, md, (IQR)	60.3 (103.6)	152.8 (230.7)	507.3 (728.2)	29.7 (30.5)	11.6 (6.5)	12.2 (11.3)	15.9 (10.7)	5.9 (4.6)
	P vs HC	<0.001	<0.001	<0.001	<0.001	<0.001	<0.001	<0.001	-
	W	352.00	42.00	6.00	387.00	431.00	459.00	209.00	
	P vs NTT	<0.001	<0.001	-	-	-			
	W	539	224	-	-	-	-	-	-
Tau plasma	n	168	150	141	53	25	24	19	96
	conc, md (IQR)	7.0 (18.8)	3.0 (4.1)	3.0 (3.5)	1.4 (1.1)	1.2 (1.1)	1.3 (1.0)	1.3 (0.7)	1.2 (1.0)
	P vs HC	<0.001	<0.001	<0.001	1.00	1.00	1.00	1.00	-
	W	1630.00	2708.00	2451.00	1777.00	1210.00	1039.00	944.00	
	P vs NTT	<0.001	<0.001	-	-	-	-	-	-
	W	466.00	469.00	-	-	-	-	-	
UCH-L1 plasma	n	168	150	141	47	22	23	17	91
	conc, md (IQR)	97.6 (155.9)	30.6 (35.4)	27.6 (31.4)	4.7 (9.0)	7.3 (9.7)	13.1 (17.0)	10.8 (8.8)	4.7 (6.2)
	P vs HC	<0.001	<0.001	<0.001	1.00	1.00	0.002	1.00	-
	W	1098.00	1341	1668	1986	834	534	577	
	P vs NTT	<0.001	<0.001	-	-	-	-	-	-
	W	595.00	367.00	-	-	-	-	-	
GFAP plasma	n	167	148	141	53	25	24	19	96
	conc, md (IQR)	12590.5 (31756.0)	2052.9 (5768.9)	330.2 (434.5)	76.7 (74.5)	77.8 (65.6)	72.7 (47.0)	77.0 (77.9)	57.0 (37.4)
	P vs HC	<0.001	<0.001	<0.001	0.081	0.041	0.66	1.00	-
		162.00	163.00	469.00	1773.00	691.00	792.00	741.00	
	P vs NTT	<0.001	<0.001	-	-	-	-	-	-
	W	69.00	67.00						
S100B serum	n	181	150	138	51	25	24	19	96
	conc, md (IQR)	215.1 (338.3)	90.2 (92.9)	50.2 (48.9)	45.8 (18.9)	46.8 (24.3)	69.7 (42.5)	53.9 (41.9)	44.5 (23.5)
	P vs HC	<0.001	<0.001	0.67	1.00	1.00	0.35	0.29	-
	W	1783.00	3166.00	5951.00	2456.00	1298.00	757.00	560.00	
	P vs NTT	<0.001	0.56	-	-	-	-	-	-
	W	862.00	938.00						

Table 7. Blood biomarkers longitudinally in patients, and healthy controls

Acute 1 / V1 : days 0-10; Acute 2 / V2: days 0-10 post-trauma; subacute: ten days to six weeks post-injury. NTT: non-TBI trauma. HC: healthy control.

There was a small difference in age between TBI patients and healthy controls however a sensitivity analysis using a closely age-matched subgroup showed (n=96 HCs) showed that this had no significant effect on the results (Table 8).

	NfL (plasma)		**Tau (plasma)**		**UCH-L1 (plasma)**		**GFAP (plasma)**		**S100B (serum)**	
	P vs HC	W	P vs HC	W	P vs HC	W	P vs HC	W	P vs HC	W
TBI										
Acute 1	0.000	359	0.000	197	0.000	724	0.000	124	0.000	1453
Acute 2	0.000	38	0.000	1898	0.000	830	0.000	128	0.000	2525
Subacute	0.000	5	0.000	1705	0.000	1098	0.000	370	1.000	4573
6 month	0.000	348	1.000	1625	1.000	1474	1.000	1460	1.000	1890
1 year	0.000	395	1.000	887	1.000	618	0.598	591	1.000	985
NTT										
Acute 1	0.003	424	1.000	24	0.001	377	1.000	663	1.000	599
Acute 2	0.000	193	1.000	678	1.000	442	1.000	589	1.000	448

Table 8. Blood biomarker concentrations - age-related sensitivity analysis

Analysis with sub-group of 96 healthy controls more closely age matched to TBI patients. Acute 1: first testing timepoint in days 0-10 post-trauma; Acute 2: second testing timepoint in days 0-10 post-trauma; subacute: ten days to six weeks post-injury. NTT: non-TBI trauma. HC: healthy control.

3.4.4 Diffuse vs focal damage, and biomarkers

The relationships of fluid biomarkers to focal versus diffuse injuries was assessed. Using the system of Marshall grading on CT, taking the worst CT scan within 24 hours of injury, patients were split into those with Marshall grade I (n=23) versus Marshall grades II-VI (n=168). The latter group includes patients with mixed focal/diffuse injury (n=168), whereas only diffuse injuries are in the first group (n=23). Those with focal injuries had higher peak concentrations of UCH-L1 (W=910, P=0.033), S100B (W=776, P=0.003) and GFAP (W=779,P=0.005), but no significant difference in levels of tau and NfL versus the diffuse injury only group.

3.4.5 Biomarkers in patients with extracranial injury only

Twenty-five trauma patients with no history of recent head injury (non-TBI trauma, 'NTT') underwent acute blood biomarker assessment on a maximum of two occasions within 10 days of injury (see Table 9). Compared with healthy controls, NTT patients had significantly raised plasma NfL and UCH-L1, but not of plasma total tau, GFAP or serum S100B. Significant differences were present at both acute testing timepoints in the case of NfL.

Compared with TBI patients, blood biomarker concentrations were lower in NTTs for all blood biomarkers at both the acute testing timepoints, apart from S100B where concentrations were lower in NTTs only for the first timepoint (all P values <0.001).

Age	Sex	Mechanism	Energy	Description	Admission duration (days)	Management
30	Male	RTA	Low	Tibia & fibula fracture	14	Operative
52	Male	RTA	Low	Multiple rib fractures and clavicular fracture	2	Conservative
37	Female	Fall	High	Lumbar vertebral and calcaneal fractures	11	Operative
25	Male	Fall	Low	Tibia & fibula fracture	1	Operative
41	Male	RTA	High	Multiple rib fractures with haemopneumothorax and splenic laceration	4	Operative
53	Male	RTA	Low	Multiple rib fractures with haemopneumothorax; pulmonary contusion; scapular fracture;	7	Conservative
20	Male	Penetrating	-	Haemopneumothorax; pulmonary laceration; splenic laceration; renal injury; multiple rib fractures	7	Operative
69	Male	Fall	Low	Multiple rib fractures with haemopneumothorax; scapular fracture, pelvic fractures; thoracic spinal process fracture; sacral canal fracture	12	Operative
69	Male	RTA	Low	Hip and metatarsal fractures	9	Operative
46	Male	Fall	Low	Hepatic haematoma, rib fracture	2	Conservative
26	Male	Penetrating	-	Penetrating knee wound with vascular injury	5	Operative
23	Male	Fall	Low	Liver laceration; multiple rib fractures; splenic laceration; lumbar spinal transverse process fracture; pulmonary contusions	2	Conservative
53	Male	Fall	Low	Multiple rib fractures with haemopneumothorax; scapular fracture, pelvic fractures; thoracic spinal process fracture; sacral canal fracture	7	Conservative
55	Male	RTA	Low	Tibia & fibula fracture	8	Operative
36	Male	RTA	Low	Tibia & fibula fracture; soft tissue injury	16	Operative
33	Male	Fall	High	Multiple rib fractures with pneumothorax	3	Conservative
54	Male	Penetrating	-	Bilateral deep ankle wounds	6	Operative
68	Female	Fall	Low	Tibia & fibula fracture	5	Operative
69	Male	Fall	Low	Hip fracture	26	Operative
23	Male	Crush	-	Femoral fracture; soft tissue injury	2	Operative
68	Male	Fall	Low	Multiple rib fractures, humeral fracture	16	Conservative
37	Male	RTA	Low	Rib fractures with pneumothorax, humeral fracture, spinal endplate fractures	10	Operative
22	Male	RTA	Low	Tibia & fibula fracture	11	Operative
23	Male	Penetrating	-	Neck wound	5	Operative
60	Male	Fall	Low	Tibia & fibula fracture	11	Operative

Table 9. Non-TBI trauma patient characteristics

Injury description for extracranial injury-only trauma patients. RTA: road traffic accident; low energy defined as impact <30kmph or fall from less than 3m.

3.4.6 Evidence of axonal injury within the brain on microdialysis assessment

18 patients underwent invasive cerebral microdialysis assessment within the first 10 days of injury, allowing the validation of blood biomarker levels against samples from the microenvironment deep within the white matter (Table 10). These patients had a median age of 34 years (IQR 27.5) and were 78% male (14).

Age	Sex	GCS	ICU duration (days)	CT Marshall	Outcome (1 month)	Catheter location
54	Male	3 – 8	5	III	Survived	F. R.
31	Male	14 – 15	17	III	Survived	F. L.
25	Male	3 – 8	6	VI	Survived	F. L.
20	Male	3 – 8	23	III	Survived	F. R.
31	Male	3 – 8	16	VI	Survived	F. R.
32	Male	3 – 8	21	II	Survived	F. R.
72	Male	3 – 8	13	VI	Died	F. R.
65	Male	3 – 8	16	VI	Died	F. R.
36	Female	3 – 8	9	VI	Survived	F. R.
19	Female	3 – 8	16	VI	Died	F. L.
54	Male	3 – 8	23	II	Survived	F. R.
47	Male	3 – 8	24	V	Died	F. R.
34	Male	3 – 8	18	VI	Survived	F. R.
22	Female	3 – 8	5	II	Survived	F. R.
24	Male	3 – 8	7	III	Survived	F. R.
61	Male	3 – 8	28	III	Survived	F. R.
34	Male	9 – 13	42	IV	Survived	F. R.
56	Female	14 – 15	23	VI	Died	F. R.

Table 10. Characteristics of patients undergoing cerebral microdialysis after TBI

GCS refers to prehospital Glasgow Coma Scale. F.R. = front right; F.L. = front left.

Microdialysis catheters were inserted into uninjured-appearing frontal white matter on the right in 83% (15) and on the left side in 17% (3), to sample from white matter affected by diffuse, rather than focal injury as per Figure 11A showing indicative catheter placement on CT. Sampling was initiated rapidly, a median of 0.15 (IQR 0.3)

days post-injury and continued for a median of 144 (IQR 114) hours in total. Reflecting the severity of injury, this group had a high mortality rate of 28% (five patients) within a month of injury. Indicating the presence of DAI in this group, FA values relative to controls were significantly reduced within the whole white matter (W=339, P<0.001) and were significantly negative in white matter around the catheter insertion site (t=-3.92, P=0.002).

Concentrations of NfL, total tau, UCH-L1 and GFAP were quantified in microdialysate and plasma (Figure 11B). Concentrations were significantly higher in microdialysate than plasma across the acute sampling period (i.e. 0-10 days) (all P<0.001, Table 11). Median concentrations of NfL, tau and UCH-L1 were ~100x higher in microdialysate than plasma, in contrast to GFAP which was only ~4x higher in brain.

Biomarker	**Location**	**Biomarker concentration (pg/ml)**				**MD : plasma**	**Statistics** (MD vs plasma)	
		minimum	maximum	median	IQR	(median)	W	P
NfL	MD	86.7	163224.0	10059.0	16040.0	106.6	108017	< 0.001
	Plasma	17.8	910.0	94.4	167.0			
Tau	MD	4.5	61597.0	488.0	1730.0	105.6	107992	< 0.001
	Plasma	0.6	149.0	4.6	6.5			
UCH-L1	MD	1106.0	503373.0	3849.0	10412.0	105.5	108035	< 0.001
	Plasma	1.8	299.0	36.5	50.3			
GFAP	MD	178.0	3484315.0	19678.0	77501.0	4.3	77669	< 0.001
	Plasma	89.9	138100.0	4601.0	13416.0			

Table 11. Biomarker concentrations in plasma and microdialysate

MD = microdialysate. MD:plasma ratio refers to ratio of median levels.

A linear mixed effects model was used to assess the relationship of brain biomarker concentrations to plasma biomarker levels, accounting for time since injury and repeated measures in individual patients (see individual trajectories plotted in Figure 12). This showed a strong relationship between for NfL (t=3.3, AIC=-128.4, P=0.001) as well as total tau (t=2.9, AIC=57.8, P=0.003) and UCH-L1 (t=4.8, AIC=19.7, P<0.001) but not GFAP (P=0.76).

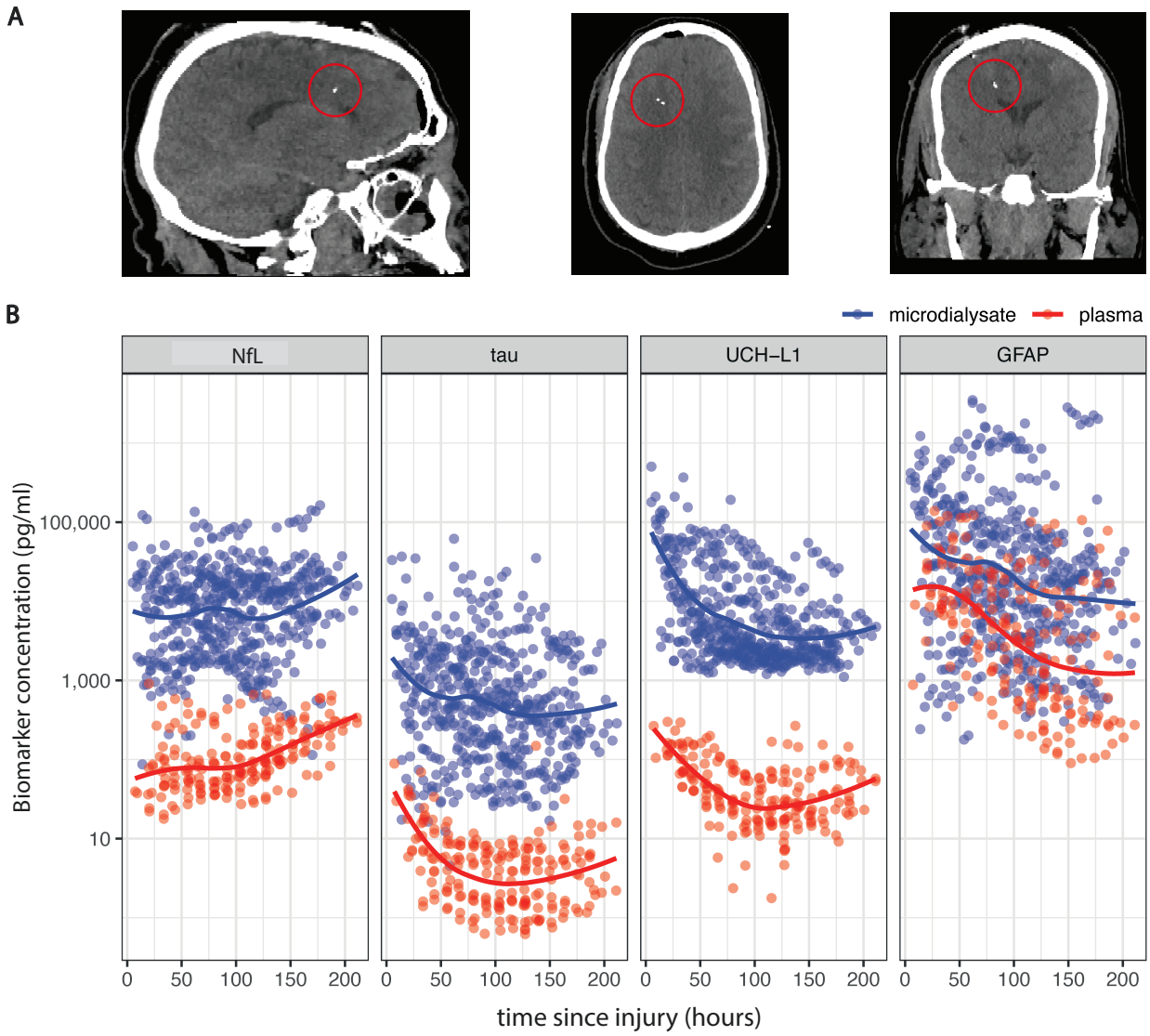

Figure 11. Cerebral microdialysis evidence of axonal injury acutely following TBI

(A) Sagittal, axial and coronal CT images showing indicative placement of catheter in deep white matter for cerebral microdialysis (B) Longitudinal trajectories of GFAP, NfL, tau and UCH-L1, measured throughout the acute phase (first 10 days) following traumatic brain injury in cerebral microdialysate across n=18 patients.

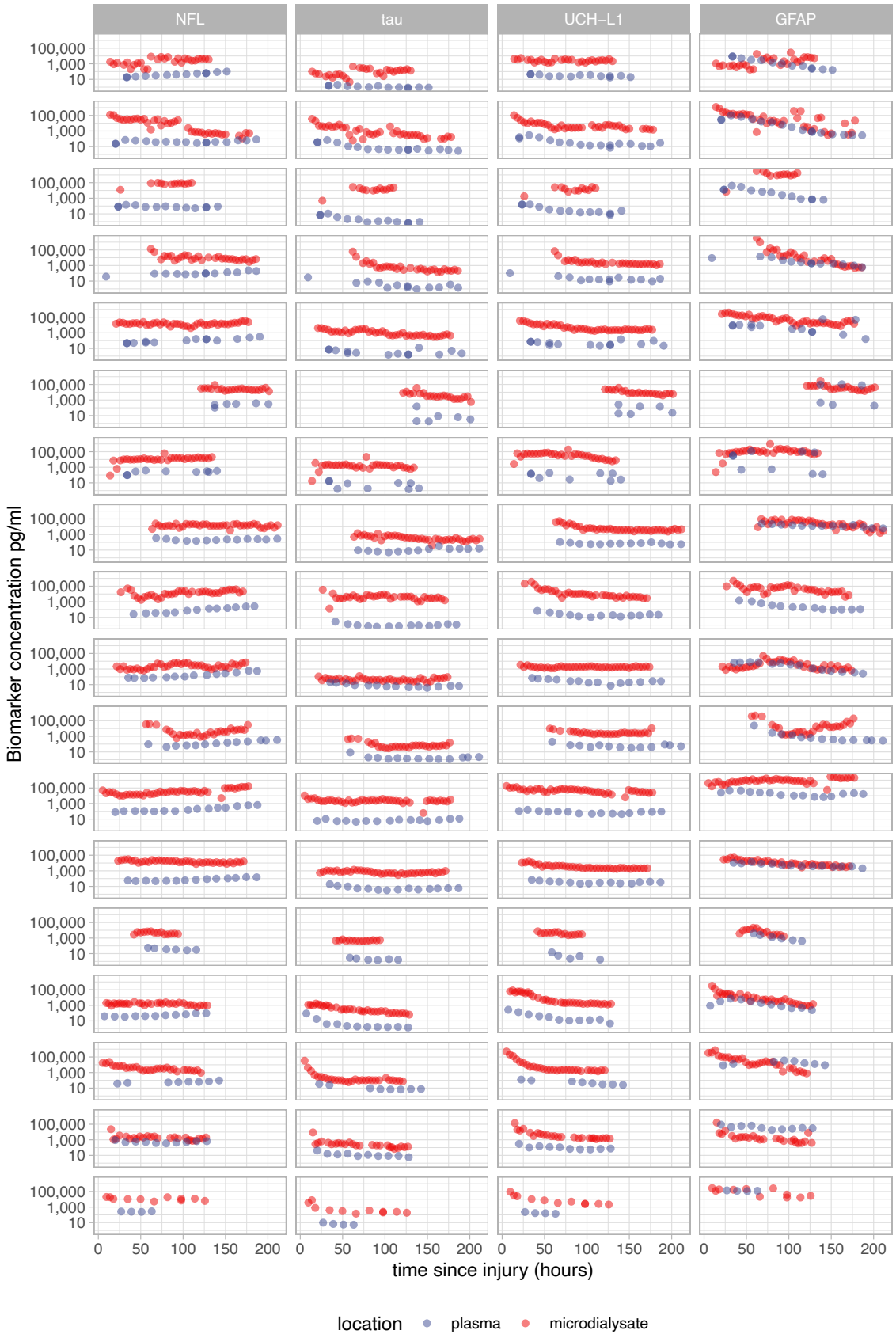

Figure 12. Microdialysis: individual patient biomarker trajectories

Biomarker concentration in microdialysate/plasma. Each row represents an individual.

3.5 Discussion

This investigation provides a detailed longitudinal description of axonal injury quantified by fluid biomarkers after moderate-severe TBI. The data show that plasma NfL is a sensitive marker of TBI with a unique time course compared to other fluid injury biomarkers. While axonal marker tau peaked in plasma within days of injury, NfL levels were maximal 10 days to six weeks after TBI indicating a clinically useful opportunity subacutely to assess patients. Concentrations were highly correlated in plasma and white matter interstitial fluid taken using invasive cerebral microdialysis.

NfL is a type IV intermediate filament which constitutes a core part of the axonal backbone, in conjunction with higher molecular weight neurofilaments medium and heavy, and other cytoplasmic proteins α-internexin and peripherin (Gafson et al., 2020, Hoffman et al., 1987). NfL has previously been studied in a range of conditions in which axonal degeneration is a feature (Gaetani et al., 2019). High expression of NfL is seen within the long myelinated axons of the cerebral deep white matter (Schlaepfer and Lynch, 1977), regions which are particularly susceptible to diffuse axonal injury arising the shearing forces of rotational acceleration during head injury (Donat et al., 2021).

Previous work in TBI has shown that plasma and CSF NfL increase after TBI, with utility in outcome prediction after single moderate-severe injury (Thelin et al., 2019, Shahim et al., 2016a, Al Nimer et al., 2015, Shahim et al., 2020a). Due to the high sensitivity of NfL changes in head injury, NfL has a role in identifying clinically significant mild TBI, for instance in impact sports (Zetterberg et al., 2006, Neselius et al., 2012). Furthermore, NfL may be of use late after injury to measure progressive neurodegeneration (Shahim et al., 2020a, Scott et al., 2018, Bernick et al., 2020, Shahim et al., 2016b), with blood levels in the chronic phase correlated to longitudinal atrophy rates in white matter (Scott et al., 2018, Shahim et al., 2020a). These characteristics may expedite trials of disease modifying treatments after TBI by identifying patients at highest neurodegenerative risk to reduce sample sizes. Akin to brain atrophy rates, there is potential utility as a surrogate trial endpoint (Cash et al., 2014, Graham and Sharp, 2019). However, the specificity of plasma NfL as a marker of TAI has not been established.

Patients with no history of TBI, but extracranial injuries alone (NTT, non-TBI trauma), had increased concentrations of plasma NFL within 10 days of injury, but to a far lesser extent than TBI patients, where these were five to 15 times higher, with a larger difference developing with increasing time since injury over the first two weeks. This increase in non-TBI patients might indicate that TBI had occurred but was not apparent on our clinical assessment. However, stringent criteria were used to exclude even mild injuries. Vertebral fractures were present in some non-TBI patients, and though there was no evidence of spinal cord injury in any case, this cannot be excluded as a possible NfL source (Kuhle et al., 2015). Furthermore, significant peripheral nerve injuries were not felt to be likely in the NTT group, who were screened for any weakness/sensory disturbance as possible signs of TBI, but this is a possible source of NfL (Sandelius et al., 2018, Kim et al., 2020). While previous work showed that *additional* extracranial injuries alongside TBI did not change the incremental value of NfL in predicting CT changes in TBI, biomarker changes in non-TBI patients had not specifically been assessed (Czeiter et al., 2020).

NfL concentrations were raised at six and 12 months post-injury. It is striking to note that in those individuals with pathologically raised NfL a year post-injury, there was no evidence of a higher preceding peak level, or steeper decline in concentration in the run-up to sampling at 12 months. This suggests that elevated concentrations at a year are not simply a feature of greater initial injury severity, and support the hypothesis that in a proportion of individuals, axonal injury triggers a progressive neurodegenerative process. Chronic elevation of GFAP was also seen, as has been reported by others in the setting of moderate-severe TBI, suggesting chronic astrogliosis/glial activation in the context of ongoing degeneration (Shahim et al., 2020b).

This investigation shows that microdialysate taken directly from damaged white matter contains very high levels of NfL, with concentrations around 100 times higher than plasma. Diffusion imaging performed subsequently shows significantly reduced FA in the region sampled by the catheter, confirming the presence of TAI. There is a strong correlation between plasma and microdialysate NfL concentrations, suggesting that plasma NfL reflects the release of NfL in damaged white matter. For the first time the

Simoa platform was used to perform ultrasensitive analysis of microdialysate. This means that using a very small volume of fluid, concentrations in brain extracellular fluid can be ascertained simultaneously across NfL, UCH-L1, GFAP and S100B. Previously such analyses were impossible due to the large volumes of fluid required. Further, this is the first simultaneous comparison of plasma and microdialysate injury biomarker concentrations sampled over the same period. This was facilitated by the novel use of Dextran 500 perfusion fluid, a commercially available standardised approach to improving protein recovery, which means data from multiple research sites can be combined, increasing statistical power.

GFAP concentrations have not previously been reported in cerebral microdialysate studies. The difference in concentrations between plasma and microdialysate was strikingly smaller than for other markers, reflecting very raised plasma GFAP. This may reflect the role of astroglial endfeet within the BBB, whose traumatic disruption could lead to large GFAP release into blood. A complex interaction between glial injury and BBB permeability may account for the lack of correlation between the two compartments over time.

One potential limitation is that there can be some variability in the Simoa assay between different reagents. To minimise the chance of introducing noise into the comparison of biomarkers in blood and cerebral microdialysate, these tests were run on the Simoa platform in one batch with a single set of reagents.

In conclusion, plasma NfL is a sensitive marker of TBI peaking around 20 days after moderate-severe TBI and remains raised at a year post-injury. I show that concentrations increase after extracranial injuries, but to a far lesser extent than TBI. Trends are strikingly different for the axonal marker tau which peaked within 24 hours of injury, alongside UCH-L1, S100B and GFAP. These findings suggest that plasma biomarker assessment including tau/NfL, depending on the time since injury, provides a feasible approach to assess axonal damage, with peripheral assessment providing a valid measure of dynamics within the brain as confirmed by invasive cerebral microdialysis.

4 Neuroimaging evidence of axonal injury and neurodegeneration after acute TBI, and relationship to fluid biomarkers and outcomes

In this Chapter I extend the fluid biomarker results within Chapter 3 with neuroimaging results of the BIO-AX-TBI study, reporting and relating neuroimaging changes to fluid biomarkers, and outcomes. These data have been collected and prepared for publication with Mr Karl Zimmerman (KZ) who assisted with the study. KZ performed the diffusion analyses and comparison of marker concentrations relating to focal lesions. Content within these Chapters has been jointly written-up with KZ and submitted for publication in Science Translational Medicine.

4.1 Abstract

Diffusion tensor imaging and volumetric MRI were acquired longitudinally in participants in the BIO-AX-TBI study (see Chapter 3 for demographic, injury and fluid biomarker results). Focal post-traumatic lesions were identified and excluded voxelwise from analyses of diffuse traumatic axonal injury pathologies. Individualised measures of brain volume change were generated, revealing increased rates of brain atrophy in grey matter subacutely to six months, and within white matter in the chronic phase from six to twelve months post-TBI. Grey matter atrophy was predicted by peak plasma tau, whereas late white matter atrophy was predicted by peak NfL. DTI evidenced widespread axonal injury after TBI, which was highly correlated with plasma NfL levels at the subacute timepoint. Factor analysis of injury biomarkers showed that peak NfL and white matter fractional anisotropy loaded highly on the same factor, suggesting that these measure the same biological substrate. NfL had strong predictive performance in relation to functional GOSE outcomes at six and twelve months post-injury. Overall, these data suggest that plasma NfL is a feasible and clinically informative measure of axonal injury following moderate-severe TBI, which outcomes and progressive white matter neurodegeneration, and which is particularly

amenable to assessment in the subacute phase where symptoms and injury diagnosis may be highly uncertain.

4.2 Introduction

Traumatic axonal injury (TAI) is not sensitively identified by traditional neuroimaging measures such as CT or conventional MRI. Indeed, even measures such as the presence of microbleeds on blood sensitive sequences such as SWI are more likely indicators of diffuse vascular injury rather than DAI (Griffin et al., 2019). Imaging approaches may be complementary to fluid biomarker measures of DAI discussed in Chapter 3.

Diffusion tensor imaging (DTI) provides measures of axonal integrity such as fractional anisotropy (FA). This measure is sensitive to alterations in tissue microstructure and hence can reflect local associations of injury such as demyelination, alongside reduced axonal density or changes in diameter (Jones et al., 2013). FA is validated against tissue evidence of reduced axonal density after experimental injury (Mac Donald et al., 2007a), and helps predict long-term clinical outcome after TBI (Sidaros et al., 2008). A relationship of plasma NfL to FA has previously been suggested, and confirming this correlation would strengthen the case for axonal integrity assessment using plasma NfL alone (Shahim et al., 2020a).

Progressive neurodegeneration can be sensitively measured using serial volumetric T1 MRI after trauma (Cole et al., 2018a) which provides a further means to test whether axonal damage predicts subsequent brain volume. Such a correlation, between NfL and atrophy, was not evident in samples taken early post-injury in previous work (Shahim et al., 2020a). However, this study focused on a limited number of pre-defined brain regions, highlights the need for a broader, spatially unrestricted longitudinal description of NfL in the context of brain structural change. Without a-priori assumptions about where damage may occur, this may be even more sensitive to relationships between neuroimaging change and NfL. Relating NfL and atrophy rates allows a dose-response relationship of damage and progressive atrophy to be tested, however moving beyond this to a voxelwise measure of TAI, the spatial pattern of volume loss can be related to the spatial pattern of injury providing mechanistic detail.

In this chapter I assess how these measures relate to radiological measures of axonal injury and clinical outcomes, testing the following hypotheses: (a) plasma NfL will correlate highly with other axonal injury measures including reduced FA on DTI; (b) plasma NfL will predict clinical outcomes at 6 and 12 months post-injury; and (c) plasma NfL will predict neurodegeneration in white matter measured using serial volumetric MRI.

4.3 Methods

4.3.1 Human MRI acquisition

Participants in all sites had a high resolution structural T1 MPRAGE, T2 fluid-attenuated inversion recovery (FLAIR), susceptibility-weighted imaging (SWI) and diffusion tensor imaging (DTI). DTI sequences were aligned at each site and acquired in 64 directions with an isotropic voxel size of 2mm^3, b = 1000 s/mm^3, four images with b = 0 s/mm^2 except in a single site (Santa Chiara Hospital – 'Trento') where only 60 directions were acquired and with a 1mm x 2mm x 2mm voxelwise (Table 12.).

Site	**Niguarda**	**Lausanne**	**Ljubljana**	**Florence**	**Milan**	**Trento**
Scanner						
manufacturer	Philips	Siemens	Siemens	Siemens	Philips	GE
model	Achieva	Skyra Fit	Trio Tim	Aera	Achieva	Optima
field strength	1.5T	3T	3T	1.5T	3T	1.5T
Voxel size (mm)						
MPRAGE	1x1x1	1x1x1	1x1x1	1x1x1	1x1x1	0.5x0.5x1
DTI	2x2x2	2x2x2	2x2x2	2x2x2	2x2x2	1x2x2
DTI parameters						
receiver coil channels	8	64	32	20	32	8
directions	64	64	64	64	64	60
b-value	1000	1000	1000	1000	1000	1000

Table 12. European scanner details

Advanced neuroimaging acquisition across European study sites. London scanner details are as per general methods described in Chapter 2.

Two travelling volunteers were scanned at each site and oversaw harmonisation of scanning protocols. FA measures per white matter region of interest were all under 5% coefficient of variation (Palacios et al., 2017). A physical N-tridecane phantom was scanned repeatedly at each site to ensure acquisition quality throughout the study. Further details for scanners and acquisition parameters can be found in the study protocol (Graham et al., 2020a). Patients and controls were scanned using the same protocols within each centre and this protocol was kept consistent for the duration of the study.

Structural MRI scans from all study sites were reviewed by a team of neuroradiologists in London and reported using an electronic case report forms adapted from the National Institute of Neurological Disorders and Stroke (NINDS) TBI Imaging common data elements, providing a gold standard readout of imaging abnormalities over time.

4.3.2 MRI analysis

Focal lesions identified were manually segmented using an in-house tool “ImSeg” (BioMedIA, Imperial College London). FLAIR sequences were co-registered to native space T1 scans and lesion masks were manually created. This was performed at each scanner session for each individual. Two neuroimaging researchers undertook the segmentations, defining acute contusions, oedema, chronic contusions, subarachnoid blood, subdural and extradural haematomas. The two individuals underwent a training period whereby both produced segmentations on the same ~ 10 studies, to help standardise approaches to lesion boundaries.

Lesion masks were then registered to MNI152 standard space and DTI-TK standard space using affine linear registration in FSL. An individual’s lesions were incorporated into the voxelwise analysis by including the lesioned voxels as voxelwise regressors in the general linear model. In analyses of atrophy rates, a conservative approach was selected, such that the lesion mask for the first of the scan pair was used on the temporal average-space image. Lesion mask data are presented in Figure 13. Data were analysed using approaches described in Chapter 2.

4.3.3 DTI processing and normalisation across centres

Quality control procedures were harmonised within the BIO-AX-TBI study across sites, performed at the London centre. The mean Pearson correlation coefficient of the neighbouring diffusion weighted images and slice-wise signal dropout for each slice was calculated. All data passed the criteria of baseline and follow-up having no difference in mean Pearson correlation coefficient > 0.1, while two scans from the same participant were removed due to signal dropout being higher than 0.1% of the total slice number (Yeh et al., 2019). In total twelve diffusion scans were removed due to failing quality control checks. Images were normalised across centres to account for site differences via a z-scoring approach.

Raw FA maps in patients were normalised in a voxelwise manner to the locally recruited age-matched healthy controls. The following equation was used at each voxel:

$$zFA_{patient} = (\text{ raw } FA_{patient} - \text{mean } FA_{control\ group}) / \text{standard deviation } FA_{control\ group}$$

This generates an individualised, normalised z-scored FA map for each patient which can then be compared between different sites.

Mean z-scored FA was calculated for the whole white matter skeleton, and to account for any potential issues with scan quality diminishing at the boundaries, zFA was also sampled within the corpus callosum, a large, robust, central tract, while excluding sampling in areas with lesions. Previous work has shown that this region is extremely sensitive to the presence of traumatic damage (Jolly et al., 2021) and would facilitate later comparisons with animal modelling considered at the study design stage (Donat et al., 2021).

4.3.4 Statistical analyses

The approach to multiple comparisons corrections is as described in Chapter 3 (ie. accounting for number of groups, timepoints, and other than in the case of NfL, the number of biomarkers). Prediction of atrophy rates in patients was performed only for those tissue classes and testing timepoints where this was abnormal: ie. grey matter atrophy over the subacute-6 month interval, and white matter atrophy from 6 to 12

months. Given the potential clinical utility of using *early* biomarkers to predict outcomes, predictions were performed using the peak fluid biomarker levels within 6 weeks of injury (capturing greatest variance and coverage across the group) and using the subacute (ie. earliest) FA measurement. Factor analysis of biomarkers was performed using the base R function 'Factanal' using the maximum likelihood method, varixmax rotation and cut-off loading score of 0.1.

4.4 Results

4.4.1 Traumatic abnormalities on MRI after moderate-severe TBI

Subacute MRI was performed between ten days to six weeks post-injury in 71% (140) of patients, a time-window chosen to ensure stabilisation of dynamic diffusion changes.

Focal lesions were identified and lesion maps were hand-drawn for each study for each individual, to be accounted for in the imaging analysis (Figure 13A). At the subacute visit, parenchymal contusions were present in 85% (119) of patients, with subarachnoid haemorrhage in 21% (30), subdural haematomas in 68% (95), extradural haematomas in 4% (6), oedema in 27% (38) and microhaemorrhages in 69% (97) (Figure 13B).

Overall a largely fronto-temporal distribution of parenchymal abnormality was noted which as expected, diminished in spatial extent over time Figure 13C,D)

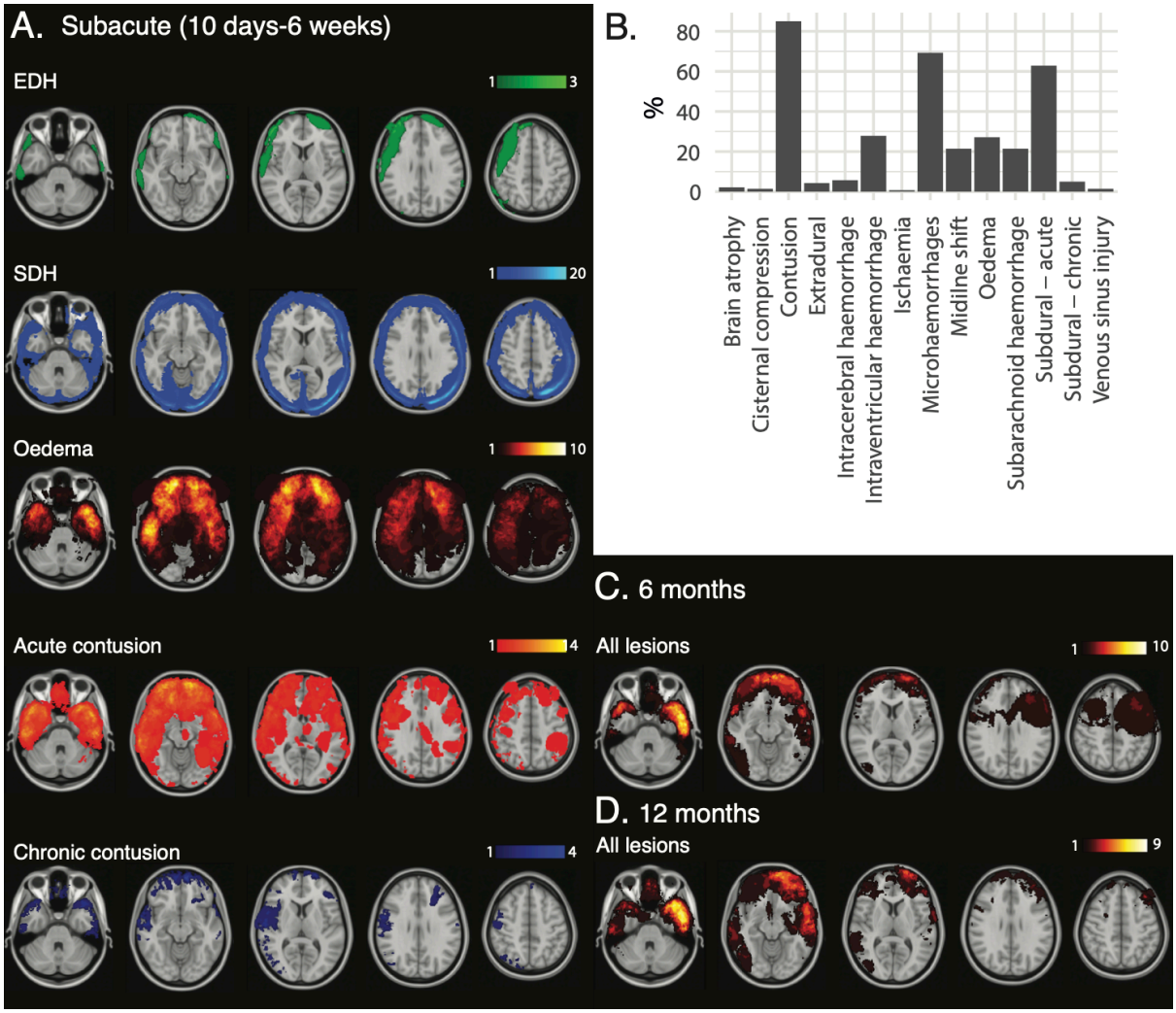

Figure 13. Distribution and longitudinal evolution of focal lesions post-TBI

EDH: extradural haematoma; SDH: subdural haematoma. A. Focal pathologies at the subacute 10 day to 6 week assessment timepoint. B. Subacute pathologies breakdown. C. Combined map of all lesions at 6 months post-TBI. D. Combined map at 12 months post-TBI.

4.4.2 Traumatic axonal injury on diffusion tensor imaging

On DTI assessment of white matter organisation excluding focally lesioned regions, group comparisons of patients and healthy controls provided evidence of traumatic axonal injury in patients. Using z-scored FA (zFA) generated from within-site comparisons of patients and controls to account for scanner specific site differences, significant group differences were present across the whole white matter skeleton

(P<0.001, see Table 13) at the subacute scanning visit, at six and twelve months post-injury (Figure 14A). Likewise, significant differences were present when restricting the analysis to the corpus callosum. Voxelwise comparisons of patients and controls demonstrated a widespread spatial distribution of these changes at all scanning visits (Figure 14B).

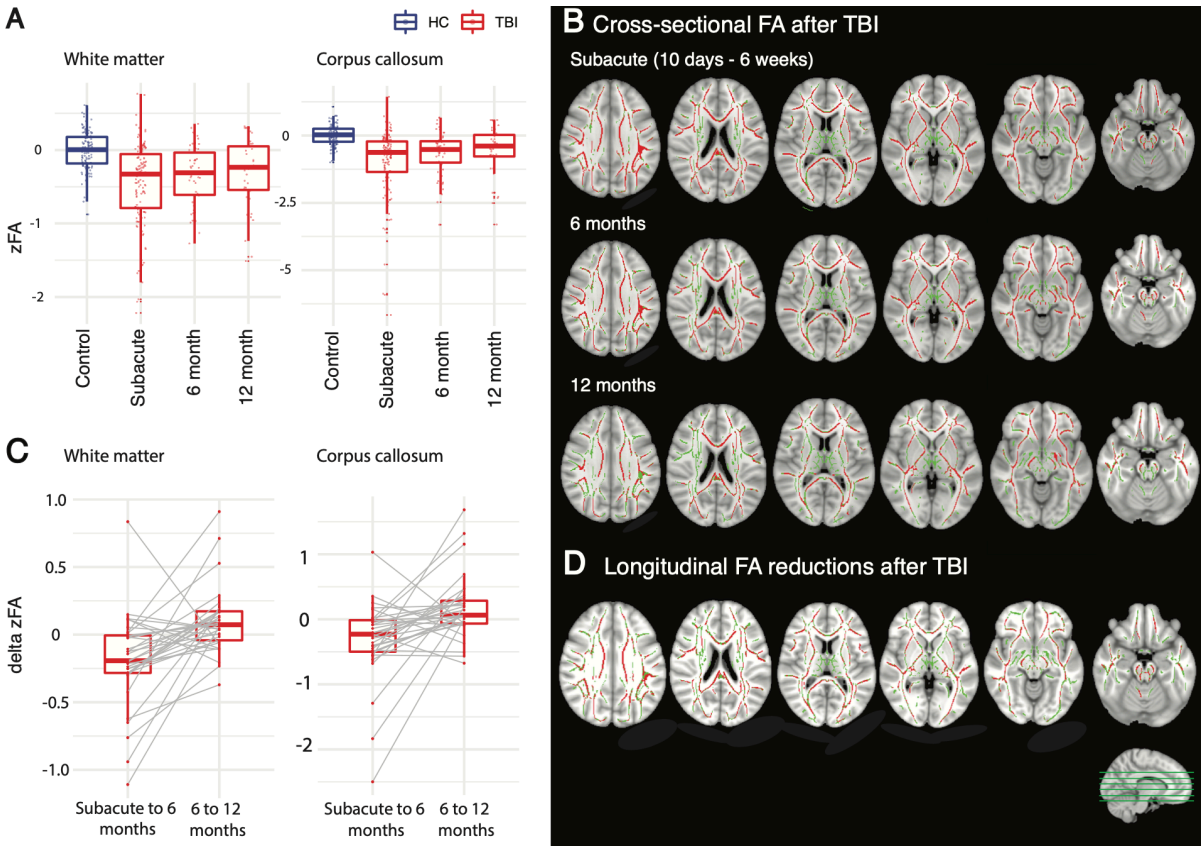

Figure 14. Diffusion tensor imaging evidence of axonal injury

(A) White matter (WM) organisation assessment using FA (z-scored vs healthy controls at each study site) in the whole WM (upper part) and the corpus callosum (CC, lower part). Controls are in blue, TBI patients in red. (B) Voxelwise comparison of zFA in patients and healthy controls with significant differences in red, overlaid on the WM skeleton in green. Significant differences at subacute (upper part), 6 month (middle) and 12 month (lower) visits. (C) Longitudinal change in FA after TBI in WM and CC regions. (D) Voxelwise map of regions with significant within-subject

reductions in FA between subacute and 6 months post-injury. No significant regions of change were present from 6-12 months or subacute to 12 months.

Longitudinal analysis showed a reduction in whole white matter zFA within the whole white matter from the first (subacute) visit to the six-month timepoint (N=49, V=975, P<0.001). However there was no significant reduction from six to twelve months (Figure 14C). A similar pattern of change was observed in the corpus callosum. Within-subject longitudinal voxelwise analysis supported the region of interest results with widespread areas of significant FA reductions from subacute to six-month visits, but no change from six to twelve months (Figure 14D).

	Traumatic Brain Injury			**Healthy Control**
Cross-sectional assessment	Subacute visit	6 month visit	12 month visit	Single visit
Days since injury, median (IQR)	20 (14.5)	189 (23)	372 (20)	-
Diffusion tensor imaging, N	132	53	39	121
mean WM zFA, median (IQR)	-0.338 (0.798)	-0.329 (0.585)	-0.242 (0.649)	0.004 (0.360)
test statistic vs HC (W)	11720	4556	3112	-
significance (P)	<0.001	<0.001	<0.001	-
mean callosum zFA, median (IQR)	-0.999 (1.278)	-0.662 (0.810)	-0.599 (0.957)	0.002 (0.402)
test statistic vs HC (W)	12485	4720	3138	-
significance (P)	<0.001	<0.001	<0.001	-
Longitudinal assessment	N/A	Subacute – 6m	6 -12m	-
Serial vol. imaging, N	-	58	38	30
GM JD, median (IQR)	-	-0.007 (0.015)	-0.001 (0.005)	0.000 (0.002)
test statistic vs HC (W)	-	469	504	-
significance (P)	-	<0.001	NS (0.421)	-
WM JD, median (IQR)	-	0.000 (0.021)	-0.007 (0.016)	-0.001 (0.005)
test statistic vs HC (W)	-	803	309	-
significance (P)	-	NS (0.558)	0.001	-
CSF JD, median (IQR)	-	0.016 (0.08)	0.012 (0.016)	0.004 (0.006)
test statistic vs HC (W)	-	1214	769	-
significance (P)	-	0.002	0.005	-

Table 13. Quantitative neuroimaging results after TBI and in healthy controls

JD: Jacobian determinant rate. WM: white matter; GM: grey matter; Vol: volumetric

4.4.3 Brain atrophy over time post-TBI

Brain volume changes were investigated over time to assess neurodegeneration in different tissue classes while excluding lesioned areas of the brain (Figure 15A). Grey matter JD atrophy rates were increased in patients during the first interval of six months post-injury (W=469, P<0.001) with concomitant raised CSF expansion rates in patients (W=1214, P=0.002). At the second interval between six and twelve months post-injury, white matter atrophy rates were significantly elevated in patients (W=309, P=0.001), with concomitant CSF expansion (W=769, P=0.005) but without significantly raised chronic grey matter atrophy rates. A linear mixed-effects model was used to assess the relationship between JD values in GM/WM tissue classes in TBI patients, using individual as a random effect. There was a significant interaction between tissue class and interval (F 8.4; DF 2; P<0.001) with greater GM atrophy over the first six months post-injury in contrast to greater WM atrophy in the chronic phase from 6 to 12 months. Tissue class was a significant determinant of JD (F 37.1, DF 2, P<0.001) however, alone, interval was not (F 3.0, DF 1, P=0.085).

Voxelwise analyses (Figure 15B) localised significant longitudinal white matter atrophy during the chronic 6-12 month timepoint to the right retrolenticular part of the internal capsule and posterior thalamic radiation. No other significant group differences were present voxelwise between patients and controls at the first interscan interval, or for other tissue classes at the second interscan interval.

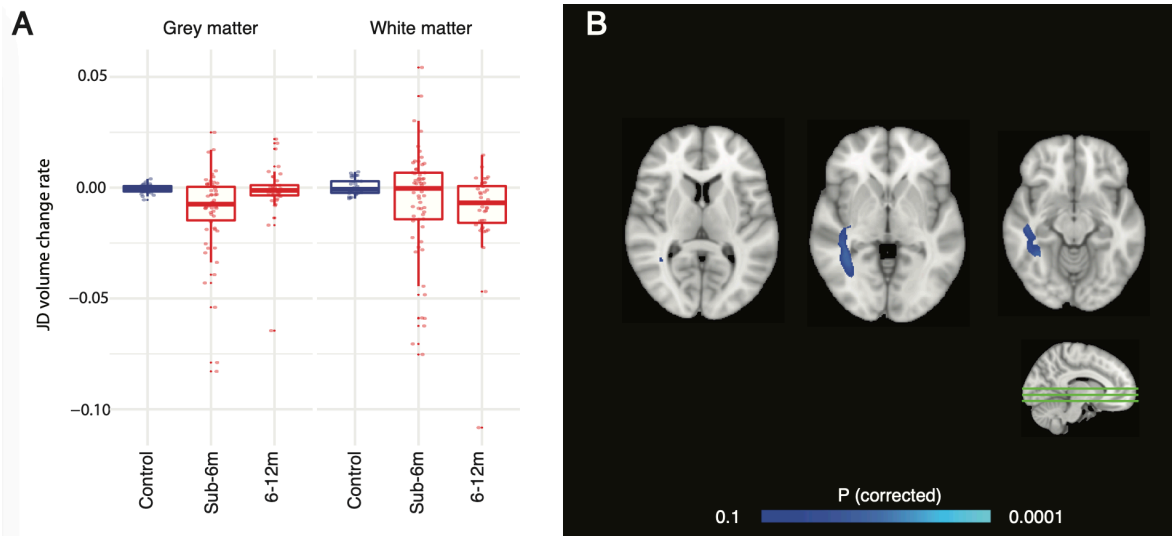

Figure 15. Longitudinal brain atrophy after TBI

(A) Jacobian determinant (JD) atrophy rates in grey matter (GM) and white matter (WM) in healthy controls and patients after TBI. (B) Voxelwise map of significant longitudinal reduction in WM volume (in blue) between 6-12 months post-injury with reduction seen in inferior longitudinal fasciculus / fronto-occipital fasciculus.

		Fluid markers					**Imaging markers**	
		NfL (peak)	Tau (peak)	UCH-L1 (peak)	GFAP (peak)	S100B (peak)	zFA WM (subacute)	zFA CC (subacute)
GOSE								
6m (n=126)	R^2 *	0.24	0.04	0.12	0.12	0.16	0.11	0.18
	AUC	0.83	0.77	0.77	0.73	0.81	0.69	0.76
	95% CI	0.75-0.91	0.68-0.87	0.68-0.86	0.63-0.82	0.72-0.89	0.59-0.80	0.66-0.85
	P	0.000	0.128	0.000	0.000	0.000	0.001	0.000
12m (n=108)	R^2 *	0.28	0.05	0.12	0.13	0.16	0.22	0.25
	AUC	0.85	0.85	0.81	0.78	0.83	0.79	0.81
	95% CI	0.77-0.94	0.78-0.92	0.72-0.89	0.69-0.86	0.74-0.91	0.68-0.91	0.70-0.92
	P	0.000	0.168	0.002	0.001	0.000	0.000	0.000
Atrophy Rate								
subacute to 6 months (n=53)								
Grey matter	Adj. R^2	0.20	0.34	0.25	0.27	0.21	0.00	0.00
	P	0.001	0.000	0.001	0.001	0.004	1.000	1.000
6 to 12 months (n=33)								
White matter	Adj. R^2	0.14	-0.03	-0.02	0.02	0.06	0.08	0.06
	P	0.037	1.000	1.000	1.000	1.000	0.667	1.000

Table 14. Injury markers and outcome predictions after TBI

** denotes McFadden's pseudo R^2. Adj = adjusted. GOSE = Glasgow outcome score extended. zFA = z-scored fractional anisotropy.*

4.4.4 Axonal markers tau and NfL predict grey and white matter atrophy

The relationships of early biomarker levels with longitudinal changes in brain volume were tested (Figure 16A). White matter atrophy rates, which were elevated compared to healthy controls in the six- to twelve-month interval, was predicted only by plasma NfL in the first six weeks post-injury (adj. R^2 0.14, P=0.037). Grey matter atrophy rates in the subacute period up to six months post-injury were predicted by the maximum level of each of the fluid biomarkers in the preceding six weeks (all P<0.004, adj. R^2 0.20 to 0.34, see Table 10), but not by the DTI zFA measures. This relationship was strongest with tau (adj. R^2 0.34, P<0.001).

To test the spatial relationship between microstructural damage acutely, indicated by each individual's z-scored FA map and chronic white matter neurodegeneration (6-12 month white matter JD map), voxelwise correlation was performed (Figure 16B). This demonstrated significant correlations between baseline FA and longitudinal white matter atrophy rates most notably centrally within the corpus callosum, right corona radiata, and left cerebral peduncle, suggesting that progressive WM atrophy relates to the pattern of damage sustained at the time of injury.

4.4.5 Blood and neuroimaging markers predict outcome

Favourable long-term functional outcome was best predicted by the maximal plasma NfL concentration in the first six weeks post-injury, during the subacute time period (Figure 16C, Table 14). In predicting binarised GOSE at 6 months and 12 months (using a score of six or higher to indicate favourable outcomes), a model including only plasma NfL had good fit (pseudo-R^2 0.24 and 0.28 respectively) and discrimination (AUC 0.83 and 0.85) on the receiver operator curve.

NfL had the highest pseudo R^2 explaining the greatest variance in outcome of all the biomarkers assessed, with z-scored FA in the corpus callosum the second strongest predictor of outcome at 6 and 12 months (pseudo-R^2 0.18 and 0.25; AUC 0.76 and 0.81, respectively).

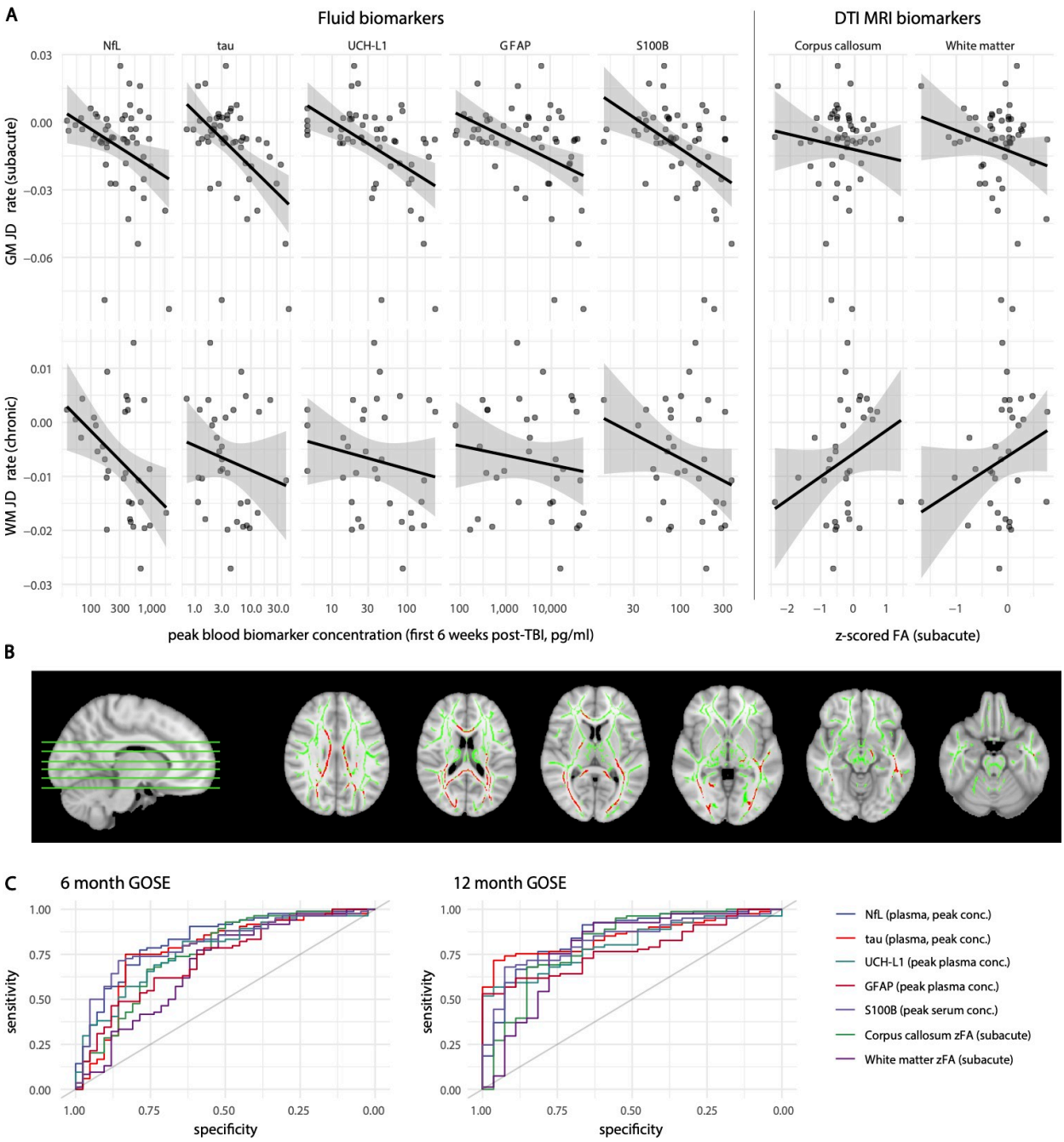

Figure 16. Predicting outcomes with biomarkers

Peak blood biomarker levels in the first six weeks post-TBI used for predictions, alongside the subacute zFA in corpus callosum (zFA CC) or white matter (zFA WM). (A) Peak concentrations and atrophy rates in GM from the subacute to six-month visit (most strongly predicted by tau), and in WM from six to twelve months post injury (predicted by NfL). (B) Areas of significant correlation between subacute FA and atrophy at 6-12 months post-injury. (C) ROC curves predicting Glasgow Outcome Score Extended (GOSE) >4 post-TBI at six (left) and twelve (right) months.

4.4.6 Cross-validation of axonal markers

The relationship between different fluid and imaging measures was assessed. Plasma NfL and fractional anisotropy (DTI) measures of axonal damage were significantly correlated (Figure 17A). Plasma NfL showed a modest negative correlation with FA (ρ=-0.44, P<0.001) as did plasma tau (ρ=-0.34, P<0.001).

Factor analysis of the five blood biomarkers and the zFA in the corpus callosum was performed to assess the latent variable structure underlying these observations in a data-driven manner (Figure 17B). Three factors explained 71% of the variance in the data structure, of which each factor explained approximately an equal proportion. One factor loaded heavily on the corpus callosum zFA (-0.99) and heavily on plasma NfL (0.56), while two further factors were identified and were loaded more broadly across the fluid biomarkers. Of these, one was most highly loaded on tau, whereas the other was most highly loaded on GFAP.

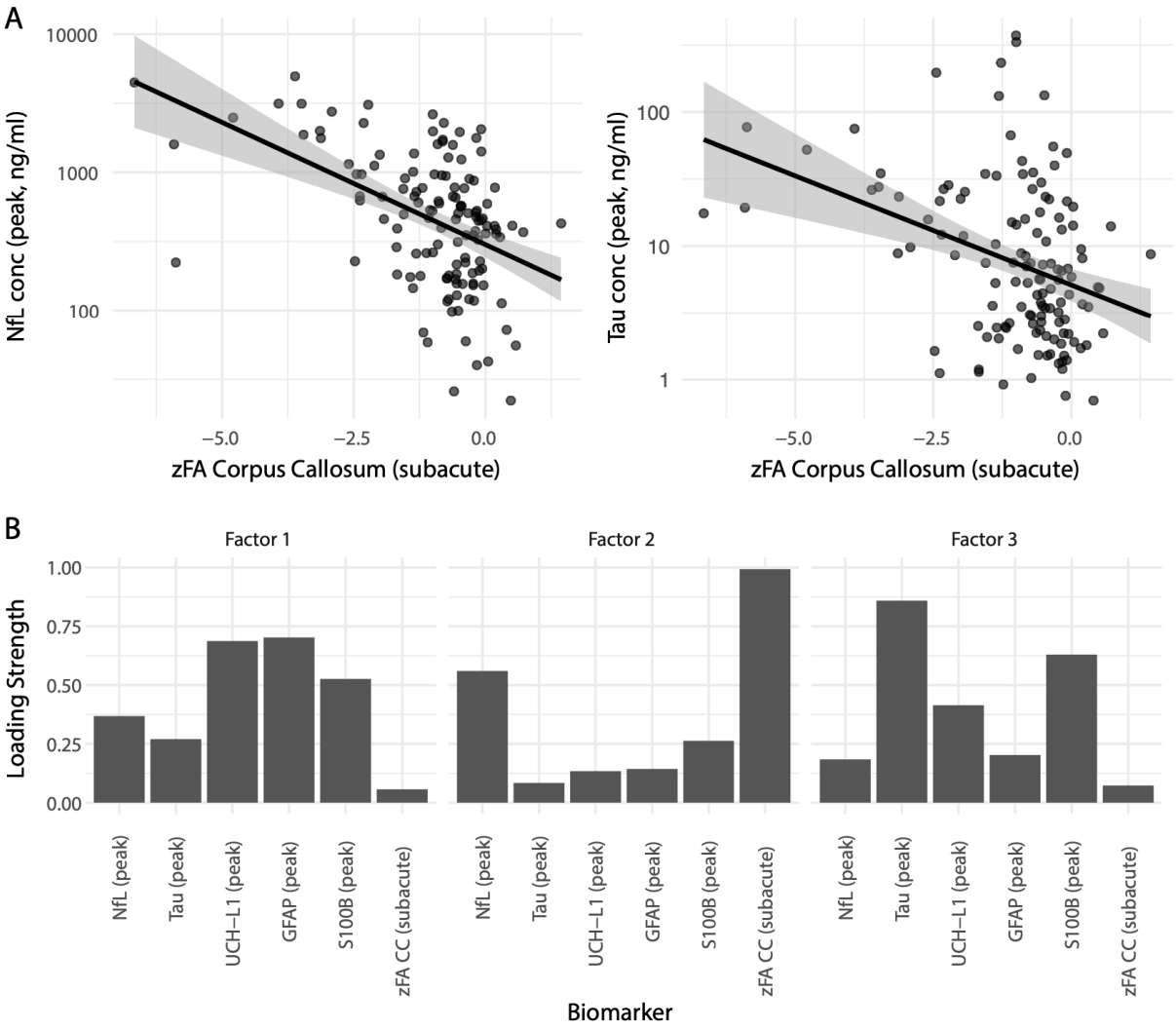

Figure 17. Correlations between axonal injury biomarkers and factor structure

(A) Relationships of peak axonal injury plasma biomarker concentrations and subacute z-scored fractional anisotropy (zFA) in the corpus callosum (CC) showing significant correlations. (B) Factor analysis showing three factors explaining latent variable structure of biomarkers, with axonal markers NfL and corpus callosum zFA both loading strongly on Factor two.

4.5 Discussion

This discussion relates to material described in Chapters 3 and 4.

Across these investigations performed longitudinally over one year after TBI, I show that the axonal injury marker plasma NfL, assessed in the subacute phase after moderate-severe injury, performs well in predicting clinical outcomes at six and twelve months. It has higher predictive performance than putative fluid markers tau or UCH-L1, or glial markers GFAP or S100B. NfL levels remained elevated in plasma at twelve months post-injury, suggesting ongoing post-traumatic neurodegeneration, which was supported by increased rates of white matter atrophy in the chronic phase on MRI. Supporting the hypothesis that acute axonal injury triggers progressive neurodegeneration, levels of NfL subacutely predicted the extent of progressive white matter loss, and furthermore, the spatial pattern of this progressive change was predicted by the distribution of axonal damage on diffusion MRI subacutely.

These data provide evidence of the validity of NfL as an axonal injury marker. Peak post-injury NfL levels were highly correlated with subacute diffusion MRI, which was used to quantify the extent of TAI. DTI provides a sensitive measure of axonal damage which can be overlooked with conventional imaging (Jolly et al., 2021). In keeping with previous work widespread FA reductions were seen after injury across a large number of white matter tracts including the corpus callosum (Kinnunen et al., 2011, Sidaros et al., 2008). A previous study has shown that serum NfL at 30 days post-injury correlates with corpus callosum FA at this time (Shahim et al., 2020a). We extend this work by showing that NfL measured subacutely correlates with diffusion MRI measures of TAI. This relationship was stronger for NfL than tau, and a factor analysis provided further evidence that plasma NfL and DTI are closely related in quantifying underlying axonal injury in an unbiased data-driven manner.

It is notable that elevated white matter atrophy was present voxelwise between six and twelve months in the posterior limb of the internal capsule and posterior thalamic radiation on the right side only. Damage in these regions has previously been reported in DTI studies, relating to visuomotor problems after injury (Caeyenberghs et al., 2010), however, previous work has suggested more spatially widespread voxelwise white matter atrophy in this phase after injury (Cole et al., 2018a). It may be that the

relatively smaller numbers of patients imaged at one year and a conservative excluding focally lesioned voxels from analyses meant that this voxelwise analysis was underpowered to detect more widespread change.

Levels of tau were raised after TBI peaking in the first 24 hours post-injury. Tau is particularly expressed in cortical interneurons (Trabzuni et al., 2012), in contrast to NfL which is associated with large, myelinated axons. For the first time, I show that plasma tau levels are closely correlated with the rate of grey matter atrophy in the first six months post-injury, a period during which this is pathologically increased.

An important question is the extent to which fluid biomarkers are sensitive to diffuse axonal injury, versus focal pathologies after trauma. I found high peak levels of NfL in patients irrespective of whether there was focal vs diffuse damage on CT. This analysis was replicated at the subacute timepoint using focal lesions identified on MRI at the subacute scanning timepoint, again showing no difference in concentrations depending on the presence of focal lesions. As expected however, in those individuals where focal lesions were present, lesion volume did correlate with NfL plasma concentration. This supports clinical use of NfL as a measure of diffuse axonal injury in this setting, rather than as simply an indicator of focal damage.

NfL is used widely as a neurodegeneration marker (Gaetani et al., 2019) and it has previously been shown that concentrations correlate with atrophy rates in Alzheimer's (Mattsson et al., 2017), and other diseases (Johnson et al., 2018, Rohrer et al., 2016, Barro et al., 2018). Further to our finding that NfL predicted white matter atrophy, it was found that peak tau plasma levels also predicted grey matter atrophy in the first six months after injury. These observations suggest that plasma NfL and diffusion measures of TAI provide information about the extent of the white matter predominant post-traumatic neurodegeneration after TBI, and may be useful biomarkers for clinical trials aimed at limiting the late effects of TBI (Graham and Sharp, 2019).

Although DTI has been widely used in TBI research but the anatomical specificity of the approach is a potential limitation. Acquiring or processing DWI imaging data differently may have increased power to detect differences, potentially strengthening correlations between fluid and imaging markers, or imaging markers and outcomes. For example, the DTI representation of diffusion signal does not make assumptions

about the biological composition of the underlying tissue within each voxel, increasing noise in regions of complex architecture (eg. crossing fibres) or partial volume such as in close proximity to the ventricles (Jones et al., 2013, Jeurissen et al., 2013). Alternative tools such as multi-shell diffusion models, leveraging DWI data acquired with several *b* values may have a superior performance in localising abnormalities to sub-compartments of the white matter (Assaf and Basser, 2005, Zhang et al., 2012).

In conclusion, the data described in this Chapter and Chapter 3 suggest that (a) axonal injury can be sensitively quantified using plasma NfL and tau; (b) the optimal timepoint to sample NfL is around 20 days post-injury, where levels peak; (c) levels of tau and NfL sampled peripherally mirror closely the dynamic changes within injured white matter, tested using invasive cerebral microdialysis; (d) that changes reflect diffuse axonal injury and are relatively resilient to the presence of focal brain pathologies / non-TBI traumatic injuries; (e) that axonal injury is a trigger for progressive neurodegeneration defined by MRI atrophy, which can be quantified by early tau / subacute NfL and (f) that there is direct clinical value in assessing these markers, which in addition to measuring neurodegeneration risk, relate well to clinical outcomes at six and 12 months post-injury.

5 Diffusion tensor imaging evidence of axonal injury and progressive neurodegeneration in the chronic phase post-TBI

In this Chapter I examine the relationship between diffusion tensor MRI assessment of axonal injury and progressive neurodegeneration in the chronic phase after TBI. Data within this Chapter have been published in Brain (Graham et al., 2020b).

5.1 Abstract

Experimental injury models relate axonal injury to chronic neurodegenerative pathologies, however in humans the link between DAI and subsequent chronic neurodegeneration has not previously been established. Here I test the hypothesis that the severity and location of diffuse axonal injury predicts the degree of progressive post-traumatic neurodegeneration in the chronic phase after TBI.

Fifty-five patients with moderate-severe TBI and 19 healthy controls underwent diffusion-weighted MRI, with FA extracted using DTI as a measure of DAI. Jacobian determinant atrophy rates were calculated from serial volumetric T1 scans as a measure of post-traumatic neurodegeneration. A range of potential predictors of neurodegeneration were tested, and I compared the variance in brain atrophy that they explained.

Patients showed widespread evidence of DAI, with reductions of FA at baseline and follow-up in large parts of the white matter. No significant changes in FA over time were observed. In contrast, abnormally high rates of brain atrophy were seen in both the grey and white matter. The location and extent of DAI predicted the degree of atrophy. These relationships were most strong in central white matter tracts such as the body of the corpus callosum, regions most commonly affected by diffuse axonal injury. DAI predicted more variability in atrophy than other factors, including baseline brain volume, age, clinical measures of injury severity and microbleeds.

In summary, diffusion MRI measures of DAI are a strong predictor of chronic post-traumatic neurodegeneration. This supports a causal link between axonal injury and

progressive neuronal loss. The assessment of diffuse axonal injury with diffusion MRI is likely to improve prognostic accuracy and help identify those at greatest neurodegenerative risk.

5.2 Introduction

Traumatic brain injury is a risk factor for dementia and neurodegeneration (Li et al., 2017). Experimental injury models implicate diffuse axonal injury (DAI) in the development of progressive proteinopathies after TBI (Tagge et al., 2018, Smith et al., 2013, Johnson et al., 2010). Traumatic cytoskeletal disruption can lead to axonal swelling and bulb formation, in which amyloid precursor protein accumulates with cleaving enzymes β secretase and presenilin 1 to produce amyloid β (Johnson et al., 2013b). Early pathologies of hyperphosphorylated tau (P-tau) also arise as acute traumatic axonal damage promotes tau dissociation from microtubules, leading to aberrant phosphorylation, miscompartmentalisation and distal spread (Tagge et al., 2018, Goldstein et al., 2012, Kondo et al., 2015). Progressive post-traumatic neurodegeneration may arise from prion-like propagation of traumatic proteinopathy distally; indeed animal models have demonstrated the transmissibility of tau generated in experimental injury (Zanier et al., 2018).

In humans, direct evidence for DAI triggering progressive neurodegeneration is lacking. However, neuroimaging tools are now available to estimate the location and severity of DAI as well as the extent of brain atrophy over time, allowing the hypothesis that patterns of injury predict the location and severity of subsequent atrophy to be tested. Patterns of DAI can be sensitively and accurately measured in vivo using diffusion MRI, providing a validated measure of post-traumatic axonal injury (Mac Donald et al., 2007a, Mac Donald et al., 2007b). Fractional anisotropy (FA) is the most widely used diffusion metric and provides a way to estimate white matter structure that is relatively stable in the chronic phase after TBI. Reduced FA is associated with damage to axons and associated structures, with surrounding inflammation (Mac Donald et al., 2007a, Scott et al., 2018) in addition to brain network dysfunction, poorer functional outcomes and cognitive impairment after TBI (Sidaros et al., 2008, Bonnelle et al., 2011, Kinnunen et al., 2011).

Post-traumatic neurodegeneration is particularly apparent in the degeneration of cerebral white matter first described in the 1950s (Smith et al., 2013, Strich, 1956). This is commonly seen after TBI and can be accurately measured *in vivo* using changes in brain volume estimated from serial volumetric T1 MRI scans (Bobinski et al., 2000, Cole et al., 2018a). Small changes in brain volume can be precisely measured using metrics such as the Jacobian determinant (JD) (Ashburner and Ridgway, 2012). Atrophy after TBI is associated with worse functional and cognitive outcomes (Brezova et al., 2014, Bendlin et al., 2008, MacKenzie et al., 2002, Trivedi et al., 2007), and elevated *longitudinal* atrophy rates are associated with poorer memory function (Cole et al., 2018a, Ross et al., 2012).

At present, there is limited information about the predictors of chronic post-traumatic neurodegeneration. A range of potential clinical and neuroimaging measures have previously been investigated in the chronic phase, which have not reliably predicted white matter atrophy rates: these include the presence of focal lesions and severity measures such as lowest Glasgow Coma Scale (GCS), with only a small amount of variance explained by age at injury, or sex (Cole et al., 2018a). Diffusion abnormalities have previously been reported to be associated with reduced cross-sectional brain volumes (Warner et al., 2010), but it is uncertain how this relates to longitudinal atrophy rates after TBI. In healthy middle-aged adults, DTI abnormalities have been associated with greater atrophy over time (Ly et al., 2014). Assessment of DAI using MRI FLAIR, T2 and T2* sequences has been related to early progressive reduction in brainstem volume post-TBI but not significant white matter volume change (Brezova et al., 2014).

Here I test whether FA at the baseline scanning visit is related to progressive atrophy, I assess the relationship at the whole brain and voxelwise levels to determine whether the location of DAI is the major determinant of subsequent neurodegeneration, and lastly, I investigate the susceptibility of different white matter tracts to both axonal injury and neurodegeneration, controlling for the potential impact of focal traumatic lesions.

5.3 Methods

5.3.1 Study design and participant recruitment

The cohort investigated in this Chapter is a combination of patients recruited into a longitudinal study of outcomes after TBI, or more than one cross sectional study after TBI. Findings on post-traumatic neurodegeneration in many of this cohort were previously reported (n=61 patients), a portion of whom were ineligible for the current study due to a lack of diffusion-weighted MRI at the time of baseline scanning assessment (Cole et al., 2018a).

Recruitment was via outpatient TBI clinics where patients were undergoing assessment for neurological sequelae of injury. Inclusion criteria were age 18-80 years and moderate-severe TBI per the Mayo classification (Malec et al., 2007). Individuals with significant previous injury histories, major neurological or psychiatric issues (eg. substance misuse) or contraindication to MRI were excluded. Injury characteristics, such as lowest acute Glasgow Coma Scale (GCS), post-traumatic amnesia (PTA) duration, and cause of injury were recorded. PTA was defined by a combination of either prospective measurement in the acute phase post-injury, or was retrospectively ascertained, where recovery the point at which the patient could consistently remember day-to-day events.

The same criteria per TBI patients were used for healthy control recruitment, individuals who were in addition required to have no history of significant TBI. Recruitment was coordinated by local research facilities at the Hammersmith Hospital. All study participants provided written informed consent in accordance with the Declaration of Helsinki. Ethical approval was granted by the Hammersmith / Queen Charlotte's and Chelsea research ethics committee.

5.3.2 MRI acquisition and processing

Imaging was acquired on two different scanners with minor differences in protocols only. Each individual's scan pair was acquired on the same system. A Siemens 3T Verio (Siemens Healthcare) and Philips 3T Achieva (Philips Medical Systems) were used, as per general methods (Chapter 2). In addition to DTI and volumetric T1, FLAIR

imaging was performed on both scanners, with gradient echo T2* and susceptibility weighted imaging performed to facilitate assessment of focal lesions. Brain MRIs were examined by a neuroradiologist for lesions such contusions, haematomas or microbleeds using multiple imaging modalities at baseline, and lesion masks were manually drawn for later analysis.

Volumetric and diffusion MRI sequences were processed as per general methods described in detail within Chapter 2.

Harmonisation of imaging data across the two scanners (Philips / Siemens) was performed using a z-scoring approach, with the following equation at each voxel for JD maps and FA maps:

$$zFA_{patient} = (\text{ raw } FA_{patient} - \text{mean } FA_{control\ group}) / \text{standard deviation } FA_{control\ group}$$

$$zJD_{patient} = (\text{ raw } JD_{patient} - \text{mean } JD_{control\ group}) / \text{standard deviation } JD_{control\ group}$$

5.3.3 Neuropsychological testing

TBI patients underwent an established battery of neuropsychological tests during the studies comprising this dataset. To overcome multiple comparison issues, I analysed a previously defined subset of tests, sensitive to post-TBI deficits, including people and doors test, choice reaction time, trail making, and matrix reasoning (Cole et al., 2018a).

5.3.4 Statistical analysis

Analyses were performed on diffusion and volumetric neuroimaging data as described in methods Chapter 2 and summarised in (Figure 18). Wholebrain summary measures were calculated by adding grey and white matter tissue data. Volumes were normalised for participant head size by dividing into total intracranial volume, defined as the sum of grey matter, white matter and CSF volume. FSL was used to generate mean and standard deviation (SD) values at each voxel within the healthy volunteer group. These maps were used to generate z-score maps for FA and JD for each patient and control by subtracting the control group mean map and dividing by the control SD map.

FSL Randomise software was used for voxelwise statistical analyses using the general linear model (Winkler et al., 2014). These included scanner system (Philips versus Siemens MRI) and age as nuisance covariates, other than in the analysis of FA vs longitudinal atrophy rate in which only scanner system was included, based on hierarchical partitioning of the linear model.

Effect sizes for t-tests were calculated to generate Cohen's d values and confidence intervals. Categorical variables were compared using the Chi-squared test. False discovery rate (FDR) correction was used to address multiple comparison issues for the battery of neuropsychological tests across multiple timepoints (ie. four tests, with assessment at baseline, follow-up and a measure of change over time; 12 comparisons).

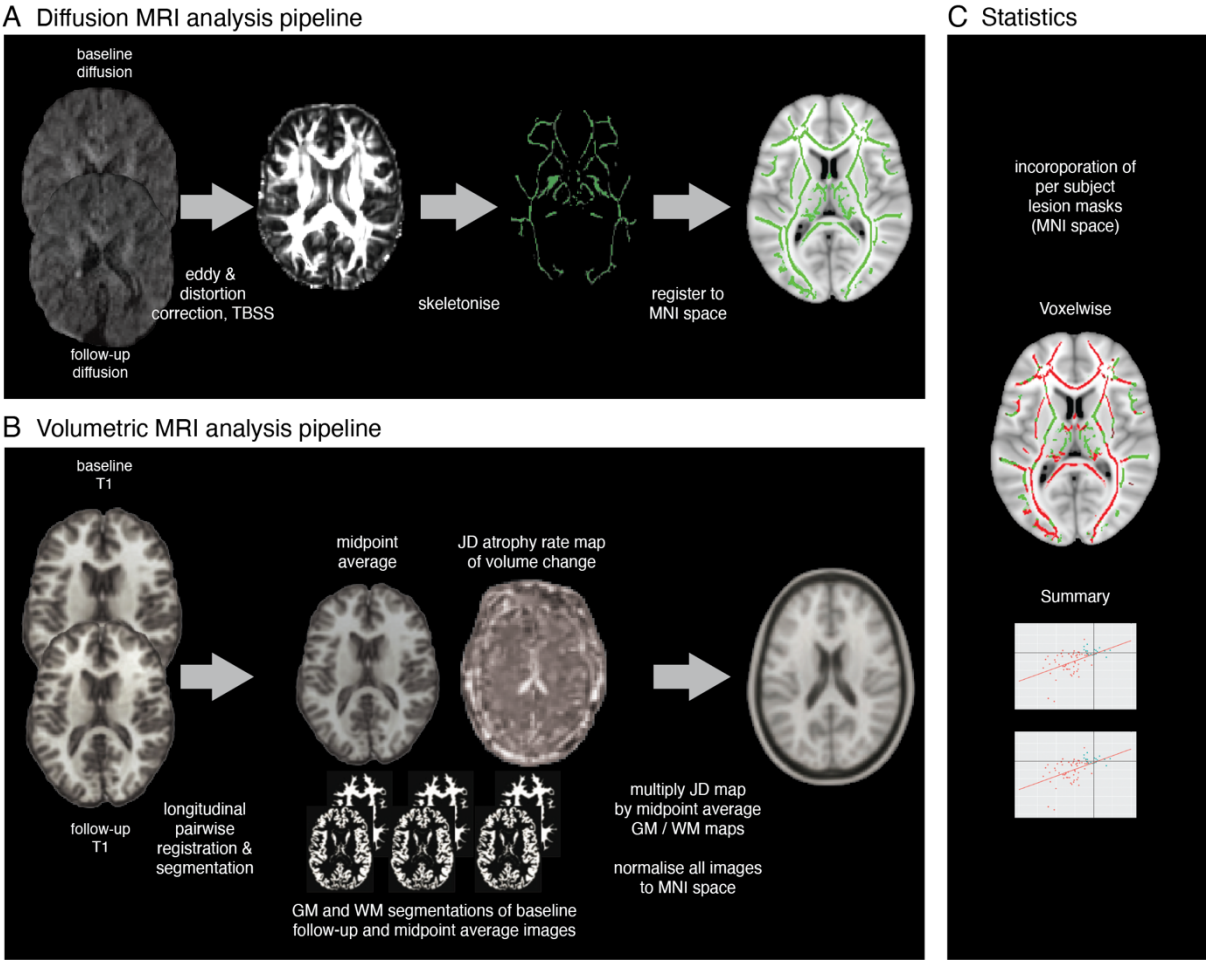

Figure 18. Approach to neuroimaging acquisition and analysis

(A) Diffusion MRI analysis pipeline to generate MNI space white matter FA map for voxelwise statistics. (B) Volumetric analysis to generate white and grey matter tissue maps from baseline and follow-up imaging, with longitudinal registration producing annualized map of change (JD rate change map) for each voxel and a midpoint average image between baseline and follow-up scans. Grey and white matter segmentations are generated, with midpoint average images multiplied by JD maps to generate tissue specific atrophy rates. All images are normalized to MNI space. (C) Voxelwise statistics assessing relationship between baseline FA and brain volume change over time (JD). Summary measures such as mean white matter FA and mean white matter JD used in linear regression.

5.4 Results

5.4.1 Clinical and demographic characteristics

Fifty-five patients were assessed after moderate-severe TBI with a mean age of 42, years (SD 13) of whom 45 were male and 10 female. Baseline MRI assessment was performed 3.5 years post-injury (mean), followed by a second MRI assessment a 12.7 months later (mean, see Table 15). Nineteen healthy controls also underwent longitudinal assessment with a mean age of 36 years at baseline (SD 9.7).

	TBI	**Healthy volunteers**	**Group comparison**
n	55	19	
Volumetric and baseline DTI	55	19	
Follow-up DTI	41	16	
Age (at scan 1), mean, years, +/- SD	42.0 ± 13.0	36.0 ± 9.7	P = 0.053
Sex, *n,* male/female	45 / 10	13 / 6	P = 0.221
Interval between scans, years	1.06	1.06	P = 0.469
Scanner system, *n*, Philips/Siemens	25 / 30	0 / 19	P < 0.001
Time since injury, mean, years ± SD	3.32 (7.97)	-	-
Post-traumatic amnesia, n (%)	50 (91)	-	-
Presence of focal lesions, n (%)	37 (67)	-	-
Lowest recorded GCS, mean ± SD	8.2 ± 5.0	-	-
Cause of injury, n	-	-	-
Road traffic accident	24	-	-
Violence / assault	13	-	-
Incidental fall	15	-	-
Sport	2	-	-
Unknown	1	-	-

Table 15. Clinical and demographic details of participants

5.4.2 Evidence of diffuse axonal injury

Following moderate-severe TBI, white matter FA, the overall measure of white matter organisation, was lower than in controls at baseline (0.43 in patients vs. 0.47 in controls; P<0.001) and at follow-up scanning visit (0.43 vs. 0.47; P<0.001; see Table 16 and Figure 19A).

	TBI	Control	**Group comparison** P value, effect size (95% CI)
White matter fractional anisotropy			
Baseline FA, mean ± SD	0.43 ± 0.02	0.47 ± 0.01	P < 0.001, d -2.20 (-2.84 to -1.56)
Follow-up FA, mean ± SD	0.43 ± 0.01	0.47 ± 0.02	P < 0.001, d -2.49 (-3.25 to -1.74)
Annualised FA change rate, mean ± SD	-0.006 ± 0.069	0.000 ± 0.009	NS (P = 0.585)
Volumes (cross-sectional)			
White matter (normalised) ± SD	-	-	-
Baseline	0.31 ± 0.03	0.34 ± 0.02	P < 0.001, d -0.93 (-1.49 to -0.38)
Follow-up	0.31 ± 0.03	0.34 ± 0.02	P < 0.001, d -1.09 (-1.65 to -0.53)
Grey matter (normalised) ± SD	-	-	-
Baseline	0.46 ± 0.04	0.49 ± 0.03	P = 0.002, d -0.73 (-1.27 to -0.19)
Follow-up	0.46 ± 0.04	0.48 ± 0.03	P < 0.001, d -0.78 (-1.33 to -0.24)
Whole brain (normalised) ± SD			
Baseline	0.77 ± 0.05	0.82 ± 0.03	P < 0.001, d -1.04 (-1.60 to -0.49)
Follow-up	0.76 ± 0.05	0.82 ± 0.03	P < 0.001, d -1.16 (-1.72 to -0.60)
Volumetric Assessment (longitudinal)			
Jacobian determinant (JD) rate ± SD	-	-	-
White matter	-0.0117 ± 0.0124	+0.0014 ± 0.0036	P < 0.001, d -1.20 (-1.77 to -0.63)
Grey matter	-0.0081 ± 0.0084	-0.0004 ± 0.0036	P < 0.001, d -1.02 (-1.58 to -0.46)
Whole brain	-0.0095 ± 0.0091	+0.0003 ± 0.0035	P < 0.001, d -1.21 (-1.77 to -0.64)

Table 16. Volumetric and white matter microstructural abnormalities after TBI

Voxelwise comparison showed widespread reductions in FA throughout the white matter in patients compared to controls at baseline, particularly within large central white matter tracts such as the corpus callosum, superior and inferior longitudinal fasciculi, the internal and external capsules (Figure 19B).

On summary measures (mean white matter FA), FA was stable over time in both patients and controls. Rates of change of FA did not differ significantly from zero in either patients or controls, nor were there significant differences in the rate of change in FA between the groups across the study duration.

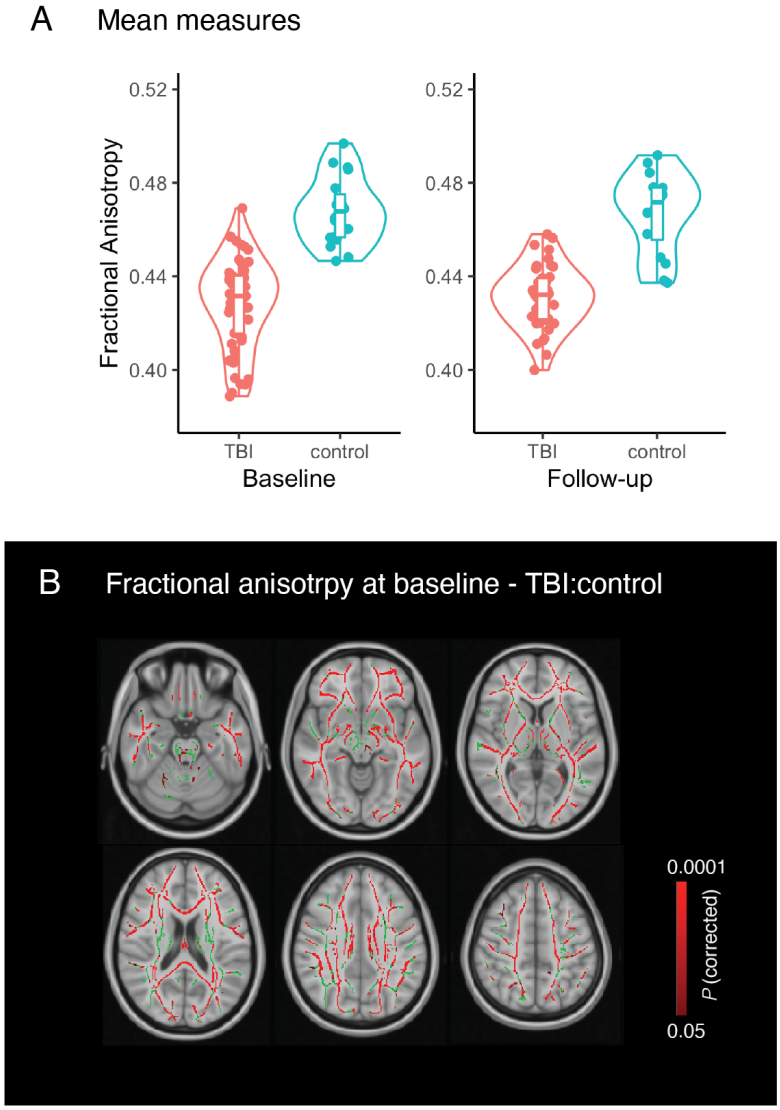

Figure 19. Diffusion tensor MRI evidence of axonal injury after TBI

(A) Boxplot showing differing mean white matter FA values between patients and controls at baseline and follow-up study visits. (B) Voxelwise contrast of white matter FA values between patients and controls. Areas of TFCE significant are in red, overlaid on mean FA skeleton in green.

5.4.3 Brain volume change over time

White and grey matter volumes were significantly lower at baseline and follow-up after TBI compared with controls (All P values < 0.002, see Table 16). Atrophy over time, indicated by lower JD rate values, was significantly greater after TBI than in controls across white matter, grey matter and whole brain tissue classes (all P values < 0.001, see Figure 20A).

Voxelwise comparisons revealed significant reductions in brain volumes cross-sectionally at baseline visit in patients versus healthy controls, involving a wide range of brain regions in both grey and white matter (Figure 20B). Specifically, baseline volume differences were present in the central white matter structures of the corpus callosum (genu, body and splenium), internal capsules, corona radiata, temporal white matter in addition to orbitofrontal grey matter particularly, alongside the temporal poles, with patchy parieto-occipital change. The spatial distribution of longitudinal atrophy over time was highly overlapping with this baseline pattern voxelwise, although with greater parieto-occipital cortical involvement and cerebellar grey matter progressive atrophy (Figure 20C).

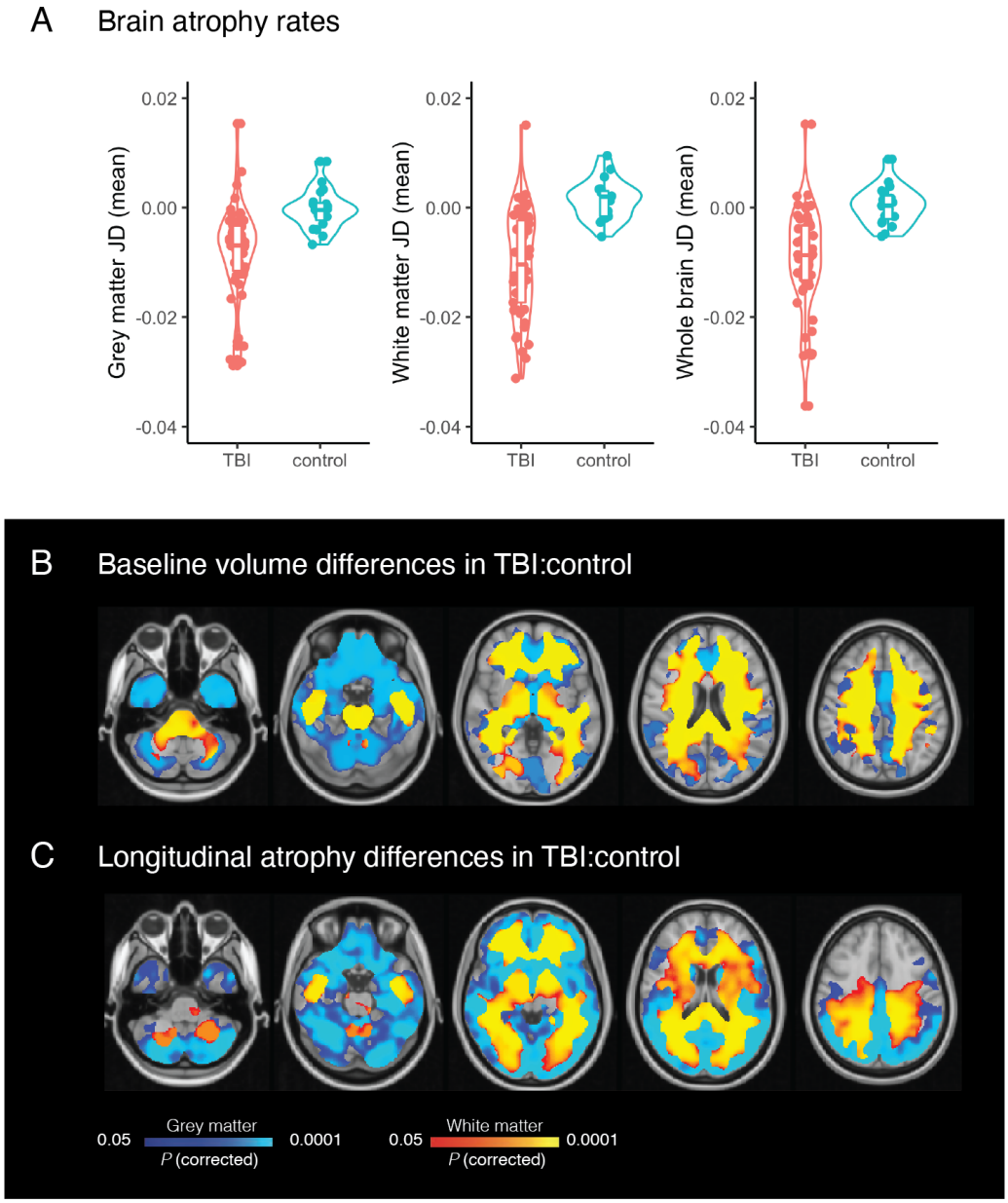

Figure 20. Brain volumetric changes over time after TBI

A. Box plots showing elevated longitudinal atrophy rates after TBI in GM, WM, and wholebrain. All comparisons are statistically significant. B. Voxelwise map comparing baseline brain volumes after TBI with healthy controls. Areas of significantly lower volume in patients (TFCE corrected) are shown in red-yellow colour for WM, blue-light blue for GM. C. Voxelwise map comparing JD atrophy rate maps after TBI and in healthy controls. Regions of significantly elevated longitudinal atrophy rates are shown: red-yellow colours indicate WM regions and light blue colours denote GM.

5.4.4 Diffuse axonal injury specifically predicts atrophy

As hypothesised (Figure 21A), there was a strong relationship between baseline diffusion MRI assessment of TAI and atrophy over time after TBI. Baseline FA predicted white matter atrophy rates (adjusted R^2 0.15, P=0.006, β_{FA} = 0.26) on multiple linear regression with scanner as a covariate. In contrast, grey matter atrophy was not predicted by baseline FA after TBI (adjusted R^2 0.03, P=0.125). In healthy controls, no significant relationship was evident between baseline FA and atrophy in either the grey or white matter (P=0.609 in white matter, P=0.566 in grey matter). Group-level results are shown graphically in Figure 21B showing the predictor variable (FA) on the x-axis against the annualised atrophy rate on the y-axis. FA and JD are z-scored for simplicity of representation. Healthy controls (blue points) cluster around the origin with very little damage or progressive atrophy, while TBI patients occupy the lower-left quadrant of the figure, with considerable diffusion MRI evidence of DAI and elevated atrophy rates.

Areas with more diffusion evidence of TAI showed greater rates of atrophy over time. Voxelwise comparison of baseline FA and JD maps, excluding lesions on a per-subject basis, showed multiple regions with significant positive relationships (Figure 21C). These included parts of the corpus callosum, superior corona radiata bilaterally, internal capsules, posterior corona radiata and thalamic radiation on the left. There were no areas where there was a negative correlation between FA and JD. The strong correlation between FA and JD is shown for the peak voxel on voxelwise analysis, situated in the body of the corpus callosum (left side, MNI co-ordinates 106 85 99; Figure 21D).

The observed relationship was not driven by the presence of focal traumatic lesions. Around two thirds of our patients had some degree of focal brain abnormality produced by their injury such as contusions, gliosis or ex-vacuo dilatation. As expected, these most frequently involved the orbitofrontal regions, temporal poles, or occipital regions. The group-level relationship between white matter damage and atrophy rates persisted when excluding lesioned voxels from each subject's mean FA / JD calculation (adjusted R^2 0.17, P=0.003, β_{FA} = 0.26). Notably, there was no significant correlation between lesion volume and white or grey matter JD atrophy rate.

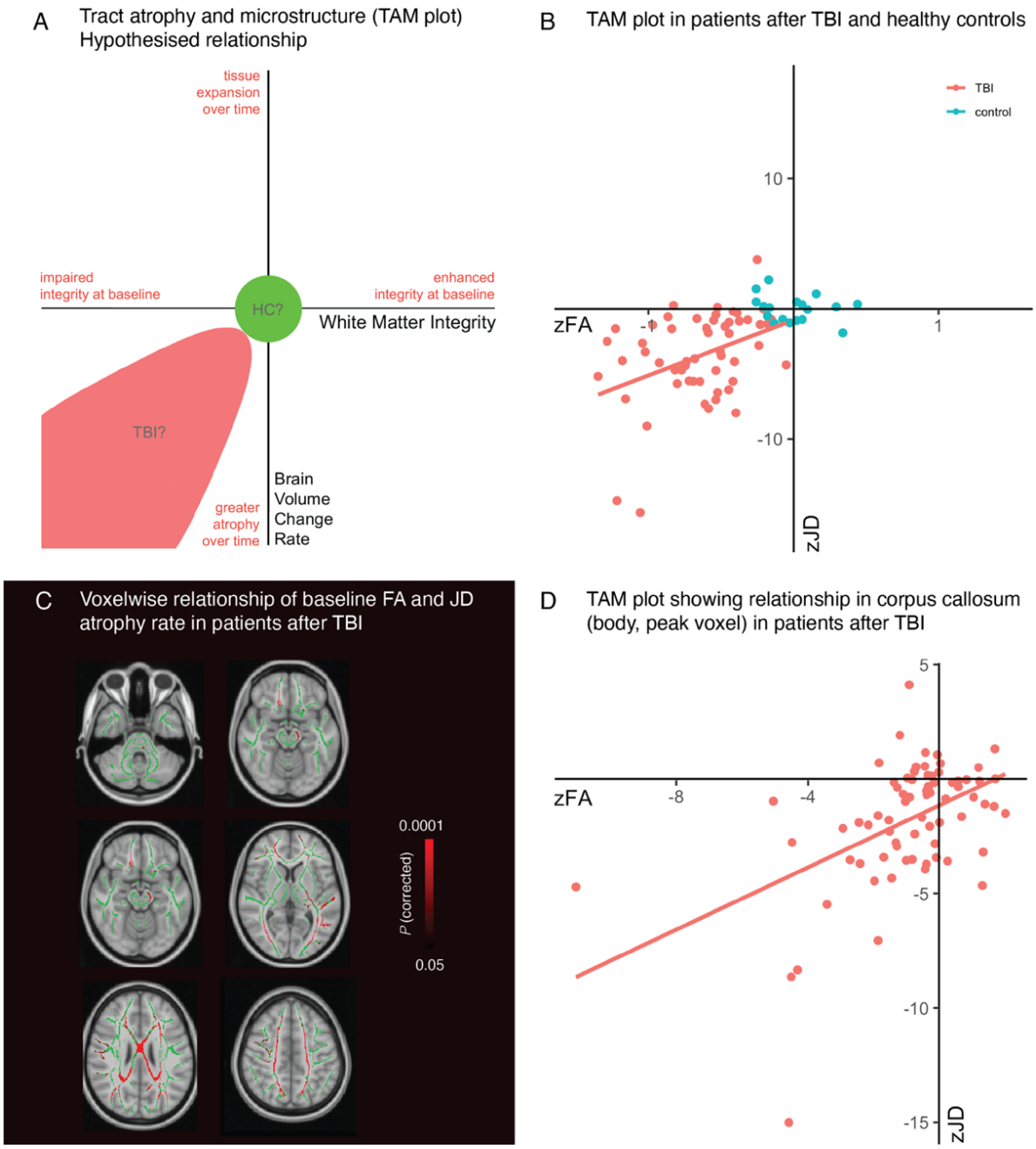

Figure 21. Relationship of TAI to neurodegeneration over time

(A) WM organisation versus atrophy plot. Z-FA, quantifying TAI vs JD, quantifying longitudinal atrophy. The green area is hypothesized to include healthy controls (HC) with undamaged WM/minimal atrophy. The red region is hypothesized to include TBI patients, with DAI that correlates with atrophy. (B) Z-FA vs mean WM JD (healthy controls blue, TBI red). (C) Voxelwise correlation of FA and JD (significant regions in red on mean FA skeleton in green). (D) The relationship between zFA and zJD atrophy rate is shown for the peak voxel from (C), within the body of the corpus callosum.

5.4.5 White matter tracts with more evidence of axonal injury show greater atrophy

The relationship between baseline FA and atrophy rate (JD rate) was investigated for different white matter tracts. Tracts show differential susceptibility to TAI, so it was hypothesised that those tracts showing more diffusion abnormalities would have greater atrophy over time.

Across the whole group of patients there were varying degrees of diffusion abnormalities and atrophy rates (Figure 22). FA and JD measures were positive correlated (adjusted R^2 0.13, P=0.0117). Larger and more midline white matter structures, such as the genu and body of the corpus callosum typically showed axonal damage and greater atrophy over time.

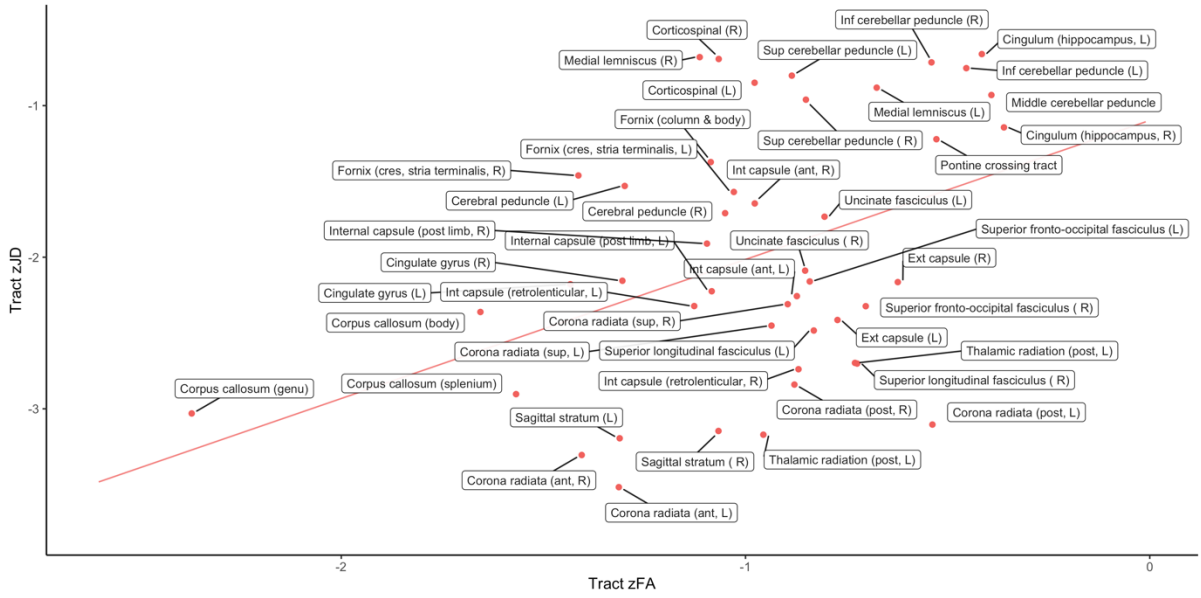

Figure 22. Tractwise relationships of axonal injury and neurodegeneration

The relationship between axonal damage (z-scored FA) and atrophy over time (z-scored JD) is shown across white matter regions derived from the Johns Hopkins University White Matter Atlas. Tracts with more evidence of axonal damage show more atrophy, most prominent within large central structures such as the corpus callosum, corona radiata, and internal capsules (adjusted R2 = 0.13, P = 0.0117).

5.4.6 Comparison with other possible predictors of atrophy

TAI severity and location explained far more of the variance in atrophy than other potential biological factors. This was explored using hierarchical partitioning of a multiple linear regression model, which showed that baseline FA explained far more of the model's variance in JD (53%) than any other biological influence.

Age, sex, time since injury, lowest recorded Glasgow Coma Scale (GCS), the presence of microbleeds or volume of focal lesions on MRI all explained less than 5% of the variance in atrophy rates (Table 17). Notably, baseline brain volume did not predict atrophy rates on either summary statistics or voxelwise (all P>0.05, including both grey and white matter tissue classes).

Predictor	**Independent Variance Explained (%)**
Baseline white matter FA	53.4
Scanner system	33.4
Presence of focal lesion	4.0
Baseline white matter volume	3.8
Time since injury	2.0
Age at baseline scanning visit	1.8
Sex	1.6

Table 17. Hierarchical partitioning of model predicting atrophy rates after TBI

5.4.7 Poorer memory performance and brain atrophy rates

I next explored the relationship between atrophy rates and levels of cognitive impairment. TBI patients showed impairment across a range of cognitive domains (Table 18). As reported previously, white and grey matter atrophy rates both correlated with a measure of memory performance (people test total score).

In patients, atrophy rate across the study period related to the performance at the follow-up assessment (white matter JD $\rho = 0.53$, $p = 0.0005$; grey matter JD $\rho = 0.54$, $p = 0.0004$) (Figure 23).

	Baseline	Follow-up	Change
People Test Total Score			
n	50	40	37
mean ± SD	23.72 ± 7.86	25.73 ± 9.07	1.86 ± 8.28
WM Jacobian determinant	ρ = 0.28, p = 0.0457*	ρ = 0.53, p = 0.0005**	ρ = 0.29, p = 0.0867
GM Jacobian determinant	ρ = 0.32, p = 0.0252*	ρ = 0.54, p = 0.0004**	ρ = 0.25, p = 0.134
Trails B minus A			
n	50	40	37
mean ± SD	34.52 ± 26.01	33.78 ± 26.73	0.39 ± 30.21
WM Jacobian determinant	ρ = -0.15, p = 0.3079	ρ = -0.26, p = 0.0984	ρ = -0.02, p = 0.8826
GM Jacobian determinant	ρ = -0.12, p = 0.4037	ρ = -0.21, p = 0.1971	ρ = -0.05, p = 0.7878
Choice Reaction Time (median)			
n	42	16	15
mean ± SD	0.49 ± 0.11	0.55 ± 0.11	0.00 ± 0.17
WM Jacobian determinant	ρ = -0.22, p = 0.1642	ρ = 0.2, p = 0.4523	ρ = 0.25, p = 0.3613
GM Jacobian determinant	ρ = -0.14, p = 0.3735	ρ = 0.14, p = 0.6062	ρ = 0.19, p = 0.506
WASI Similarities			
n	30	20	19
mean ± SD	36.27 ± 4.86	34.35 ± 6.13	-0.47 ± 7.11
WM Jacobian determinant	ρ = 0.39, p = 0.0341*	ρ = 0.04, p = 0.8765	ρ = -0.17, p = 0.4808
GM Jacobian determinant	ρ = 0.45, p = 0.0118	ρ = 0.07, p = 0.7828	ρ = -0.2, p = 0.419

Table 18. Neuropsychological and atrophy rates after TBI

** significant at P<0.05; ** significant after FDR correction for 12 independent comparisons; WM: white matter, GM: grey matter*

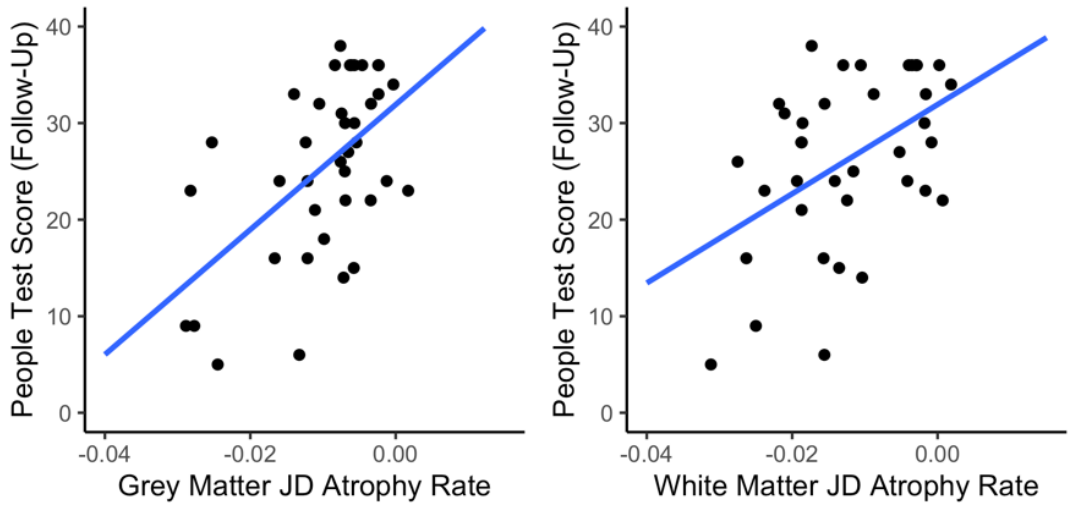

Figure 23. Atrophy rates and memory dysfunction post-injury

The relationship between brain atrophy over time in grey matter (left) and white matter (right) and a measure of memory at the follow-up visit (the People Test total score) is shown, with significant correlation in each tissue class.

5.5 Discussion

In this investigation I show that TAI measured by diffusion MRI predicts brain atrophy following single moderate-severe TBI. In the chronic phase after injury, white matter tract FA at baseline predicts the amount of volume loss seen in white matter tracts over time. I compared several factors that could influence neurodegeneration and TAI was the most important predictor. Most of the variability in atrophy rates was explained by TAI. In contrast, less than 5% of the variance in atrophy was predicted by any other hypothesised predictor, including clinical measures such as PTA and lowest GCS, as well imaging measures of evidence of diffuse vascular injury and white matter volume at baseline. This provides evidence that axonal injury causes progressive neurodegeneration of white matter tracts, an effect that persists for many years after injury.

A causal link between TAI and axonal neurodegeneration is supported by experimental models of TBI (Tagge et al., 2018). Rodent models of TBI produce a chronic and progressive degenerative process (Smith et al., 1997). In humans, this degeneration is most prominent in the white matter (Cole et al., 2018a). Wallerian

degeneration of damaged axons plays a role, particularly in the early phase after injury. This is the set of molecular and cellular events that clear degenerating axons and myelin from the central nervous system (CNS) (Vargas and Barres, 2007). Traumatic axonal injury produces degeneration of the axolemma and disintegration of the axonal cytoskeleton. This results in the disassembly of the microtubules, neurofilaments and other cytoskeletal component, resulting in fragmentation of the axon. In the peripheral nervous system Wallerian degeneration is a relatively rapid process. In CNS the process is much more chronic. The reasons for this discrepancy are not entirely clear, but may relate to the failure of CNS glial cells to fully clear myelin breakdown products, which are still seen in damaged white matter tracts many years after injury (Johnson et al., 2013a).

TAI can also trigger an active neurodegenerative process caused by toxic proteinopathies that are generated at the time of injury. Hyperphosphorylated tau and amyloid β pathology are generated within hours of injury and persist into the chronic phase. This pathology characterises many of the chronic neurodegenerative diseases associated with TBI, including CTE and AD (Smith et al., 2013). The effects of biomechanical strain on axons can trigger the generation of hyperphosphorylated tau and amyloid β pathology. Cytoskeletal disruption caused by high strain leads to tau dissociation from microtubules, aberrant phosphorylation and possible trans-synaptic spread into other neurons (Zanier et al., 2018). Amyloid pathology is also produced soon after injury. Axonal bulbs formed shortly after axonal damage provide an environment that accelerates the cleavage of amyloid precursor protein to generate amyloid β (Gentleman et al., 1993, Johnson et al., 2013b). Hence, the generation and persistence of toxic proteinopathy in combination with gradual Wallerian-like degeneration of white matter tracts affected by TBI can explain the gradual white matter neurodegeneration associated with TAI (Hill et al., 2016, Zanier et al., 2018).

I investigated the pattern and degree of axonal damage using diffusion MRI to measure FA. This is a sensitive marker of post-traumatic white matter abnormality (Mac Donald et al., 2007a, Mac Donald et al., 2007b). Widespread reductions in FA were seen in this TBI group, providing evidence for axonal injury affecting a large number of white matter tracts. FA reductions are associated with disruption of white

matter organisation, glial cell activation and myelin damage (Mac Donald et al., 2007a, Scott et al., 2018) and also predict the extent of brain network dysfunction, the degree of functional impairment and the pattern of cognitive impairment seen after TBI (Sidaros et al., 2008, Bonnelle et al., 2011, Kinnunen et al., 2011). Hence, FA measures provide a clinically relevant imaging marker of axonal damage that characterises the early stages of Wallerian degeneration and neurodegeneration that is associated with the production of toxic proteinopathies.

It is striking that while brain volumes reduced over time, this was not associated with a longitudinal reduction in FA on DTI. This suggests that these imaging measures capture different properties of white matter, lending support to the hypothesis that FA measures axonal microstructure disruption related to early post-injury damage and that volume reductions reflect gradual neuronal dropout within fibre tracts. We did not see previously described increases in FA over time (Feeney et al., 2017, Castaño-Leon et al., 2019) although these findings have varied spatially across different investigations. Replication of this work spanning early to chronic stages after TBI will help to clarify the longitudinal dynamics of FA and atrophy in white matter.

The key factor in determining the pattern of post-traumatic neurodegeneration is likely to be the biomechanics of the initial injury. DAI is caused by biomechanical forces exerted across white matter tracts at the time of injury (Gennarelli et al., 1982). The distribution of these forces is likely to determine the spatial pattern of tract damage. Hence, the pattern of initial shear forces is key to understanding which white matter tracts are most likely to degenerate over time. Midline structures such as the corpus callosum are exposed to high shearing forces after many types of injury (Ghajari et al., 2017). These tracts are particularly affected by TAI, typically showing the most prominent diffusion MRI abnormalities and the most pronounced atrophy (Kinnunen et al., 2011, Cole et al., 2018a).

White and grey matter atrophy over time correlated with a measure of memory at the follow-up visit, but not with dysfunction in other cognitive domains tested, or indeed problems at other ‘timepoints’ assessed (baseline, change over time). The lack of a broader or stronger correlation between atrophy over time and cognitive function may reflect a combination of cognitive reserve and pre-symptomatic neurodegeneration,

whereby progressive symptoms could manifest many years post-injury (Nordstrom and Nordstrom, 2018, Graham and Sharp, 2019).

The relationship between shear force, axonal injury and diffusion MRI abnormalities has recently been characterised using finite element modelling of a controlled cortical injury to predict the pattern of shear forces within the corpus callosum. These shear forces correlated with histopathological features of axonal injury and also the reduction of FA within damaged white matter. The results support a causal relationship between the biomechanics of an initial injury and axonal injury, which can be measured using diffusion MRI (Donat et al., 2021). In conjunction with this experimental work, these human results support a close relationship between initial biomechanical force, axonal injury and subsequent neurodegeneration. This is seen most clearly in tracts exposed to high shear forces such as the corpus callosum, where large abnormalities in FA are associated with high levels of tract degeneration.

There are several potential limitations of this work. One concern is whether resolving oedema might confound the measurement of atrophy or microstructure after TBI. Although this is a potential confound in the acute stages following TBI, this is not an issue for these analysis as the participants are in the chronic phase post-TBI with a mean time since injury of 3.3 years. A further potential confound is the effect of focal lesions and loss of brain tissue on estimates of microstructure and atrophy. This issue has been carefully controlled for by using an analysis pipeline that exclude focal injuries from the voxelwise analyses using lesion masking. A further potential limitation is the use of two different scanner systems for data acquisition. Although this introduces noise in the MRI measurements, this is unlikely to affect the main findings: each participant was scanned longitudinally on the same scanner, which dramatically reduces the impact of including two scanners. Hierarchical partitioning was used to systematically assess the impact of the two scanners on diffusion measures, which are particularly susceptible to different scanners. This showed that scanner system accounted for a significant amount of the explained variance in JD. Hence, scanner system was included as a nuisance covariate in analyses.

In summary, this investigation shows the novel finding that the extent and location of TAI predicts white matter degeneration after TBI. This is in line with experimental injury

models showing that axonal damage triggers progressive neurodegeneration. This will lead to an improved ability to predict those at greatest neurodegenerative risk after TBI, which should improve outcome prediction and facilitate recruitment to clinical trials of anti-neurodegenerative and neuroprotective treatments (Schott et al., 2010, Graham and Sharp, 2019).

6 Comparing post-traumatic neurodegeneration with Alzheimer's disease and healthy ageing

6.1 Abstract

TBI is an established dementia risk factor, but whether Alzheimer's disease (AD) specifically is a consequence is uncertain. Axonal injury is implicated in the development of neuropathologies of amyloid and tau, which are features of AD. Neurodegeneration after TBI, in AD or health ageing can be sensitively measured over time with volumetric MRI, allowing assessment of commonalities and differences. 45 with AD and 55 patients after TBI were assessed, alongside 46 scanner and age-matched controls, and a further 15 healthy ageing controls. Brain volumes and atrophy rates were assessed. I found that established atrophy patterns were similar in AD and healthy ageing but distinctive in TBI. Atrophy rates were increased in grey and white matter in AD, but only in white matter after TBI voxelwise. Deep central white matter atrophy was TBI-specific, with little overlap of age-related change or the cortical atrophy specific to AD. In conclusion, neurodegeneration after TBI differs from AD and healthy ageing, with a central white matter predominance reminiscent of traumatic axonal injury patterns.

6.2 Introduction

TBI is a risk factor for neurodegeneration and dementia (Graham and Sharp, 2019). The population attributable fraction of dementia due to TBI is substantial, estimated at 3% (Livingston et al., 2020). Dementia risk remains elevated for many decades after injury (Nordstrom and Nordstrom, 2018), and the association with dementia of all-subtypes is robust with a pooled relative risk of around 1.8 times across injuries of all severities (Li et al., 2017).

What is less clear is whether Alzheimer's disease (AD) in particular is more prevalent following TBI. The epidemiological data are contradictory and sometimes difficult to interpret (Graham and Sharp, 2019). This can be related to difficulty establishing dementia subtype clinically, compounded by challenges in retrospectively ascertaining head injury history. Recent meta-analysis suggested modest association of TBI and

AD (pooled relative risk ~ 1.5 times), (Li et al., 2017), however the association is less clear in those studies with neuropathological diagnosis of AD. Several large well designed studies show earlier AD onset after injury, (Schaffert et al., 2018), an association of injury and AD but only in men (Abner et al., 2014), or indeed no significant association with AD (Crane et al., 2016).

TBI can trigger the development of AD pathology. Post-mortem studies and experimental injury models demonstrate biomechanical mechanisms by which axonal damage induces shearing stress across axons at the time of injury leading to the development of proteinopathies of both amyloid-β and hyperphosphorylated tau (P-tau) (Smith et al., 2013). Specifically, traumatic damage to the neuronal cytoskeleton disrupts axonal transport and leads to swellings in which amyloid precursor protein accumulates with cleaving enzymes β-secretase-1 and presenilin-1, generating intraneuronal amyloid β. This can be seen within hours of injury and has been demonstrated in vivo using amyloid PET well into the chronic phase post-TBI (Johnson et al., 2013b, Scott et al., 2016). Likewise, microtubular damage drives dissociation of microtubule associated protein tau (tau), which is aberrantly hyperphosphorylated to generate highly toxic isoforms, which can promote neuronal degeneration and alter brain function (Tagge et al., 2018).

Proteinopathies may spread via prion-like mechanisms post-injury, possibly providing the means for injury to produce an AD-like neuropathological picture. For example, amyloid-β has long been thought to spread via prion-like mechanisms in neurodegenerative disease (Kane et al., 2000), and recent experimental modelling shows the transmissibility of trauma-induced tauopathy (Zanier et al., 2018). Neurofibrillary tangles related to TBI closely resemble AD and primary age-related tauopathy in respect of phosphorylation ratio and isoform state (Smith et al., 2013, Schmidt et al., 2001, Arena et al., 2020) although morphological distinctions have been demonstrated (Falcon et al., 2019). Neuroinflammation and in particular chronic microglial activation are common features of chronic TBI and AD, with complex roles which may be reparative or deleterious in certain circumstances (Heneka et al., 2015, Simon et al., 2017, Scott et al., 2018).

Advanced MRI may be used to define the chronic effects of TBI on the brain in-vivo relative to other neurodegenerative diseases and change associated with healthy ageing. Longitudinal volumetric T1-weighted MRI assessment of brain volume provides a way to quantify atrophy location and rates, quantifying the extent and distribution of neuronal loss, the end product of diverse degenerative pathways (Cash et al., 2015). Gross atrophy, particularly of white matter, has long been recognised following TBI (Strich, 1956) and longitudinal neuroimaging work shown abnormally raised atrophy rates in the chronic phase in vivo, indicating progressive degeneration years after injury (Cole et al., 2018a). Longitudinal MRI after TBI suggests increased rates of grey and white matter atrophy early post-injury, with ongoing white matter atrophy for months and years post-injury. This white matter atrophy is particularly prevalent in large fibre bundles such as the corpus callosum, internal and external capsules, inferior and superior longitudinal fasciculi (Sidaros et al., 2009, Cole et al., 2018a, Farbota et al., 2012). These tracts are highly susceptible to traumatic axonal injury (Jolly et al., 2021, Donat et al., 2021) and, as described in Chapters 3 and 4, I have shown that the pattern of white matter degeneration is predicted by the distribution of axonal damage (Graham et al., 2020b).

Atrophy progression in AD is often stereotyped, initially within the hippocampi and spreading to involve the temporal lobes, parietal lobes and frontal regions later in the disease process (Scahill et al., 2002). Atrophy is related to the distribution and extent of tau deposition, with relatively little contribution of amyloid (Bejanin et al., 2017, La Joie et al., 2020) and reflects neuronal loss (Bobinski et al., 2000, Zarow et al., 2005). Similarly, subcortical and cortical volume loss are features of healthy ageing. Longitudinal atrophy rates are increased in temporal and pre-frontal cortices in advanced age (Fjell et al., 2009), and though the frontal change suggests AD neuropathological change is unlikely to be an exclusive driver of age-related volume loss, one cannot exclude a contribution of preclinical AD. The landscape of non-AD pathologies which could contribute to age-related atrophy is expansive, including primary age-related tauopathy (Crary et al., 2014), aging-related tau astrogliopathy (Kovacs et al., 2016), cerebral age-related TDP-43 and sclerosis, α-synuclein and vascular pathologies (Nelson et al., 2016). Furthermore, CTE neuropathologic change

(eg. sulcal perivascular astroglial tau deposition) has been reported in healthy older people with no known head injury history (Ling et al., 2015).

Patterns of progressive atrophy have never previously been compared between TBI, AD and healthy ageing, representing an opportunity to better understand the neurodegenerative consequences of trauma. In this longitudinal cross-disease comparative study, it was hypothesised that: (a) longitudinal patterns of brain volume loss on MRI in the chronic phase after moderate-severe TBI would be distinct from late-onset Alzheimer's disease; (b) this change would be distinct from healthy ageing; and (c) that post-traumatic neurodegeneration would reflect the typical central white matter distribution of axonal injury after TBI. I used serial T1-weighted MRI to quantify brain volume changes in grey matter, white matter and CSF regions of interest as well as voxelwise, and performed group comparisons to indicate spatial similarities and differences between TBI, AD and healthy ageing.

6.3 Methods

6.3.1 Study participants

An overview of study methods is provided in Figure 24. Recruitment took place across two research sites: patients with AD and a group of healthy controls (HCs) were assessed at University College London (UCL), whereas patients after TBI were recruited at Imperial College London (ICL), alongside a group of young controls (matched to TBI patients in age, yHCs) and older controls (matched to AD patients in age, oHCs) also assessed at ICL. Baseline characteristics of the patients and healthy controls are shown in Table 19.

Forty five patients with AD and no significant history of head injury were assessed longitudinally from the Minimal Interval Resonance Imaging in Alzheimer's Disease (MIRIAD) dataset (Malone et al., 2013). This publicly shared dataset was acquired at University College London ('UCL' / 'research site 1'). This includes 46 subjects with mild-moderate probable Alzheimer's disease (NINCDS-ADRDA criteria) (McKhann et al., 1984) with volumetric T1-weighted MRI collected longitudinally (range 0.46 to 2.07 years), with all imaging acquired on the same 1.5T Signa scanner (GE Medical systems, Milwaukee, WI) and matched controls. A MIRIAD participant with AD was

not eligible for the study due to a short inter-scan interval under two months. Patients with AD were a median of 68.6 years old, (IQR 9.9) and were well matched to healthy volunteers with a median age of 68.5 years (IQR 7.5). Mini mental status examination (MMSE) was performed to assess dementia severity at baseline in the AD group, with a median score of 19, within the moderate range of this scale (IQR 9.5).

Forty eight patients after moderate-severe TBI were assessed, comprising a longitudinal cohort of patients in the chronic phase (>6 months) after moderate-severe TBI, defined by the Mayo classification (Malec et al., 2007). Data were combined across several previous cross-sectional and longitudinal studies opportunistically at ICL to provide the maximum possible inter-scan intervals and reduce noise. The presence of post-traumatic atrophy has previously been defined in members of the TBI cohort in comparison with age-matched healthy controls but no comparisons have previously been made with other neurodegenerative diseases (Cole et al., 2018a). Patients after TBI were a median of 40 years old at baseline visit (IQR 17.2) which was 1.9 years (median) after injury (IQR 6.3). Injuries were typically sustained in road traffic accidents (44%) or falls (29%), followed by assault (15%). Most of the TBI patients (92%) had a period of post-traumatic amnesia after injury. MRI scans showed evidence of focal lesions in 69% of cases and 46% (21/46 assessed) had microhaemorrhages on MRI suggestive of diffuse vascular injury. Focal lesions were present in 69%. Patients had a range of post-injury cognitive impairments as previously described, including of memory, processing speed and executive function (Cole et al., 2018a).

Healthy volunteers were assessed at both sites. Twenty-three healthy controls were assessed at UCL with a median age of 68.5 (IQR 7.5). At Imperial, 23 healthy controls (HCs) age-matched to the TBI patients were assessed (ICL HCs, median age 35 years, IQR 19.7). To define atrophy patterns associated with ageing, fifteen older healthy controls (HCs) with no history of head injury or cognitive problems were also assessed at Imperial (median age 65.8 years, IQR 7.3).

There was no significant difference in age between AD patients and healthy volunteers at UCL, or between TBI patients and the younger group of healthy controls at ICL. As expected, the older group of healthy controls at the Imperial site were not significantly

different in age from AD patients or the UCL healthy control group, but were older than TBI age-matched healthy controls (W=0, P<0.001) at Imperial. The proportion of female participants differed significantly across the five groups (X^2 24.4, df 4, P<0.001). There were no sex differences between the AD patients and age-matched controls, however the TBI group had a lower proportion of females than the age-matched control group (X^2 4.9, d=1, P=0.028), as did the older healthy controls (X^2=7.1, df=1, P=0.008).

	Alzheimer's disease	**Healthy Controls**	**Traumatic brain injury**	**Young healthy controls**	**Older healthy controls**
Participants, N	45	23	48	23	15
Age, years, median (IQR)	68.6 (9.9)	68.5 (7.5)	40.0 (17.2)	35.0 (19.7)	65.8 (7.3)
Male, N (%)	18 (40%)	12 (52%)	39 (81%)	13 (57%)	14 (93%)
Interscan interval, years, median (IQR)	1.49 (0.98)	1.49 (0.99)	2.1 (2.1)	1.1 (0.4)	1.7 (0.5)
Scanner site	UCL		ICL		

Table 19. Demographics of patients and healthy volunteers

UCL: University College London, ICL: Imperial College London; IQR: interquartile range.

6.3.2 Neuroimaging processing and analysis

At UCL, an inversion recovery prepared fast spoiled gradient recalled (IR-FSPGR) sequence was used to acquire 3D volumetric T1-weighted images in AD patients and age-matched controls longitudinally with a field of view of 24 cm, with a time to repetition of 15ms, an echo time of 5.4ms, TI of 650ms, flip angle of 15°, in a 256x256 matrix, comprising 124 contiguous 1.5 mm coronal slices, resulting in a voxel size of 0.9735mm x 0.9735mm x 1.5mm. At ICL, patients were assessed twice on the same Siemens Verio 3T system (Siemens Healthineers AG, Erlangen, Germany), alongside age-matched controls and a group of older healthy controls to assess the effect of ageing on brain structure. The MPRAGE sequence used the following parameters: slice thickness of 1mm, with 160 slices and a matrix of 256x240, with a repetition time

of 2300ms, echo time of 2.98ms, flip angle 9°, field of view of 25.6cm x 24cm, with a voxel size of 1.0 x 1.0 x 1.0 mm. When more than two scans were available for any study participant within the two cohorts, the scan pair with the longest inter-scan interval was chosen to reduce noise in the generation of atrophy rates. Exclusion criteria for healthy controls across both sites included history of significant brain injury, or neurological or psychiatric disease.

To generate multiple comparison corrected maps of disease-specific longitudinal atrophy, the threshold-free cluster enhancement (TFCE) corrected P value maps for each condition were binarised using a cut-off of 0.9. Regions of significant change were those with a one-sided t-test with $P<0.05$, reflecting the strong a-priori hypothesis that each condition would be associated with varying degrees of grey matter atrophy, WM atrophy and CSF expansion, relative to controls. An AD-specific longitudinal atrophy map was generated by multiplying the AD TFCE P-map by an inverted mask of the TBI map; the opposite approach was taken to generate a TBI-specific map. The AD-specific map was subtracted from the AD map to produce a map of shared atrophy in TBI and AD. The degree of overlap between two mask images, quantified by the Dice coefficient, was calculated using Matlab (Mathworks, R2017b). This is defined as twice the common area between the scans, divided by the total number of voxels in each mask image.

6.3.3 Statistical analyses

As described in the general methods (Chapter 2), analyses on summary measures were performed using R studio (R version 3.6.0). The following comparisons were performed at baseline for volume and for summary JD measures longitudinally: AD vs healthy controls; TBI vs young controls (ICL), TBI vs older controls (ICL), young vs older controls (ICL), and healthy controls (UCL) vs older controls (ICL). False discovery rate multiple comparison correction was used for post-hoc testing.

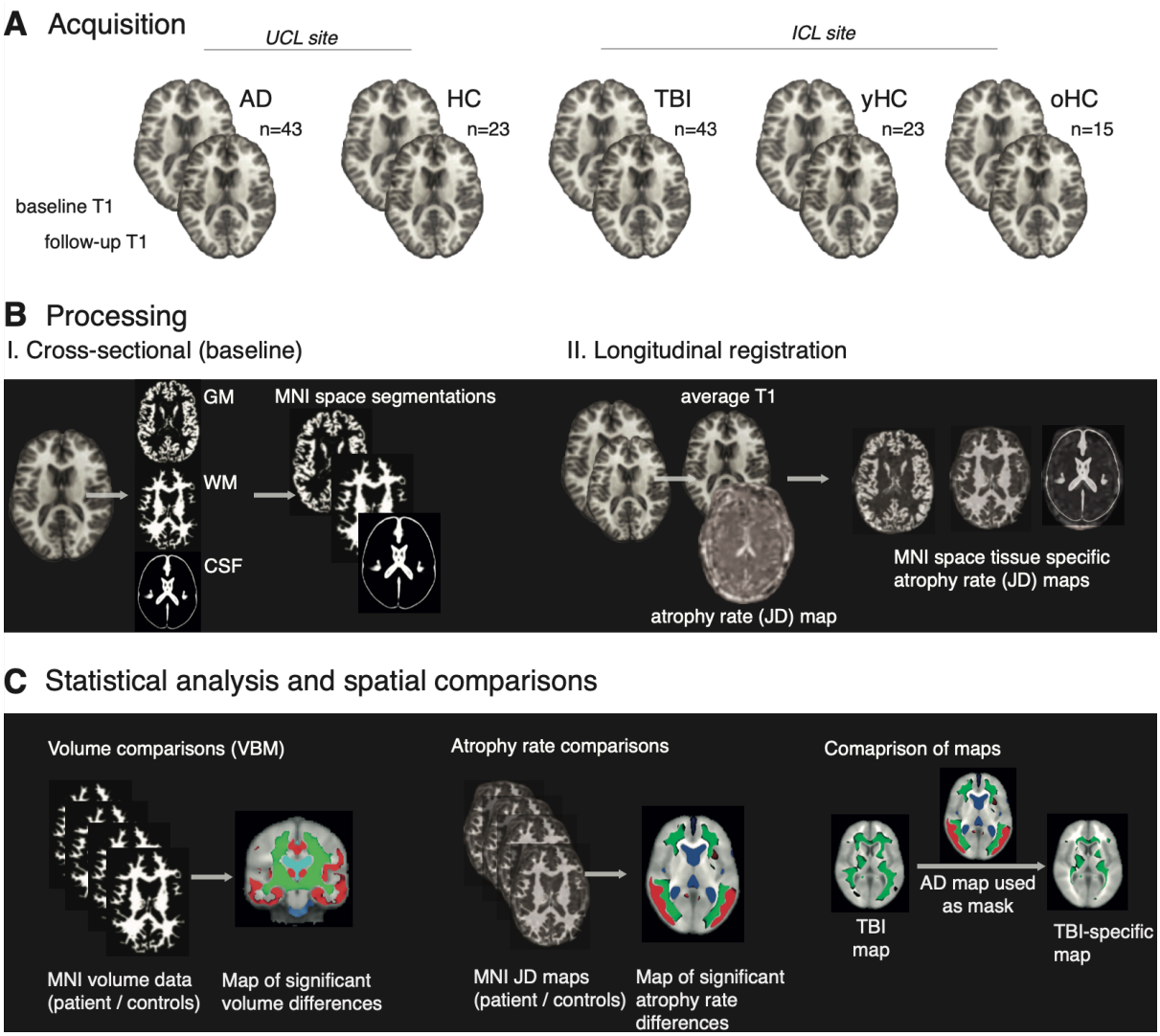

Figure 24. TBI and AD comparison methods

A. Serial volumetric T1-weighted MRIs are acquired in AD and HCs scanned at UCL, patients in chronic phase after single moderate-severe TBI, young healthy controls (yHC) and older healthy controls (oHC) at ICL. B. Cross sectional processing involved segmentation and non-linear registration to MNI space. Images are modulated to preserve volume. Longitudinal registration of scan pairs generates temporal average space T1 map and JD atrophy rate maps. The JD map is multiplied by the segmented temporal average image and registered to MNI space. C. MNI space images are used in permutation testing to assess differences in volume or atrophy rates. Subtractive analyses, using P-stat images outputted from other disease entities, are used to show disease-specific atrophy patterns or shared patterns of progressive atrophy.

6.4 Results

6.4.1 Volume loss at baseline is most substantial in Alzheimer's disease

Brain volumes were assessed at the baseline scanning visit, with normalisation for total intracranial volume as a proxy for head size (Table 20). Compared with all other groups, patients with AD had the lowest volumes of grey and white matter, and the largest CSF volume (FDR-corrected, all P values < 0.001) (Figure 25A). TBI patients had significantly lower baseline volumes compared with healthy controls in white matter (TBI median WM:TICV ratio 0.31, HC 0.33, P<0.001) and grey matter (TBI 0.45; HC median 0.48, P=0.006), with larger CSF volume (0.24 vs 0.19, P<0.001). There was no significant difference of white matter, or CSF volumes in TBI patients compared with healthy older controls, but grey matter volumes were higher in the TBI group than older controls (0.45 vs 0.43).

Voxelwise patterns of baseline cross-sectional brain atrophy and CSF expansion were assessed. AD and TBI patients were compared with their own age-matched controls, whose data were acquired on the same scanner system (Figure 25B). Older and younger healthy controls (ICL groups) were compared to assess change related to healthy ageing. In AD, significantly lower volume at baseline was evident in many areas, particularly in temporo-parietal grey matter regions. There were widespread reductions in white matter volume as well as expansion of the lateral ventricles.

Patients after TBI had limited regional grey matter atrophy within fontal and parietal regions, with limited temporal atrophy, but most notably substantial central white matter atrophy compared with age-matched controls. There were no regions with significant brain volume differences between TBI and older healthy controls at baseline.

There were similarities in the spatial distribution of atrophy when looking at the AD contrast and the older versus younger healthy volunteer contrast. Baseline atrophy was seen within temporal lobe structures in both cases, as well as frontoparietal cortical regions and subcortical white matter. However, the temporal lobe involvement was more extensive in the AD contrast, and white matter atrophy deeper and more widespread in ageing.

	Alzheimer's disease (UCL)	Healthy volunteers (UCL)	Traumatic brain injury (ICL)	Young healthy controls (ICL)	Older healthy controls (ICL)
Baseline volume, median (IQR)					
Grey matter	0.38 (0.04)	0.44 (0.04)	0.45 (0.04)	0.48 (0.02)	0.43 (0.04)
White matter	0.29 (0.03)	0.31 (0.02)	0.31 (0.03)	0.33 (0.02)	0.32 (0.02)
Whole brain	0.67 (0.05)	0.76 (0.06)	0.76 (0.05)	0.81 (0.05)	0.75 (0.03)
CSF	0.33 (0.05)	0.24 (0.06)	0.24 (0.05)	0.19 (0.05)	0.25 (0.03)
JD atrophy rate, median (IQR)					
Grey matter	-0.008 (0.008)	-0.002 (0.002)	-0.002 (0.005)	0.000 (0.005)	0.000 (0.004)
White matter	-0.009 (0.009)	-0.002 (0.003)	-0.003 (0.007)	0.001 (0.007)	-0.004 (0.006)
Whole brain	-0.009 (0.009)	-0.002 (0.003)	-0.003 (0.005)	0.001 (0.006)	-0.002 (0.004)
CSF	0.010 (0.007)	0.003 (0.003)	0.004 (0.009)	0.003 (0.006)	0.009 (0.004)

Table 20. Brain volumes and longitudinal atrophy rates

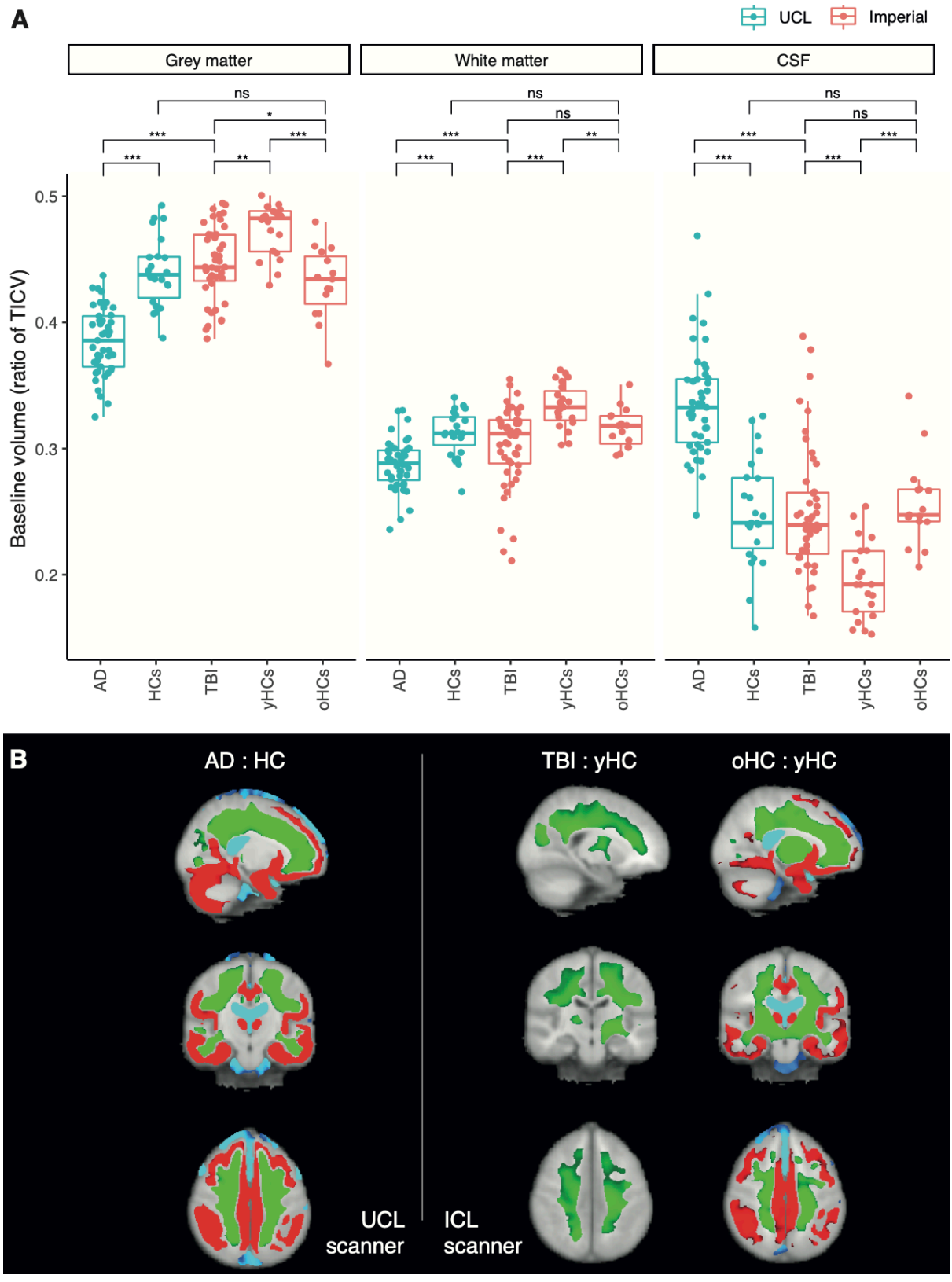

Figure 25. Brain volumes and atrophy at baseline scanning visit

A. A. Brain volumes across different groups normalised by total intracranial volume (TICV). Comparisons are between AD and HCs at UCL; AD and TBI; TBI and ICL

*young healthy controls (yHCs); TBI and ICL older healthy controls (oHCs); yHCs and oHCs; HCs at UCL and oHCs at ICL. Wilcox tests performed, P values are FDR corrected for multiple comparisons. *=P<0.05; **=P<0.01; ***=P<0.001. B. Voxelwise contrasts (TFCE corrected P value significance maps) showing patterns of white matter/grey matter atrophy and CSF expansion in AD (left); TBI vs young controls (middle) and TBI vs older controls (right)*

6.4.2 Atrophy rates are raised in AD and post-TBI, but to different extents

In comparison with age and scanner matched healthy controls, patients with AD had markedly raised atrophy rates in grey matter (median JD rate in AD -0.008 vs HC -0.002) and white matter (-0.009 vs -0.002), and higher rates of CSF expansion (0.010 vs 0.003; all P values <0.001) (Table 20, Figure 26A).

Atrophy rates were abnormally elevated in the white matter of TBI patients and were significantly higher than in young healthy controls (median WM JD -0.003 vs 0.001, P=0.019), but not different from those of older healthy controls (median WM JD -0.004). Grey matter atrophy rates were significantly raised after TBI versus age-matched controls (TBI -0.002 vs HC 0.000, P=0.05), but not when compared to older healthy controls. CSF expansion rates did not differ between TBI and young controls, but were significantly higher in older healthy controls than TBI patients (TBI median 0.004 vs older HC 0.009, P=0.040).

Directly comparing AD and TBI showed that, in AD, atrophy rates were higher in both grey (AD -0.008 vs -0.002, P<0.001) and white matter (-0.009 vs -0.003, P<0.001), with a raised rate of CSF expansion in AD (0.010 vs 0.004, P=0.003). Assessing changes in atrophy rates associated with ageing, i.e. comparing older with younger healthy controls (scanner matched), older controls had greater CSF expansion rates (0.009 vs 0.003, P=0.040) but no significant differences in either white matter or grey matter atrophy rates.

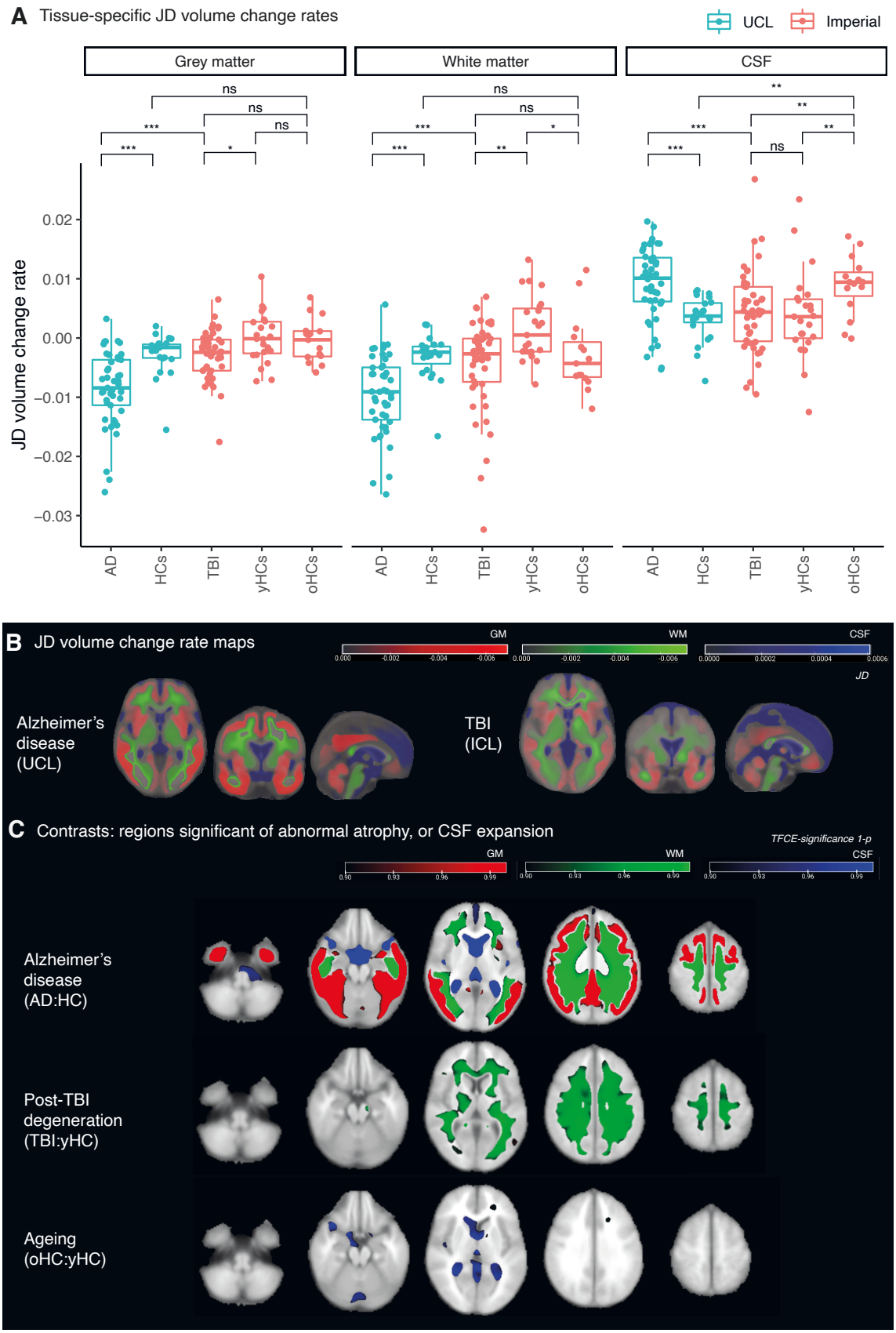

Figure 26. Longitudinal patterns of brain volume change in AD and after TBI

*A. JD volume change rates. HC: healthy control; yHC: younger healthy control (ICL) oHC: older healthy control (ICL). *=P<0.05; **=P<0.01; ***=P<0.001. B. Group average JD maps showing atrophy rates in grey matter (red) or white matter (green) and CSF expansion (blue). C. Voxelwise contrasts of JD rate maps. Regions of significantly increased atrophy rates in grey matter are in red, white matter in green, and CSF expansion in blue.*

6.4.3 Defining spatial patterns of progressive volume loss in AD, TBI and ageing

Group average JD atrophy rate maps are shown for AD and TBI (Figure 26B). A comparison of patients with Alzheimer's disease and age-matched healthy controls revealed significant AD-related grey matter atrophy with a temporo-parietal predilection but not including primary motor cortices, with high atrophy rates in much of the white matter, but not the corticospinal tracts (Figure 26C, upper row).

In TBI versus age-matched controls, there was no significant regional abnormal progressive grey matter atrophy, but elevated white matter atrophy rates were present centrally including the corpus callosum, superior longitudinal fasciculus, and descending corticospinal tracts within the corona radiata, centrum semiovale, internal capsule (Figure 26C, middle row).

To define the pattern of change in atrophy rates associated with ageing over three decades, atrophy rates in healthy older adults were compared with younger controls, revealing a small region of left frontal white matter atrophy including the anterior thalamic radiation (Figure 26C, lower row).

6.4.4 Distinct patterns of atrophy over time are present

To define atrophy patterns specific to each of Alzheimer's disease and TBI, the maps of significant regional brain volume change over time were compared (Figure 27). The similarity between the significance maps across different pathologies (TBI, AD and ageing) was compared. There was substantial overlap between the AD and TBI maps (Figure 27A) in white matter, indicated by a high Dice coefficient of 0.80, but no overlap in the grey matter (Dice = 0.00) or CSF (Dice = 0.00). The overlapping regions were predominantly subcortical rather than involving structures of the deep white matter.

Comparing post-TBI atrophy and ageing there was minimal overlap (GM Dice = 0.00, WM Dice = 0.03, CSF DICE = 0.00) as expected, given the few regions surviving multiple comparison correction on the voxelwise map of significant longitudinal volume change in ageing. Ageing and AD had overlap in CSF (Dice = 0.61), but less so in white matter (Dice = 0.31) or grey matter (Dice = 0.00).

An 'AD-specific' atrophy map was generated by subtracting regions of significant TBI-related atrophy from the AD map. This showed raised atrophy rates specific to AD within the temporal grey matter, parietal and occipital cortices and white matter regions including the inferior occipito-frontal fasciculi bilaterally, which are not seen after TBI (Figure 27B, upper row).

Using the same approach a 'TBI-specific' atrophy map (Figure 27B, middle row) was generated, by subtracting the AD image from the TBI map. This showed TBI-specific increases in atrophy rate particularly involving the corona radiata, corpus callosum, internal capsules, corticospinal tracts and cerebral peduncle (right). Lastly, for completeness, this TBI-specific map with respect to Alzheimer's disease was refined by removing regions of significant change attributable to ageing. The resulting image appeared substantially unchanged (Figure 27B, lower row).

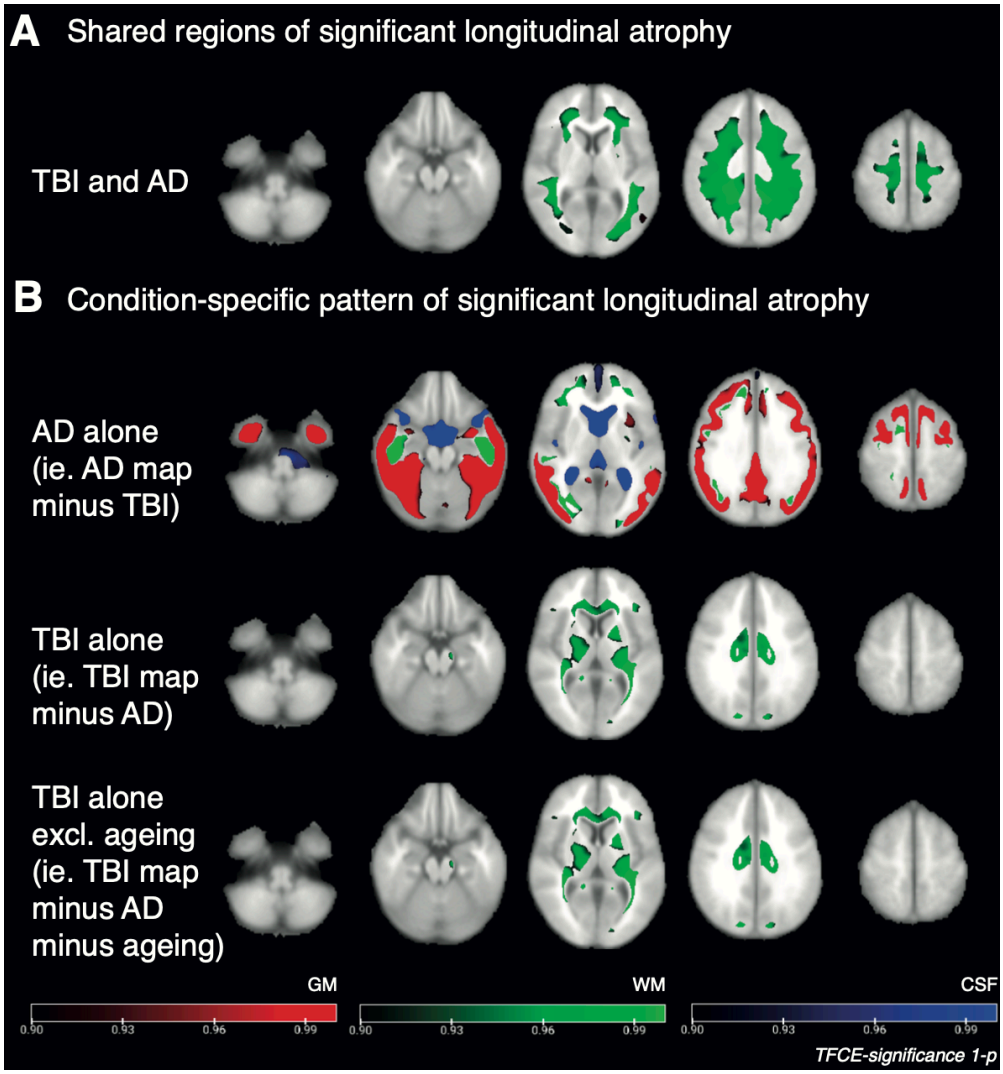

Figure 27. Comparisons of atrophy rates between AD, TBI and ageing

Composite figure showing shared significant volume change over time between TBI and AD. B. Composite significance maps: the top map indicates regions of significant volume change which are found only in Alzheimer's disease but not in TBI; the middle map shows regions significant in TBI only, but not AD; and the lowermost map shows this but with regions significantly changing in ageing also excluded.

6.5 Discussion

Here, I show that progressive brain atrophy in the chronic phase after single moderate-severe TBI differs significantly from mild-moderate late-onset AD and healthy ageing. Although atrophy rates were significantly higher in both white matter and grey matter in AD than after TBI, I demonstrate that the involvement of central white matter structures is highly specific to TBI and is not seen in AD. Progressive cortical atrophy was not widely present after trauma and appears more specific to AD.

Importantly, the age difference between patients with AD and post-TBI did not explain the progressive brain volume differences between these groups. As patients in the chronic phase after TBI were considerably younger than those with AD, I explored this in several ways. At baseline, the extent of established brain atrophy was significantly greater in AD than in either TBI or healthy ageing. There was substantial spatial similarity in the distribution of volume loss in AD and ageing over three decades. Whereas baseline volumes in patients after TBI were reduced in white matter and grey matter compared with young healthy controls age-matched to the TBI group, the magnitude of this volume loss was similar to that seen in healthy controls several decades older than the TBI patients. The spatial distribution of this established atrophy was different however: post-traumatic atrophy was predominant within the deep white matter, rather than involving temporal and frontal regions seen in both AD and ageing.

There was similarity in established atrophy patterns at baseline in AD and healthy ageing. Ageing is the foremost risk factor for a range of late-onset neurodegenerative disorders including AD (Wyss-Coray, 2016) and bran volume loss is a feature of both neurodegenerative dementias and ageing (Terry et al., 1987, Fjell et al., 2014). Overlap between healthy ageing and AD atrophy has previously been reported although frontal volume loss appears more age-related (Pichet Binette et al., 2020). This distribution may reflect presymptomatic AD in ageing individuals (Fjell et al., 2010), resulting in combination of age-related change and presymptomatic neurodegenerative disease.

The relationship between diffuse axonal injury and progressive atrophy after TBI using diffusion tensor imaging and longitudinal volumetric data has been investigated (see Chapter 5, (Graham et al., 2020b)). The distribution of TBI-specific atrophy, in

comparison with AD and ageing, is highly reminiscent of the common pattern of axonal injury reported after head injury, attributable to shear forces affecting central white matter structures (Kinnunen et al., 2011). Axonal injury is likely to drive chronic central white matter atrophy via slow Wallerian degeneration of these damaged structures (Hill et al., 2016) or perhaps via toxic proteinopathies (Smith et al., 2013). Although grey matter atrophy rates were increased in the TBI group versus age-matched controls, as in previous work (Graham et al., 2020b), this was not as extensive voxelwise, perhaps relating to the slightly smaller number of patients or composition of the groups.

The similarity in brain atrophy rates between TBI and healthy older volunteers may suggest that TBI accelerates brain ageing. Indeed, machine-learning approaches to analysis of brain structure on MRI after TBI does suggests that post-traumatic brains appear 'older' than would be expected given the patients' chronological age (Cole et al., 2015). However, these approaches also show higher 'brain ages' in more advanced AD (Beheshti et al., 2018) and I did not find spatial congruence between atrophy patterns over time in TBI and ageing in this investigation. Indeed, after removing regions of age-related brain atrophy, there remained a clear TBI-specific pattern of longitudinal atrophy involving the corpus callosum and corticospinal tracts.

This investigation has several potential limitations, which I have sought to mitigate. One consideration is the high sensitivity but poor molecular specificity of brain atrophy as a measure of neurodegeneration, limiting the inferences which can be made from this work. However, this feature is useful if the underlying molecular basis of volume loss is unclear a-priori, such as in this comparison. Importantly for this work, there is clear evidence that atrophy patterns frequently have spatial specificity for underlying pathology, for example atrophy patterns mirror the distribution of tau pathology in AD (La Joie et al., 2020). Two research sites (Imperial and University College London) were used to acquire the imaging data. Each individual was always imaged on the same scanner, such that longitudinal atrophy rates are essentially normalised with each acting as his/her own 'control', mitigating the effects of scanner differences. The presence of focal lesions may have influenced our findings, but I do not suspect a significant effect on these conclusions in spite of the non-availability of lesion masks

for the TBI group. First, the overall presence or absence of focal lesions was included as a nuisance regressor in voxelwise analyses to mitigate this. Second, previous work assessing longitudinal atrophy in an overlapping TBI cohort did not show any change in atrophy rates / patterns when excluding individuals without focal lesions (Cole et al., 2018a). The TBI patients were established within the chronic phase at approximately two years post-event, making significant ongoing evolution of focal lesions or resolution of oedema extremely unlikely.

In conclusion, this investigation provides evidence that chronic post-traumatic neurodegeneration is distinct from Alzheimer's disease and healthy aging, which showed similarities. Patterns of volume loss within the deep cerebral white matter are highly reminiscent of typical patterns of diffuse axonal injury and appear specific to TBI. Indicating the magnitude of brain atrophy after TBI, I show that rates are similar post-injury to healthy individuals three decades older than our patient group. Future investigation should characterise the molecular signatures of post-traumatic atrophy, using tools such as positron emission tomography and blood biomarker assessment alongside serial MRI. A better understanding of the relationship between injury and progressive sequelae would help to focus strategies to prevent dementia after TBI, and to target clinical trials of anti-neurodegenerative treatments.

7 Discussion

7.1 Summary of findings

The aim of this programme of investigation was to characterise the relationship between axonal injury and post-traumatic neurodegeneration after TBI.

Chapter 3 describes a longitudinal investigation of axonal injury acutely after TBI measured using fluid biomarkers. I provide evidence that NfL has a unique time course in plasma peaking subacutely around 20 days post-injury, making it particularly amenable to clinical sampling at this time where symptoms may not map well to the underlying pathologies, and where there may be diagnostic uncertainty. For NfL, tau and UCH-L1, I show that levels within brain extracellular fluid are approximately 100 times higher than in plasma early post-injury, and that the two are highly correlated. This provides important evidence that sampling plasma levels provides a meaningful readout of extensive traumatic tissue damage deep within injured white matter. In addition, I describe biomarker results in a group of patients with traumatic extracranial injuries only, and show that concentrations of fluid biomarkers are significantly lower in these individuals than following TBI, highlighting the specificity and clinical applicability of this approach.

In Chapter 4 I present the aligned neuroimaging results of the BIO-AX-TBI study and relate these to fluid biomarker dynamics and clinical outcomes. I show that there is a strong correlation between the peak plasma NfL levels and evidence of axonal injury on DTI. This relationship is supported further in a data-driven way using factor analysis, with DTI FA and plasma NfL loading heavily on the same factor, suggesting these measure the same underlying biological substrate i.e. axonal damage after injury. This provides further mechanistic validation of NfL as an axonal injury measure, given that DTI has been validated against histopathological change (Mac Donald et al., 2007a, Mac Donald et al., 2007b). Importantly, I show that plasma NfL sampled at this subacute timepoint point reliably predicts the extent of accelerated neurodegeneration in white matter following injury up to a year post-TBI. Further evidencing the utility of assessing axonal injury with fluid biomarkers after TBI I show that the cortical axonal marker tau peaks within days of injury, and in contrast to NfL,

closely correlates with the extent of subsequent grey matter atrophy after TBI. Together these investigations show that there is clinical utility in assessing axonal injury after TBI in the acute phase, that NfL is amenable to a clinical assessment subacutely and that levels in plasma reflect damage to white matter within in the brain.

In Chapter 5 I investigate the relationship between axonal injury evidenced by diffusion tenser MRI in the chronic phase after moderate-severe TBI and assess how this relates to progressive brain atrophy, in particular testing whether this predicts neurodegeneration better than other available clinical and neuroimaging measures. I showed that there was significant evidence of TAI in the TBI group and that atrophy rates were increased longitudinally. Notably, the diffusion findings were stable over time suggesting that DTI and volume represent different dimensions of white matter health. For the first time in adults in the chronic phase after moderate-severe injuries, I show that damage on DTI at the baseline scanning timepoint reliably predicts white matter atrophy over time, and does so more accurately than the other putative predictors. Furthermore, I found that elevated atrophy rates were associated with poorer performance on neuropsychological testing, evidencing the potential utility of atrophy rates as a surrogate outcome measure. This evidence supports the hypothesis that TAI triggers progressive neurodegeneration over time, when assessed relatively late after injury.

In Chapter 6 I seek to better define the neurodegenerative consequences of axonal injury. Using longitudinal volumetric MRI in the chronic phase after TBI, in late-onset Alzheimer's disease and healthy ageing, I compare patterns of atrophy while accounting for the age differences between groups. I show that although there is marked similarity between ageing over three decades and atrophy in AD at baseline and that patterns of established and longitudinal change in TBI are distinctive. Post-traumatic atrophy occurs in a distribution highly reminiscent of axonal injury distributions, with extensive deep white matter loss within the corpus callosum and of the corticospinal tracts. In contrast, atrophy patterns in AD and ageing included substantial temporal cortical change, with atrophy of frontal regions to a varying extent. These data support the hypothesis that axonal injury triggers neuropathological

change locally, and that this determines atrophy patterns which are similar in magnitude to ageing over three decades, but spatially different from AD and ageing.

7.2 Interpretation

These findings provide evidence that TAI, measured in several different ways at different timepoints after TBI is mechanistically linked to progressive post-TBI neurodegeneration, of key importance given the established epidemiological relationship between head injuries and dementia. My investigations show that after acute moderate-severe TBI, there is extensive damage and release of axonal proteins including NfL and tau. Concentrations were very significantly elevated in brain extracellular fluid measured directly within diffusely injured white matter, changes which are accurately reflected in blood. Traumatic damage, quantified with markers such as NfL, tau and DTI FA was associated with progressive brain volume loss, in investigations which spanned a range of time periods post injury. One possible mechanism is prion-like spread of proteinopathies generated early after injury. While AD neuropathological change of tau and amyloid may be key underlying mechanisms, I did not find convincing evidence to support a typical AD *distribution* of late neurodegeneration after TBI, with post-traumatic atrophy patterns similar to axonal damage patterns rather than AD or ageing.

7.3 Practical implications

Providing evidence relating axonal injury to progressive neurodegeneration after TBI is important clinically and for public health interventions aimed at reducing dementia risk. Widespread, clinically feasible approaches to quantifying axonal injury will be important in understanding and protecting brain health in future, and the validation of peripheral sampling of NfL in plasma post-TBI is an important step towards translating this marker into widespread clinical use. NfL is one of most promising markers of damage across a range of neurological diseases where axonal degeneration is a feature (Gaetani et al., 2019) and has a unique double role after TBI, quantifying both early injury and chronic degeneration. However, lack of detailed examination in moderate-severe TBI previously is notable, as was the historic challenge of sampling this in CSF, requiring lumbar puncture. Cross-validation of plasma NfL with DTI FA

adds to limited earlier work showing that these are correlated (Shahim et al., 2020a) and the finding that central levels tested using microdialysis correlate with peripheral levels is both novel and significant for this sampling approach. Testing patients at around the 20-day timepoint, where NfL concentrations peak in plasma, appears optimal. Assessment at this point could provide clinicians with greater confidence about the presence of significant TAI underlying symptoms, which are frequently poor markers of damage (Sharp and Jenkins, 2015). While there were elevations of blood biomarkers in non-TBI trauma, concentrations were far higher after TBI, providing reassurance that this tool will be of use in practice where mixed injuries are common. Further data to help define normal and pathological ranges would be helpful, with data collected in peripheral nerve injuries and spinal injuries of particular interest.

Defining the temporal trends of different TAI biomarkers is important for translation. For example, plasma tau provides an early readout of axonal injury, followed by NfL subacutely or diffusion-weighted MRI / NfL late after injury. The imaging approach provides more opportunity to define the spatial pattern rather than total amount of axonal damage or degeneration, and also a baseline measure of brain volume which could be used longitudinally to define degenerative consequences of injury if progressive problems arise. There are a wide range of opportunities of these tools to assist in axonal injury diagnosis, TBI prognostication and monitoring/diagnosis of neurodegenerative sequelae.

Improving the diagnostic categorisation of injury would be an important consequence of widespread biomarker use. What may appear to be a clinically severe injury could in reality involve little parenchymal damage / TAI. Although a patient with a traumatic extradural haematoma requiring urgent evacuation would be graded as moderate-severe on the Mayo classification and is likely to require ICU care, fluid or imaging markers may well reflect the absence of substantial marked damage. A more precise injury classification based on biomarker levels studied over time at the individual level would be clinically helpful, in contrast to broad categories which encompass vast heterogeneity of injury. This is likely a more informative approach than traditional clinical measures of severity which can be highly variable in practice.

7.4 Barriers to overcome

Translation necessitates the demonstration of satisfactory analytical performance at various stages, including the accuracy of the test, precision and reproducibility over time or across test kits, operators or centres, and issues around the stability of samples. This work has begun in relation to NfL which appears to be stable across freeze-thaw cycles, but clinical laboratory-grade approval for the Simoa assay is not yet complete (Keshavan et al., 2018).

New fluid biomarker assays are extremely sensitive to neurotrauma. This raises a question of what cut-offs would be diagnostically relevant in clinical practice. One approach to this high sensitivity combined with uncertainty is to utilise the diagnostic value of a *negative* test: for instance, a highly sensitive combined test for UCH-L1 and GFAP has received approval in the setting of mild injuries. If levels are non-elevated, the clinician can be confident of an extremely low probability of the presence of abnormality on CT (Bazarian et al., 2018). While this represents an important step for the field, it would be helpful to use biomarker approaches to move beyond diagnosing the absence of pathology, and to move towards diagnosing the presence of clinically important pathologies. In relation to diagnosis, in the acute setting, this likely necessitates marker assessment across a wide range of injury severities where outcomes are known. Large collaborative international research consortia in TBI and the use of common data elements mean that this is feasible to produce.

The quantitative use of atrophy on MRI necessitates some changes in our current practice and a shift away from qualitative radiologist reports. In order that scans can be reliably co-registered and atrophy rates generated, we will have to take more care to undertake serial clinical scans on the same scanner system, and to increase expertise on post-processing and analysis within departments. Such changes may be most easily promoted by the manufacturers of MRI systems. Given its established use in the highly regulated clinical trials setting as an outcome measure, it would seem appropriate for atrophy rates to be incorporated into clinical decision making particularly around diagnosis of neurodegenerative disease.

Further work with the neuroimaging analysis methods used in this programme of investigation will be important prior to clinical use: for example, tools such as tensor-

based morphometry and TBSS were not specifically developed for the TBI setting, which can be associated with significant and highly variable anatomical change. This introduces noise at the group-level, which can be reduced with approaches such as lesion-masking. This strengthens effect sizes and is likely to be adequate for clinical trials. However, for clinical use at the individual level, future work will need to find ways to reliably dissect meaningful signal from artefact, and prove that this works across a range of post-traumatic pathologies.

7.5 Related questions

Given the convincing mechanistic relationship between traumatic axonal injury and the generation of toxic species, it is notable that not all individuals with significant TBI including axonal damage develop neurodegenerative disorders. Understanding the heterogeneity of outcome here is likely to hinge not just on an accurate assessment of the true extent of axonal damage (as above) but upon the other contributing factors which interact with injury. Genetic risk is likely to be important, even if this is a non-modifiable consideration for post-TBI change. For example, it has already been shown that APOE status, the major genetic risk factor for sporadic late-onset AD, relates to injury outcomes (Hayes et al., 2017). However, using microarrays or whole genome sequencing to assess polymorphisms across a range of genomic loci (Escott-Price et al., 2015), it may be possible to capture far more information about the polygenic risk of neurodegeneration after injury. This may capture abnormalities in several important pathways.

One consideration is the clearance of abnormal proteins from the brain, which like any physiological process is likely to vary between individual patients. This could affect diagnostic biomarker levels, for example generating a spuriously low/high NfL, or indeed interfere with biochemical cascades following axonal damage, such as where poor clearance of a protein seed promotes greater neurodegeneration. The presence of abnormal species of hyperphosphorylated tau found post-mortem in teenage athletes who died within days of mild TBI (Tagge et al., 2018) and the lack of ubiquity of CTE tau pathology in brain banks suggests that changes are not inexorability progressive. The function of glymphatic systems is implicated in tau accumulation post-injury, and may potentially vary depending on injury (Iliff et al., 2014). A balance

between generation and clearance is better characterised in the case of amyloid: neprilysin is involved in the enzymatic degradation of amyloid β (Iwata et al., 2000), with polymorphisms in the neprilysin gene significantly influencing the presence of plaques post-TBI (Johnson et al., 2009, Chen et al., 2009).

Neurodegeneration may be perpetuated by abnormal chronic neuroinflammation post-injury, which is likely to vary between individuals and may be amenable to intervention to different extents, although there is complexity in defining helpful versus deleterious immunological responses to injury (Scott et al., 2018). Chronic abnormalities of the blood brain barrier (Hay et al., 2015) may further influence this and need to be better understood longitudinally post-injury, perhaps facilitated by non-invasive tools such as DCE-MRI (Varatharaj et al., 2019).

7.6 Future directions

The biomarkers described provide a toolbox to sensitively identify TAI, measure its consequences and test treatments in early clinical trial stages. NfL has been used as a neurodegeneration measure in clinical trials but so far, its use after TBI for this purpose has been more limited. Interpretation has been challenging in several trials where concentrations have risen unexpectedly, in the context of otherwise positive outcome signals. Examples include a dose-dependent elevation NfL in response to antisense oligonucleotide treatment in Huntington's disease, where several follow-up studies have since been discontinued for as-yet uncertain reasons (Tabrizi et al., 2019) or with minocycline treatment of chronic inflammation after TBI (Scott et al., 2018). These situations warrant careful investigation to establish whether NfL rises are necessarily deleterious as is widely thought, or if situations exist in which a rise is tolerable, or indeed physiologically beneficial. In TBI, a therapeutic focus on maintaining axonal integrity may be beneficial, extending preclinical work in which Wallerian degeneration has been successfully slowed in vivo, for example by inhibition of the neurofilament-degrading enzyme calpain (Wang et al., 2012).

The epidemiological data relating head injuries, traumatic axonal damage and subsequent dementia are likely to be improved by more detailed assessment and definition of the entities on either side of this equation, using many of the techniques

discussed in this thesis. For example, observational studies which define injuries using tools such as plasma tau / NfL will have an accurate readout of the initial insult, which can then be related to specific neurodegenerative pathologies, evolving over time and quantified using tools such as NfL, amyloid and tau PET. This would address key historic issues of injury definition and lack of certainty of neurodegenerative diagnosis. More detail is needed in respect of the typical fluctuations of biomarkers over hours, days and months within and between individuals and to define what constitutes a significant deviation from normal in various settings. Successful demonstration that new PET tracers are sensitive to post-traumatic conformations of tau will be an important step, given the limited sensitivity of earlier generations of ligand.

The link between TBI and dementia is both an important public health challenge and a remarkable potential therapeutic opportunity. This reflects our ability to define the neurological insult driving subsequent neurodegeneration at the individual level and the presence of a substantial time period following injury where a disease-modifying treatment could be given. Improved diagnosis and prognostication using biomarkers have the potential to improve clinical care very rapidly. In conjunction with intervention trials, future longitudinal observational studies will be able to relate injury exposures to patterns of damage and clinical outcomes over extended durations, with detailed phenotyping using biomarkers. These data will help to focus public health messaging on injury prevention, to promote long-term brain health and assist individuals in making informed choices about participation in activities with a high risk of significant injury.

8 References

ABNER, E. L., NELSON, P. T., SCHMITT, F. A., BROWNING, S. R., FARDO, D. W., WAN, L., JICHA, G. A., COOPER, G. E., SMITH, C. D., CABAN-HOLT, A. M., VAN ELDIK, L. J. & KRYSCIO, R. J. 2014. Self-reported head injury and risk of late-life impairment and AD pathology in an AD center cohort. *Dement Geriatr Cogn Disord,* 37**,** 294-306.

AL NIMER, F., THELIN, E., NYSTRÖM, H., DRING, A. M., SVENNINGSSON, A., PIEHL, F., NELSON, D. W. & BELLANDER, B.-M. 2015. Comparative Assessment of the Prognostic Value of Biomarkers in Traumatic Brain Injury Reveals an Independent Role for Serum Levels of Neurofilament Light. *PLOS ONE,* 10**,** e0132177.

AMERICAN PSYCHIATRIC ASSOCIATION 2013. Diagnostic and Statistical Manual of Mental Disorders. 5th ed. Washington, DC.

ANDERSON, R. E., HANSSON, L. O., NILSSON, O., DIJLAI-MERZOUG, R. & SETTERGREN, G. 2001. High serum S100B levels for trauma patients without head injuries. *Neurosurgery,* 48**,** 1255-8; discussion 1258-60.

ARENA, J. D., SMITH, D. H., LEE, E. B., GIBBONS, G. S., IRWIN, D. J., ROBINSON, J. L., LEE, V. M.-Y., TROJANOWSKI, J. Q., STEWART, W. & JOHNSON, V. E. 2020. Tau immunophenotypes in chronic traumatic encephalopathy recapitulate those of ageing and Alzheimer's disease. *Brain,* 143**,** 1572-1587.

ARMON, C. 2007. Sports and trauma in amyotrophic lateral sclerosis revisited. *J Neurol Sci,* 262**,** 45-53.

ARMON, C. & NELSON, L. M. 2012. Is head trauma a risk factor for amyotrophic lateral sclerosis? An evidence based review. *Amyotroph Lateral Scler,* 13**,** 351-6.

ARNOLD, D. L. & DE STEFANO, N. 2013. Preventing brain atrophy should be the gold standard of effective therapy in multiple sclerosis (after the first year of treatment): Commentary. *Mult Scler,* 19**,** 1007-8.

ASHBURNER, J. 2007. A fast diffeomorphic image registration algorithm. *Neuroimage,* 38**,** 95-113.

ASHBURNER, J. & RIDGWAY, G. R. 2012. Symmetric diffeomorphic modeling of longitudinal structural MRI. *Front Neurosci,* 6**,** 197.

ASSAF, Y. & BASSER, P. J. 2005. Composite hindered and restricted model of diffusion (CHARMED) MR imaging of the human brain. *Neuroimage,* 27**,** 48-58.

BACIOGLU, M., MAIA, L. F., PREISCHE, O., SCHELLE, J., APEL, A., KAESER, S. A., SCHWEIGHAUSER, M., ENINGER, T., LAMBERT, M., PILOTTO, A., SHIMSHEK, D. R., NEUMANN, U., KAHLE, P. J., STAUFENBIEL, M., NEUMANN, M., MAETZLER, W., KUHLE, J. & JUCKER, M. 2016. Neurofilament Light Chain in Blood and CSF as Marker of Disease Progression in Mouse Models and in Neurodegenerative Diseases. *Neuron,* 91**,** 56-66.

BARNES, D. E., BYERS, A. L., GARDNER, R. C., SEAL, K. H., BOSCARDIN, W. J. & YAFFE, K. 2018. Association of Mild Traumatic Brain Injury With and Without Loss of Consciousness With Dementia in US Military Veterans. *JAMA Neurol,* 75**,** 1055-1061.

BARRIO, J. R., SMALL, G. W., WONG, K. P., HUANG, S. C., LIU, J., MERRILL, D. A., GIZA, C. C., FITZSIMMONS, R. P., OMALU, B., BAILES, J. & KEPE, V. 2015. In vivo characterization of chronic traumatic encephalopathy using [F-18]FDDNP PET brain imaging. *Proc Natl Acad Sci U S A,* 112**,** E2039-47.

BARRO, C., BENKERT, P., DISANTO, G., TSAGKAS, C., AMANN, M., NAEGELIN, Y., LEPPERT, D., GOBBI, C., GRANZIERA, C., YALDIZLI, Ö., MICHALAK, Z., WUERFEL, J., KAPPOS, L., PARMAR, K. & KUHLE, J. 2018. Serum neurofilament as a predictor of disease worsening and brain and spinal cord atrophy in multiple sclerosis. *Brain,* 141**,** 2382-2391.

BAZARIAN, J. J., BIBERTHALER, P., WELCH, R. D., LEWIS, L. M., BARZO, P., BOGNER-FLATZ, V., GUNNAR BROLINSON, P., BUKI, A., CHEN, J. Y., CHRISTENSON, R. H., HACK, D., HUFF, J. S., JOHAR, S., JORDAN, J. D., LEIDEL, B. A., LINDNER, T., LUDINGTON, E., OKONKWO, D. O., ORNATO, J., PEACOCK, W. F., SCHMIDT, K., TYNDALL, J. A., VOSSOUGH, A. & JAGODA, A. S. 2018. Serum GFAP and UCH-L1 for prediction of absence of intracranial injuries on head CT (ALERT-TBI): a multicentre observational study. *Lancet Neurol,* 17**,** 782-789.

BEHESHTI, I., MAIKUSA, N. & MATSUDA, H. 2018. The association between "Brain-Age Score" (BAS) and traditional neuropsychological screening tools in Alzheimer's disease. *Brain and behavior,* 8**,** e01020-e01020.

BEJANIN, A., SCHONHAUT, D. R., LA JOIE, R., KRAMER, J. H., BAKER, S. L., SOSA, N., AYAKTA, N., CANTWELL, A., JANABI, M., LAURIOLA, M., O'NEIL, J. P., GORNO-TEMPINI, M. L., MILLER, Z. A., ROSEN, H. J., MILLER, B. L., JAGUST, W. J. & RABINOVICI, G. D. 2017. Tau pathology and neurodegeneration contribute to cognitive impairment in Alzheimer's disease. *Brain,* 140**,** 3286-3300.

BENDLIN, B. B., RIES, M. L., LAZAR, M., ALEXANDER, A. L., DEMPSEY, R. J., ROWLEY, H. A., SHERMAN, J. E. & JOHNSON, S. C. 2008. Longitudinal changes in patients with traumatic brain injury assessed with diffusion-tensor and volumetric imaging. *Neuroimage,* 42**,** 503-14.

BERNICK, C., SHAN, G., ZETTERBERG, H., BANKS, S., MISHRA, V. R., BEKRIS, L., LEVERENZ, J. B. & BLENNOW, K. 2020. Longitudinal change in regional brain volumes with exposure to repetitive head impacts. *Neurology,* 94**,** e232-e240.

BIENIEK, K. F., ROSS, O. A., CORMIER, K. A., WALTON, R. L., SOTO-ORTOLAZA, A., JOHNSTON, A. E., DESARO, P., BOYLAN, K. B., GRAFF-RADFORD, N. R., WSZOLEK, Z. K., RADEMAKERS, R., BOEVE, B. F., MCKEE, A. C. & DICKSON, D. W. 2015. Chronic traumatic encephalopathy pathology in a neurodegenerative disorders brain bank. *Acta Neuropathol,* 130**,** 877-89.

BOBINSKI, M., DE LEON, M. J., WEGIEL, J., DESANTI, S., CONVIT, A., SAINT LOUIS, L. A., RUSINEK, H. & WISNIEWSKI, H. M. 2000. The histological validation of post mortem magnetic resonance imaging-determined hippocampal volume in Alzheimer's disease. *Neuroscience,* 95**,** 721-5.

BOGOSLOVSKY, T., WILSON, D., CHEN, Y., HANLON, D., GILL, J., JEROMIN, A., SONG, L., MOORE, C., GONG, Y., KENNEY, K. & DIAZ-ARRASTIA, R. 2017. Increases of Plasma Levels of Glial Fibrillary Acidic Protein, Tau, and Amyloid beta up to 90 Days after Traumatic Brain Injury. *J Neurotrauma,* 34**,** 66-73.

BONNELLE, V., LEECH, R., KINNUNEN, K. M., HAM, T. E., BECKMANN, C. F., DE BOISSEZON, X., GREENWOOD, R. J. & SHARP, D. J. 2011. Default mode network connectivity predicts sustained attention deficits after traumatic brain injury. *J Neurosci,* 31**,** 13442-51.

BREZOVA, V., MOEN, K. G., SKANDSEN, T., VIK, A., BREWER, J. B., SALVESEN, O. & HABERG, A. K. 2014. Prospective longitudinal MRI study of brain volumes and diffusion changes during the first year after moderate to severe traumatic brain injury. *Neuroimage Clin,* 5**,** 128-40.

CAEYENBERGHS, K., LEEMANS, A., GEURTS, M., TAYMANS, T., LINDEN, C. V., SMITS-ENGELSMAN, B. C. M., SUNAERT, S. & SWINNEN, S. P. 2010. Brain-behavior relationships in young traumatic brain injury patients: Fractional anisotropy measures are highly correlated with dynamic visuomotor tracking performance. *Neuropsychologia,* 48**,** 1472-1482.

CASH, D. M., FROST, C., IHEME, L. O., UNAY, D., KANDEMIR, M., FRIPP, J., SALVADO, O., BOURGEAT, P., REUTER, M., FISCHL, B., LORENZI, M., FRISONI, G. B., PENNEC, X., PIERSON, R. K., GUNTER, J. L., SENJEM, M. L., JACK, C. R., JR., GUIZARD, N., FONOV, V. S., COLLINS, D. L., MODAT, M., CARDOSO, M. J., LEUNG, K. K., WANG, H., DAS, S. R., YUSHKEVICH, P. A., MALONE, I. B., FOX, N. C., SCHOTT, J. M. & OURSELIN, S. 2015. Assessing atrophy measurement techniques in dementia: Results from the MIRIAD atrophy challenge. *Neuroimage,* 123**,** 149-64.

CASH, D. M., ROHRER, J. D., RYAN, N. S., OURSELIN, S. & FOX, N. C. 2014. Imaging endpoints for clinical trials in Alzheimer's disease. *Alzheimers Res Ther,* 6**,** 87.

CASTAÑO-LEON, A. M., CICUENDEZ, M., NAVARRO, B., PAREDES, I., MUNARRIZ, P. M., CEPEDA, S., HILARIO, A., RAMOS, A., GOMEZ, P. A. & LAGARES, A. 2019. Longitudinal Analysis of Corpus Callosum Diffusion Tensor Imaging Metrics and Its Association with Neurological Outcome. *J Neurotrauma,* 36**,** 2785-2802.

CHEN, H., RICHARD, M., SANDLER, D. P., UMBACH, D. M. & KAMEL, F. 2007. Head injury and amyotrophic lateral sclerosis. *Am J Epidemiol,* 166**,** 810-6.

CHEN, X. H., JOHNSON, V. E., URYU, K., TROJANOWSKI, J. Q. & SMITH, D. H. 2009. A lack of amyloid beta plaques despite persistent accumulation of amyloid beta in axons of long-term survivors of traumatic brain injury. *Brain Pathol,* 19**,** 214-23.

CHIO, A., BENZI, G., DOSSENA, M., MUTANI, R. & MORA, G. 2005. Severely increased risk of amyotrophic lateral sclerosis among Italian professional football players. *Brain,* 128**,** 472-6.

CHIO, A., CALVO, A., DOSSENA, M., GHIGLIONE, P., MUTANI, R. & MORA, G. 2009. ALS in Italian professional soccer players: the risk is still present and could be soccer-specific. *Amyotroph Lateral Scler,* 10**,** 205-9.

CLAVAGUERA, F., HENCH, J., GOEDERT, M. & TOLNAY, M. 2015. Invited review: Prion-like transmission and spreading of tau pathology. *Neuropathol Appl Neurobiol,* 41**,** 47-58.

COLE, J. H., JOLLY, A., DE SIMONI, S., BOURKE, N., PATEL, M. C., SCOTT, G. & SHARP, D. J. 2018a. Spatial patterns of progressive brain volume loss after moderate-severe traumatic brain injury. *Brain,* 141**,** 822-836.

COLE, J. H., LEECH, R., SHARP, D. J. & ALZHEIMER'S DISEASE NEUROIMAGING, I. 2015. Prediction of brain age suggests accelerated atrophy after traumatic brain injury. *Ann Neurol,* 77**,** 571-81.

COLE, J. H., MARIONI, R. E., HARRIS, S. E. & DEARY, I. J. 2019. Brain age and other bodily 'ages': implications for neuropsychiatry. *Mol Psychiatry,* 24**,** 266-281.

COLE, J. H., RITCHIE, S. J., BASTIN, M. E., VALDES HERNANDEZ, M. C., MUNOZ MANIEGA, S., ROYLE, N., CORLEY, J., PATTIE, A., HARRIS, S. E., ZHANG, Q., WRAY, N. R., REDMOND, P., MARIONI, R. E., STARR, J. M., COX, S. R., WARDLAW, J. M., SHARP, D. J. & DEARY, I. J. 2018b. Brain age predicts mortality. *Mol Psychiatry,* 23**,** 1385-1392.

CORRAINI, P., HENDERSON, V. W., ORDING, A. G., PEDERSEN, L., HORVATH-PUHO, E. & SORENSEN, H. T. 2017. Long-Term Risk of Dementia Among Survivors of Ischemic or Hemorrhagic Stroke. *Stroke,* 48**,** 180-186.

CRANE, P. K., GIBBONS, L. E., DAMS-O'CONNOR, K., TRITTSCHUH, E., LEVERENZ, J. B., KEENE, C. D., SONNEN, J., MONTINE, T. J., BENNETT, D. A., LEURGANS, S., SCHNEIDER, J. A. & LARSON, E. B. 2016. Association of Traumatic Brain Injury With Late-Life Neurodegenerative Conditions and Neuropathologic Findings. *JAMA Neurol,* 73**,** 1062-9.

CRARY, J. F., TROJANOWSKI, J. Q., SCHNEIDER, J. A., ABISAMBRA, J. F., ABNER, E. L., ALAFUZOFF, I., ARNOLD, S. E., ATTEMS, J., BEACH, T. G., BIGIO, E. H., CAIRNS, N. J., DICKSON, D. W., GEARING, M., GRINBERG, L. T., HOF, P. R., HYMAN, B. T., JELLINGER, K., JICHA, G. A., KOVACS, G. G., KNOPMAN, D. S., KOFLER, J., KUKULL, W. A., MACKENZIE, I. R., MASLIAH, E., MCKEE, A., MONTINE, T. J., MURRAY, M. E., NELTNER, J. H., SANTA-MARIA, I., SEELEY, W. W., SERRANO-POZO, A., SHELANSKI, M. L., STEIN, T., TAKAO, M., THAL, D. R., TOLEDO, J. B., TRONCOSO, J. C., VONSATTEL, J. P., WHITE, C. L., 3RD, WISNIEWSKI, T., WOLTJER, R. L., YAMADA, M. & NELSON, P. T. 2014. Primary age-related tauopathy (PART): a common pathology associated with human aging. *Acta Neuropathol,* 128**,** 755-66.

CSUKA, E., MORGANTI-KOSSMANN, M. C., LENZLINGER, P. M., JOLLER, H., TRENTZ, O. & KOSSMANN, T. 1999. IL-10 levels in cerebrospinal fluid and serum of patients with severe traumatic brain injury: relationship to IL-6, TNF-alpha, TGF-beta1 and blood-brain barrier function. *J Neuroimmunol,* 101**,** 211-21.

CZEITER, E., AMREIN, K., GRAVESTEIJN, B. Y., LECKY, F., MENON, D. K., MONDELLO, S., NEWCOMBE, V. F. J., RICHTER, S., STEYERBERG, E. W., VYVERE, T. V., VERHEYDEN, J., XU, H., YANG, Z., MAAS, A. I. R., WANG, K. K. W. & BÜKI, A. 2020. Blood biomarkers on admission in acute traumatic brain injury: Relations to severity, CT findings and care path in the CENTER-TBI study. *EBioMedicine,* 56.

DEUTSCH, M. B., MENDEZ, M. F. & TENG, E. 2015. Interactions between traumatic brain injury and frontotemporal degeneration. *Dement Geriatr Cogn Disord,* 39**,** 143-53.

DICKSTEIN, D. L., PULLMAN, M. Y., FERNANDEZ, C., SHORT, J. A., KOSTAKOGLU, L., KNESAUREK, K., SOLEIMANI, L., JORDAN, B. D., GORDON, W. A., DAMS-O'CONNOR, K., DELMAN, B. N., WONG, E., TANG, C. Y., DEKOSKY, S. T., STONE, J. R., CANTU, R. C., SANO, M., HOF, P. R. & GANDY, S. 2016. Cerebral [(18) F]T807/AV1451 retention pattern in clinically probable CTE resembles pathognomonic distribution of CTE tauopathy. *Transl Psychiatry,* 6**,** e900.

DONAT, C. K., YANEZ-LOPEZ, M., SASTRE, M., BAXAN, N., GOLDFINGER, M., SEEAMBER, R., MÜLLER, F., DAVIES, P., HELLYER, P., SIEGKAS, P., GENTLEMAN, S., SHARP, D. J. & GHAJARI, M. 2021. From biomechanics to pathology: predicting axonal injury from patterns of strain after traumatic brain injury. *Brain,* 144**,** 70-91.

ESCOTT-PRICE, V., SIMS, R., BANNISTER, C., HAROLD, D., VRONSKAYA, M., MAJOUNIE, E., BADARINARAYAN, N., MORGAN, K., PASSMORE, P., HOLMES, C., POWELL, J., BRAYNE, C., GILL, M., MEAD, S., GOATE, A., CRUCHAGA, C., LAMBERT, J. C., VAN DUIJN, C., MAIER, W., RAMIREZ, A., HOLMANS, P., JONES, L., HARDY, J., SESHADRI, S., SCHELLENBERG, G. D., AMOUYEL, P. & WILLIAMS, J. 2015. Common polygenic variation enhances risk prediction for Alzheimer's disease. *Brain,* 138**,** 3673-84.

FALCON, B., ZIVANOV, J., ZHANG, W., MURZIN, A. G., GARRINGER, H. J., VIDAL, R., CROWTHER, R. A., NEWELL, K. L., GHETTI, B., GOEDERT, M. & SCHERES, S. H. W. 2019. Novel tau filament fold in chronic traumatic encephalopathy encloses hydrophobic molecules. *Nature,* 568**,** 420-423.

FANN, J. R., RIBE, A. R., PEDERSEN, H. S., FENGER-GRON, M., CHRISTENSEN, J., BENROS, M. E. & VESTERGAARD, M. 2018. Long-term risk of dementia among people with traumatic brain injury in Denmark: a population-based observational cohort study. *Lancet Psychiatry,* 5**,** 424-431.

FARBOTA, K. D., SODHI, A., BENDLIN, B. B., MCLAREN, D. G., XU, G., ROWLEY, H. A. & JOHNSON, S. C. 2012. Longitudinal volumetric changes following traumatic brain injury: a tensor-based morphometry study. *J Int Neuropsychol Soc,* 18**,** 1006-18.

FEENEY, C., SHARP, D. J., HELLYER, P. J., JOLLY, A. E., COLE, J. H., SCOTT, G., BAXTER, D., JILKA, S., ROSS, E., HAM, T. E., JENKINS, P. O., LI, L. M., GORGORAPTIS, N., MIDWINTER, M. & GOLDSTONE, A. P. 2017. Serum insulin-like growth factor-I levels are associated with improved white matter recovery after traumatic brain injury. *Ann Neurol,* 82**,** 30-43.

FJELL, A. M., WALHOVD, K. B., FENNEMA-NOTESTINE, C., MCEVOY, L. K., HAGLER, D. J., HOLLAND, D., BLENNOW, K., BREWER, J. B., DALE, A. M. & INITIATIVE, T. A. S. D. N. 2010. Brain Atrophy in Healthy Aging Is Related to CSF Levels of Aβ1-42. *Cerebral Cortex,* 20**,** 2069-2079.

FJELL, A. M., WALHOVD, K. B., FENNEMA-NOTESTINE, C., MCEVOY, L. K., HAGLER, D. J., HOLLAND, D., BREWER, J. B. & DALE, A. M. 2009. One-Year Brain Atrophy Evident in Healthy Aging. *The Journal of Neuroscience,* 29**,** 15223-15231.

FJELL, A. M., WESTLYE, L. T., GRYDELAND, H., AMLIEN, I., ESPESETH, T., REINVANG, I., RAZ, N., DALE, A. M., WALHOVD, K. B. & ALZHEIMER DISEASE NEUROIMAGING, I. 2014. Accelerating cortical thinning: unique to dementia or universal in aging? *Cerebral cortex (New York, N.Y. : 1991),* 24**,** 919-934.

FLEMINGER, S., OLIVER, D. L., LOVESTONE, S., RABE-HESKETH, S. & GIORA, A. 2003. Head injury as a risk factor for Alzheimer's disease: the evidence 10 years on; a partial replication. *Journal of Neurology Neurosurgery and Psychiatry,* 74**,** 857-862.

GAETANI, L., BLENNOW, K., CALABRESI, P., DI FILIPPO, M., PARNETTI, L. & ZETTERBERG, H. 2019. Neurofilament light chain as a biomarker in neurological disorders. *Journal of Neurology, Neurosurgery & Psychiatry,* 90**,** 870-881.

GAFSON, A. R., BARTHÉLEMY, N. R., BOMONT, P., CARARE, R. O., DURHAM, H. D., JULIEN, J.-P., KUHLE, J., LEPPERT, D., NIXON, R. A., WELLER, R. O., ZETTERBERG, H. & MATTHEWS, P. M. 2020. Neurofilaments: neurobiological foundations for biomarker applications. *Brain: A Journal of Neurology*.

GAIOTTINO, J., NORGREN, N., DOBSON, R., TOPPING, J., NISSIM, A., MALASPINA, A., BESTWICK, J. P., MONSCH, A. U., REGENITER, A., LINDBERG, R. L., KAPPOS, L., LEPPERT, D., PETZOLD, A., GIOVANNONI, G. & KUHLE, J. 2013. Increased neurofilament light chain blood levels in neurodegenerative neurological diseases. *PLoS One,* 8**,** e75091.

GARDNER, R. C., BYERS, A. L., BARNES, D. E., LI, Y., BOSCARDIN, J. & YAFFE, K. 2018. Mild TBI and risk of Parkinson disease: A Chronic Effects of Neurotrauma Consortium Study. *Neurology,* 90**,** e1771-e1779.

GENNARELLI, T. A., THIBAULT, L. E., ADAMS, J. H., GRAHAM, D. I., THOMPSON, C. J. & MARCINCIN, R. P. 1982. Diffuse axonal injury and traumatic coma in the primate. *Ann Neurol,* 12**,** 564-74.

GENTLEMAN, S. M., NASH, M. J., SWEETING, C. J., GRAHAM, D. I. & ROBERTS, G. W. 1993. Beta-Amyloid Precursor Protein (Beta-App) as a Marker for Axonal Injury after Head-Injury. *Neuroscience Letters,* 160**,** 139-144.

GHAJARI, M., HELLYER, P. J. & SHARP, D. J. 2017. Computational modelling of traumatic brain injury predicts the location of chronic traumatic encephalopathy pathology. *Brain,* 140**,** 333-343.

GIORGI-COLL, S., THELIN, E. P., LINDBLAD, C., TAJSIC, T., CARPENTER, K. L. H., HUTCHINSON, P. J. A. & HELMY, A. 2020. Dextran 500 Improves Recovery of Inflammatory Markers: An In Vitro Microdialysis Study. *J Neurotrauma,* 37**,** 106-114.

GISSLÉN, M., PRICE, R. W., ANDREASSON, U., NORGREN, N., NILSSON, S., HAGBERG, L., FUCHS, D., SPUDICH, S., BLENNOW, K. & ZETTERBERG, H. 2016. Plasma Concentration of the Neurofilament Light Protein (NFL) is a Biomarker of CNS Injury in HIV Infection: A Cross-Sectional Study. *EBioMedicine,* 3**,** 135-140.

GOLDSTEIN, L. E., FISHER, A. M., TAGGE, C. A., ZHANG, X. L., VELISEK, L., SULLIVAN, J. A., UPRETI, C., KRACHT, J. M., ERICSSON, M., WOJNAROWICZ, M. W., GOLETIANI, C. J., MAGLAKELIDZE, G. M., CASEY, N., MONCASTER, J. A., MINAEVA, O., MOIR, R. D., NOWINSKI, C. J., STERN, R. A., CANTU, R. C., GEILING, J., BLUSZTAJN, J. K., WOLOZIN, B. L., IKEZU, T., STEIN, T. D., BUDSON, A. E., KOWALL, N. W., CHARGIN, D., SHARON, A., SAMAN, S., HALL, G. F., MOSS, W. C., CLEVELAND, R. O., TANZI, R. E., STANTON, P. K. & MCKEE, A. C. 2012. Chronic traumatic encephalopathy in blast-exposed military veterans and a blast neurotrauma mouse model. *Sci Transl Med,* 4**,** 134ra60.

GORGORAPTIS, N., LI, L. M., WHITTINGTON, A., ZIMMERMAN, K. A., MACLEAN, L. M., MCLEOD, C., ROSS, E., HESLEGRAVE, A., ZETTERBERG, H., PASSCHIER, J., MATTHEWS, P. M., GUNN, R. N., MCMILLAN, T. M. & SHARP, D. J. 2019. In vivo detection of cerebral tau pathology in long-term survivors of traumatic brain injury. *Science Translational Medicine,* 11**,** eaaw1993.

GRAHAM, N. S. & SHARP, D. J. 2019. Understanding neurodegeneration after traumatic brain injury: from mechanisms to clinical trials in dementia. *J Neurol Neurosurg Psychiatry*.

GRAHAM, N. S., ZIMMERMAN, K. A., BERTOLINI, G., MAGNONI, S., ODDO, M., ZETTERBERG, H., MORO, F., NOVELLI, D., HESLEGRAVE, A., CHIEREGATO, A., FAINARDI, E., FLEMING, J. M., GARBERO, E., ABED-MAILLARD, S., GRADISEK, P., BERNINI, A. & SHARP, D. J. 2020a. Multicentre longitudinal study of fluid and neuroimaging BIOmarkers of AXonal injury after traumatic brain injury: the BIO-AX-TBI study protocol. *BMJ Open,* 10**,** e042093.

GRAHAM, N. S. N., JOLLY, A., ZIMMERMAN, K., BOURKE, N. J., SCOTT, G., COLE, J. H., SCHOTT, J. M. & SHARP, D. J. 2020b. Diffuse axonal injury predicts neurodegeneration after moderate–severe traumatic brain injury. *Brain*.

GRIFFIN, A. D., TURTZO, L. C., PARIKH, G. Y., TOLPYGO, A., LODATO, Z., MOSES, A. D., NAIR, G., PERL, D. P., EDWARDS, N. A., DARDZINSKI, B. J., ARMSTRONG, R. C., RAY-CHAUDHURY, A., MITRA, P. P. & LATOUR, L. L. 2019. Traumatic microbleeds suggest vascular injury and predict disability in traumatic brain injury. *Brain,* 142**,** 3550-3564.

HANSSON, O., JANELIDZE, S., HALL, S., MAGDALINOU, N., LEES, A. J., ANDREASSON, U., NORGREN, N., LINDER, J., FORSGREN, L., CONSTANTINESCU, R., ZETTERBERG, H. & BLENNOW, K. 2017. Blood-based NfL: A biomarker for differential diagnosis of parkinsonian disorder. *Neurology,* 88**,** 930-937.

HAY, J. R., JOHNSON, V. E., YOUNG, A. M., SMITH, D. H. & STEWART, W. 2015. Blood-Brain Barrier Disruption Is an Early Event That May Persist for Many Years After Traumatic Brain Injury in Humans. *J Neuropathol Exp Neurol,* 74**,** 1147-57.

HAYES, J. P., LOGUE, M. W., SADEH, N., SPIELBERG, J. M., VERFAELLIE, M., HAYES, S. M., REAGAN, A., SALAT, D. H., WOLF, E. J., MCGLINCHEY, R. E., MILBERG, W. P., STONE, A.,

SCHICHMAN, S. A. & MILLER, M. W. 2017. Mild traumatic brain injury is associated with reduced cortical thickness in those at risk for Alzheimer's disease. *Brain,* 140**,** 813-825.

HELLYER, P. J., LEECH, R., HAM, T. E., BONNELLE, V. & SHARP, D. J. 2013. Individual prediction of white matter injury following traumatic brain injury. *Ann Neurol,* 73**,** 489-99.

HENEKA, M. T., CARSON, M. J., EL KHOURY, J., LANDRETH, G. E., BROSSERON, F., FEINSTEIN, D. L., JACOBS, A. H., WYSS-CORAY, T., VITORICA, J., RANSOHOFF, R. M., HERRUP, K., FRAUTSCHY, S. A., FINSEN, B., BROWN, G. C., VERKHRATSKY, A., YAMANAKA, K., KOISTINAHO, J., LATZ, E., HALLE, A., PETZOLD, G. C., TOWN, T., MORGAN, D., SHINOHARA, M. L., PERRY, V. H., HOLMES, C., BAZAN, N. G., BROOKS, D. J., HUNOT, S., JOSEPH, B., DEIGENDESCH, N., GARASCHUK, O., BODDEKE, E., DINARELLO, C. A., BREITNER, J. C., COLE, G. M., GOLENBOCK, D. T. & KUMMER, M. P. 2015. Neuroinflammation in Alzheimer's disease. *The Lancet. Neurology,* 14**,** 388-405.

HILL, C. S., COLEMAN, M. P. & MENON, D. K. 2016. Traumatic Axonal Injury: Mechanisms and Translational Opportunities. *Trends in neurosciences,* 39**,** 311-324.

HOFFMAN, P. N., CLEVELAND, D. W., GRIFFIN, J. W., LANDES, P. W., COWAN, N. J. & PRICE, D. L. 1987. Neurofilament gene expression: a major determinant of axonal caliber. *Proc Natl Acad Sci U S A,* 84**,** 3472-6.

HONG, Y. T., VEENITH, T., DEWAR, D., OUTTRIM, J. G., MANI, V., WILLIAMS, C., PIMLOTT, S., HUTCHINSON, P. J., TAVARES, A., CANALES, R., MATHIS, C. A., KLUNK, W. E., AIGBIRHIO, F. I., COLES, J. P., BARON, J. C., PICKARD, J. D., FRYER, T. D., STEWART, W. & MENON, D. K. 2014. Amyloid imaging with carbon 11-labeled Pittsburgh compound B for traumatic brain injury. *JAMA Neurol,* 71**,** 23-31.

HUA, X., LEE, S., YANOVSKY, I., LEOW, A. D., CHOU, Y. Y., HO, A. J., GUTMAN, B., TOGA, A. W., JACK, C. R., JR., BERNSTEIN, M. A., REIMAN, E. M., HARVEY, D. J., KORNAK, J., SCHUFF, N., ALEXANDER, G. E., WEINER, M. W., THOMPSON, P. M. & ALZHEIMER'S DISEASE NEUROIMAGING, I. 2009. Optimizing power to track brain degeneration in Alzheimer's disease and mild cognitive impairment with tensor-based morphometry: an ADNI study of 515 subjects. *Neuroimage,* 48**,** 668-81.

IACONO, W. G. 2018. Endophenotypes in psychiatric disease: prospects and challenges. *Genome medicine,* 10**,** 11-11.

ILIFF, J. J., CHEN, M. J., PLOG, B. A., ZEPPENFELD, D. M., SOLTERO, M., YANG, L., SINGH, I., DEANE, R. & NEDERGAARD, M. 2014. Impairment of glymphatic pathway function promotes tau pathology after traumatic brain injury. *J Neurosci,* 34**,** 16180-93.

ILIFF, J. J., WANG, M., LIAO, Y., PLOGG, B. A., PENG, W., GUNDERSEN, G. A., BENVENISTE, H., VATES, G. E., DEANE, R., GOLDMAN, S. A., NAGELHUS, E. A. & NEDERGAARD, M. 2012. A Paravascular Pathway Facilitates CSF Flow Through the Brain Parenchyma and the Clearance of Interstitial Solutes, Including Amyloid β. *Science Translational Medicine,* 4**,** 147ra111.

ISENSEE, F., SCHELL, M., PFLUEGER, I., BRUGNARA, G., BONEKAMP, D., NEUBERGER, U., WICK, A., SCHLEMMER, H.-P., HEILAND, S., WICK, W., BENDSZUS, M., MAIER-HEIN, K. H. & KICKINGEREDER, P. 2019. Automated brain extraction of multisequence MRI using artificial neural networks. *Human Brain Mapping,* 40**,** 4952-4964.

IVERSON, G. L., KEENE, C. D., PERRY, G. & CASTELLANI, R. J. 2018. The Need to Separate Chronic Traumatic Encephalopathy Neuropathology from Clinical Features. *J Alzheimers Dis,* 61**,** 17-28.

IWATA, N., TSUBUKI, S., TAKAKI, Y., WATANABE, K., SEKIGUCHI, M., HOSOKI, E., KAWASHIMA-MORISHIMA, M., LEE, H. J., HAMA, E., SEKINE-AIZAWA, Y. & SAIDO, T. C. 2000. Identification of the major Abeta1-42-degrading catabolic pathway in brain parenchyma: suppression leads to biochemical and pathological deposition. *Nat Med,* 6**,** 143-50.

JAFARI, S., ETMINAN, M., AMINZADEH, F. & SAMII, A. 2013. Head injury and risk of Parkinson disease: a systematic review and meta-analysis. *Mov Disord,* 28**,** 1222-9.

JAMES, O. G., DORAISWAMY, P. M. & BORGES-NETO, S. 2015. PET Imaging of Tau Pathology in Alzheimer's Disease and Tauopathies. *Front Neurol,* 6**,** 38.

JEURISSEN, B., LEEMANS, A., TOURNIER, J. D., JONES, D. K. & SIJBERS, J. 2013. Investigating the prevalence of complex fiber configurations in white matter tissue with diffusion magnetic resonance imaging. *Hum Brain Mapp,* 34**,** 2747-66.

JOHNSON, E. B., BYRNE, L. M., GREGORY, S., RODRIGUES, F. B., BLENNOW, K., DURR, A., LEAVITT, B. R., ROOS, R. A., ZETTERBERG, H., TABRIZI, S. J., SCAHILL, R. I. & WILD, E. J. 2018. Neurofilament light protein in blood predicts regional atrophy in Huntington disease. *Neurology,* 90**,** e717-e723.

JOHNSON, V. E., STEWART, J. E., BEGBIE, F. D., TROJANOWSKI, J. Q., SMITH, D. H. & STEWART, W. 2013a. Inflammation and white matter degeneration persist for years after a single traumatic brain injury. *Brain,* 136**,** 28-42.

JOHNSON, V. E., STEWART, W., GRAHAM, D. I., STEWART, J. E., PRAESTGAARD, A. H. & SMITH, D. H. 2009. A neprilysin polymorphism and amyloid-beta plaques after traumatic brain injury. *J Neurotrauma,* 26**,** 1197-202.

JOHNSON, V. E., STEWART, W. & SMITH, D. H. 2010. Traumatic brain injury and amyloid-β pathology: a link to Alzheimer's disease? *Nature Reviews Neuroscience,* 11**,** 361-370.

JOHNSON, V. E., STEWART, W. & SMITH, D. H. 2012. Widespread tau and amyloid-beta pathology many years after a single traumatic brain injury in humans. *Brain Pathol,* 22**,** 142-9.

JOHNSON, V. E., STEWART, W. & SMITH, D. H. 2013b. Axonal pathology in traumatic brain injury. *Experimental neurology,* 246**,** 35-43.

JOLLY, A. E., BALAET, M., AZOR, A., FRIEDLAND, D., SANDRONE, S., GRAHAM, N. S. N., ZIMMERMAN, K. & SHARP, D. J. 2021. Detecting axonal injury in individual patients after Traumatic Brain Injury. *Brain,* 144**,** 92-113.

JONES, D. K., KNÖSCHE, T. R. & TURNER, R. 2013. White matter integrity, fiber count, and other fallacies: the do's and don'ts of diffusion MRI. *Neuroimage,* 73**,** 239-54.

JUCKER, M. & WALKER, L. C. 2013. Self-propagation of pathogenic protein aggregates in neurodegenerative diseases. *Nature,* 501**,** 45-51.

KALKONDE, Y. V., JAWAID, A., QURESHI, S. U., SHIRANI, P., WHEATON, M., PINTO-PATARROYO, G. P. & SCHULZ, P. E. 2012. Medical and environmental risk factors associated with frontotemporal dementia: a case-control study in a veteran population. *Alzheimers Dement,* 8**,** 204-10.

KAMNITSAS, K., LEDIG, C., NEWCOMBE, V. F. J., SIMPSON, J. P., KANE, A. D., MENON, D. K., RUECKERT, D. & GLOCKER, B. 2017. Efficient multi-scale 3D CNN with fully connected CRF for accurate brain lesion segmentation. *Med Image Anal,* 36**,** 61-78.

KANE, M. D., LIPINSKI, W. J., CALLAHAN, M. J., BIAN, F., DURHAM, R. A., SCHWARZ, R. D., ROHER, A. E. & WALKER, L. C. 2000. Evidence for seeding of beta -amyloid by intracerebral infusion of Alzheimer brain extracts in beta -amyloid precursor protein-transgenic mice. *J Neurosci,* 20**,** 3606-11.

KATZ, D. I., BERNICK, C., DODICK, D. W., MEZ, J., MARIANI, M. L., ADLER, C. H., ALOSCO, M. L., BALCER, L. J., BANKS, S. J., BARR, W. B., BRODY, D. L., CANTU, R. C., DAMS-O'CONNOR, K., GEDA, Y. E., JORDAN, B. D., MCALLISTER, T. W., PESKIND, E. R., PETERSEN, R. C., WETHE, J. V., ZAFONTE, R. D., FOLEY, É. M., BABCOCK, D. J., KOROSHETZ, W. J., TRIPODIS, Y., MCKEE, A. C., SHENTON, M. E., CUMMINGS, J. L., REIMAN, E. M. & STERN, R. A. 2021. National Institute of Neurological Disorders and Stroke Consensus Diagnostic Criteria for Traumatic Encephalopathy Syndrome. *Neurology***,** 10.1212/WNL.0000000000011850.

KEMPTON, M. J., ETTINGER, U., SCHMECHTIG, A., WINTER, E. M., SMITH, L., MCMORRIS, T., WILKINSON, I. D., WILLIAMS, S. C. & SMITH, M. S. 2009. Effects of acute dehydration on brain morphology in healthy humans. *Hum Brain Mapp,* 30**,** 291-8.

KESHAVAN, A., HESLEGRAVE, A., ZETTERBERG, H. & SCHOTT, J. M. 2018. Stability of blood-based biomarkers of Alzheimer's disease over multiple freeze-thaw cycles. *Alzheimers Dement (Amst),* 10**,** 448-451.

KIM, S.-H., CHOI, M. K., PARK, N. Y., HYUN, J.-W., LEE, M. Y., KIM, H. J., JUNG, S. K. & CHA, Y. 2020. Serum neurofilament light chain levels as a biomarker of neuroaxonal injury and severity of oxaliplatin-induced peripheral neuropathy. *Scientific Reports,* 10**,** 7995.

KINNUNEN, K. M., GREENWOOD, R., POWELL, J. H., LEECH, R., HAWKINS, P. C., BONNELLE, V., PATEL, M. C., COUNSELL, S. J. & SHARP, D. J. 2011. White matter damage and cognitive impairment after traumatic brain injury. *Brain,* 134**,** 449-63.

KONDO, A., SHAHPASAND, K., MANNIX, R., QIU, J., MONCASTER, J., CHEN, C. H., YAO, Y., LIN, Y. M., DRIVER, J. A., SUN, Y., WEI, S., LUO, M. L., ALBAYRAM, O., HUANG, P., ROTENBERG, A., RYO, A., GOLDSTEIN, L. E., PASCUAL-LEONE, A., MCKEE, A. C., MEEHAN, W., ZHOU, X. Z. & LU, K. P. 2015. Antibody against early driver of neurodegeneration cis P-tau blocks brain injury and tauopathy. *Nature,* 523**,** 431-436.

KOSHINAGA, M., KATAYAMA, Y., FUKUSHIMA, M., OSHIMA, H., SUMA, T. & TAKAHATA, T. 2000. Rapid and widespread microglial activation induced by traumatic brain injury in rat brain slices. *J Neurotrauma,* 17**,** 185-92.

KOVACS, G. G., FERRER, I., GRINBERG, L. T., ALAFUZOFF, I., ATTEMS, J., BUDKA, H., CAIRNS, N. J., CRARY, J. F., DUYCKAERTS, C., GHETTI, B., HALLIDAY, G. M., IRONSIDE, J. W., LOVE, S., MACKENZIE, I. R., MUNOZ, D. G., MURRAY, M. E., NELSON, P. T., TAKAHASHI, H., TROJANOWSKI, J. Q., ANSORGE, O., ARZBERGER, T., BABORIE, A., BEACH, T. G., BIENIEK, K. F., BIGIO, E. H., BODI, I., DUGGER, B. N., FEANY, M., GELPI, E., GENTLEMAN, S. M., GIACCONE, G., HATANPAA, K. J., HEALE, R., HOF, P. R., HOFER, M., HORTOBAGYI, T., JELLINGER, K., JICHA, G. A., INCE, P., KOFLER, J., KOVARI, E., KRIL, J. J., MANN, D. M., MATEJ, R., MCKEE, A. C., MCLEAN, C., MILENKOVIC, I., MONTINE, T. J., MURAYAMA, S., LEE, E. B., RAHIMI, J., RODRIGUEZ, R. D., ROZEMULLER, A., SCHNEIDER, J. A., SCHULTZ, C., SEELEY, W., SEILHEAN, D., SMITH, C., TAGLIAVINI, F., TAKAO, M., THAL, D. R., TOLEDO, J. B., TOLNAY, M., TRONCOSO, J. C., VINTERS, H. V., WEIS, S., WHARTON, S. B., WHITE, C. L., 3RD, WISNIEWSKI, T., WOULFE, J. M., YAMADA, M. & DICKSON, D. W. 2016. Aging-related tau astrogliopathy (ARTAG): harmonized evaluation strategy. *Acta Neuropathol,* 131**,** 87-102.

KUHLE, J., BARRO, C., ANDREASSON, U., DERFUSS, T., LINDBERG, R., SANDELIUS, A., LIMAN, V., NORGREN, N., BLENNOW, K. & ZETTERBERG, H. 2016. Comparison of three analytical platforms for quantification of the neurofilament light chain in blood samples: ELISA, electrochemiluminescence immunoassay and Simoa. *Clin Chem Lab Med,* 54**,** 1655-61.

KUHLE, J., GAIOTTINO, J., LEPPERT, D., PETZOLD, A., BESTWICK, J. P., MALASPINA, A., LU, C. H., DOBSON, R., DISANTO, G., NORGREN, N., NISSIM, A., KAPPOS, L., HURLBERT, J., YONG, V. W., GIOVANNONI, G. & CASHA, S. 2015. Serum neurofilament light chain is a biomarker of human spinal cord injury severity and outcome. *J Neurol Neurosurg Psychiatry,* 86**,** 273-9.

LA JOIE, R., VISANI, A. V., BAKER, S. L., BROWN, J. A., BOURAKOVA, V., CHA, J., CHAUDHARY, K., EDWARDS, L., IACCARINO, L., JANABI, M., LESMAN-SEGEV, O. H., MILLER, Z. A., PERRY, D. C., O'NEIL, J. P., PHAM, J., ROJAS, J. C., ROSEN, H. J., SEELEY, W. W., TSAI, R. M., MILLER, B. L., JAGUST, W. J. & RABINOVICI, G. D. 2020. Prospective longitudinal atrophy in Alzheimer's disease correlates with the intensity and topography of baseline tau-PET. *Science Translational Medicine,* 12**,** eaau5732.

LAGARDE, J., SARAZIN, M. & BOTTLAENDER, M. 2018. In vivo PET imaging of neuroinflammation in Alzheimer's disease. *Journal of Neural Transmission,* 125**,** 847-867.

LEDIG, C., KAMNITSAS, K., KOIKKALAINEN, J., POSTI, J. P., TAKALA, R. S. K., KATILA, A., FRANTZEN, J., ALA-SEPPALA, H., KYLLONEN, A., MAANPAA, H. R., TALLUS, J., LOTJONEN, J., GLOCKER, B., TENOVUO, O. & RUECKERT, D. 2017. Regional brain morphometry in patients with traumatic brain injury based on acute- and chronic-phase magnetic resonance imaging. *PLoS One,* 12**,** e0188152.

LEHMAN, E. J., HEIN, M. J., BARON, S. L. & GERSIC, C. M. 2012. Neurodegenerative causes of death among retired National Football League players. *Neurology,* 79**,** 1970-4.

LI, Y., LI, Y., LI, X., ZHANG, S., ZHAO, J., ZHU, X. & TIAN, G. 2017. Head Injury as a Risk Factor for Dementia and Alzheimer's Disease: A Systematic Review and Meta-Analysis of 32 Observational Studies. *PLoS One,* 12**,** e0169650.

LING, H., HOLTON, J. L., SHAW, K., DAVEY, K., LASHLEY, T. & REVESZ, T. 2015. Histological evidence of chronic traumatic encephalopathy in a large series of neurodegenerative diseases. *Acta Neuropathol,* 130**,** 891-3.

LIVINGSTON, G., HUNTLEY, J., SOMMERLAD, A., AMES, D., BALLARD, C., BANERJEE, S., BRAYNE, C., BURNS, A., COHEN-MANSFIELD, J., COOPER, C., COSTAFREDA, S. G., DIAS, A., FOX, N., GITLIN, L. N., HOWARD, R., KALES, H. C., KIVIMÄKI, M., LARSON, E. B., OGUNNIYI, A., ORGETA, V., RITCHIE, K., ROCKWOOD, K., SAMPSON, E. L., SAMUS, Q., SCHNEIDER, L. S., SELBÆK, G., TERI, L. & MUKADAM, N. 2020. Dementia prevention, intervention, and care: 2020 report of the Lancet Commission. *The Lancet,* 396**,** 413-446.

LJUNGQVIST, J., ZETTERBERG, H., MITSIS, M., BLENNOW, K. & SKOGLUND, T. 2017. Serum Neurofilament Light Protein as a Marker for Diffuse Axonal Injury: Results from a Case Series Study. *J Neurotrauma,* 34**,** 1124-1127.

LOBUE, C., WILMOTH, K., CULLUM, C. M., ROSSETTI, H. C., LACRITZ, L. H., HYNAN, L. S., HART, J., JR. & WOMACK, K. B. 2016. Traumatic brain injury history is associated with earlier age of onset of frontotemporal dementia. *J Neurol Neurosurg Psychiatry,* 87**,** 817-20.

LOLEKHA, P., PHANTHUMCHINDA, K. & BHIDAYASIRI, R. 2010. Prevalence and risk factors of Parkinson's disease in retired Thai traditional boxers. *Mov Disord,* 25**,** 1895-901.

LU, C. H., MACDONALD-WALLIS, C., GRAY, E., PEARCE, N., PETZOLD, A., NORGREN, N., GIOVANNONI, G., FRATTA, P., SIDLE, K., FISH, M., ORRELL, R., HOWARD, R., TALBOT, K., GREENSMITH, L., KUHLE, J., TURNER, M. R. & MALASPINA, A. 2015. Neurofilament light chain: A prognostic biomarker in amyotrophic lateral sclerosis. *Neurology,* 84**,** 2247-57.

LY, M., CANU, E., XU, G. F., OH, J., MCLAREN, D. G., DOWLING, N. M., ALEXANDER, A. L., SAGER, M. A., JOHNSON, S. C. & BENDLIN, B. B. 2014. Midlife measurements of white matter microstructure predict subsequent regional white matter atrophy in healthy adults. *Human Brain Mapping,* 35**,** 2044-2054.

MAAS, A. I. R., MENON, D. K., ADELSON, P. D., ANDELIC, N., BELL, M. J., BELLI, A., BRAGGE, P., BRAZINOVA, A., BUKI, A., CHESNUT, R. M., CITERIO, G., COBURN, M., COOPER, D. J., CROWDER, A. T., CZEITER, E., CZOSNYKA, M., DIAZ-ARRASTIA, R., DREIER, J. P., DUHAIME, A. C., ERCOLE, A., VAN ESSEN, T. A., FEIGIN, V. L., GAO, G., GIACINO, J., GONZALEZ-LARA, L. E., GRUEN, R. L., GUPTA, D., HARTINGS, J. A., HILL, S., JIANG, J. Y., KETHARANATHAN, N., KOMPANJE, E. J. O., LANYON, L., LAUREYS, S., LECKY, F., LEVIN, H., LINGSMA, H. F., MAEGELE, M., MAJDAN, M., MANLEY, G., MARSTELLER, J., MASCIA, L., MCFADYEN, C., MONDELLO, S., NEWCOMBE, V., PALOTIE, A., PARIZEL, P. M., PEUL, W., PIERCY, J., POLINDER, S., PUYBASSET, L., RASMUSSEN, T. E., ROSSAINT, R., SMIELEWSKI, P., SODERBERG, J., STANWORTH, S. J., STEIN, M. B., VON STEINBUCHEL, N., STEWART, W., STEYERBERG, E. W., STOCCHETTI, N., SYNNOT, A., TE AO, B., TENOVUO, O., THEADOM, A., TIBBOEL, D., VIDETTA, W., WANG, K. K. W., WILLIAMS, W. H., WILSON, L., YAFFE, K. & INVESTIGATORS, I. P. A. 2017. Traumatic brain injury: integrated approaches to improve prevention, clinical care, and research. *Lancet Neurol,* 16**,** 987-1048.

MAC DONALD, C. L., DIKRANIAN, K., BAYLY, P., HOLTZMAN, D. & BRODY, D. 2007a. Diffusion Tensor Imaging Reliably Detects Experimental Traumatic Axonal Injury and Indicates Approximate Time of Injury. *The Journal of Neuroscience,* 27**,** 11869.

MAC DONALD, C. L., DIKRANIAN, K., SONG, S. K., BAYLY, P. V., HOLTZMAN, D. M. & BRODY, D. L. 2007b. Detection of traumatic axonal injury with diffusion tensor imaging in a mouse model of traumatic brain injury. *Exp Neurol,* 205**,** 116-31.

MACKENZIE, J. D., SIDDIQI, F., BABB, J. S., BAGLEY, L. J., MANNON, L. J., SINSON, G. P. & GROSSMAN, R. I. 2002. Brain atrophy in mild or moderate traumatic brain injury: a longitudinal quantitative analysis. *AJNR Am J Neuroradiol,* 23**,** 1509-15.

MACLAREN, J., HAN, Z., VOS, S. B., FISCHBEIN, N. & BAMMER, R. 2014. Reliability of brain volume measurements: a test-retest dataset. *Sci Data,* 1**,** 140037.

MAGNONI, S., ESPARZA, T. J., CONTE, V., CARBONARA, M., CARRABBA, G., HOLTZMAN, D. M., ZIPFEL, G. J., STOCCHETTI, N. & BRODY, D. L. 2012. Tau elevations in the brain extracellular space correlate with reduced amyloid-beta levels and predict adverse clinical outcomes after severe traumatic brain injury. *Brain,* 135**,** 1268-80.

MAGNONI, S., MAC DONALD, C. L., ESPARZA, T. J., CONTE, V., SORRELL, J., MACRI, M., BERTANI, G., BIFFI, R., COSTA, A., SAMMONS, B., SNYDER, A. Z., SHIMONY, J. S., TRIULZI, F., STOCCHETTI, N. & BRODY, D. L. 2015. Quantitative assessments of traumatic axonal injury in human brain: concordance of microdialysis and advanced MRI. *Brain,* 138**,** 2263-77.

MALEC, J. F., BROWN, A. W., LEIBSON, C. L., FLAADA, J. T., MANDREKAR, J. N., DIEHL, N. N. & PERKINS, P. K. 2007. The mayo classification system for traumatic brain injury severity. *J Neurotrauma,* 24**,** 1417-24.

MALONE, I. B., CASH, D., RIDGWAY, G. R., MACMANUS, D. G., OURSELIN, S., FOX, N. C. & SCHOTT, J. M. 2013. MIRIAD--Public release of a multiple time point Alzheimer's MR imaging dataset. *Neuroimage,* 70**,** 33-6.

MARQUIÉ, M., AGÜERO, C., AMARAL, A. C., VILLAREJO-GALENDE, A., RAMANAN, P., CHONG, M. S. T., SÁEZ-CALVERAS, N., BENNETT, R. E., VERWER, E. E., KIM, S. J. W., DHAYNAUT,

M., ALVAREZ, V. E., JOHNSON, K. A., MCKEE, A. C., FROSCH, M. P. & GÓMEZ-ISLA, T. 2019. [(18)F]-AV-1451 binding profile in chronic traumatic encephalopathy: a postmortem case series. *Acta Neuropathol Commun,* 7**,** 164.

MATTSSON, N., ANDREASSON, U., ZETTERBERG, H. & BLENNOW, K. 2017. Association of Plasma Neurofilament Light With Neurodegeneration in Patients With Alzheimer Disease. *JAMA Neurol,* 74**,** 557-566.

MAXWELL, W. L., BARTLETT, E. & MORGAN, H. 2015. Wallerian degeneration in the optic nerve stretch-injury model of traumatic brain injury: a stereological analysis. *J Neurotrauma,* 32**,** 780-90.

MCKEE, A. C., CAIRNS, N. J., DICKSON, D. W., FOLKERTH, R. D., KEENE, C. D., LITVAN, I., PERL, D. P., STEIN, T. D., VONSATTEL, J. P., STEWART, W., TRIPODIS, Y., CRARY, J. F., BIENIEK, K. F., DAMS-O'CONNOR, K., ALVAREZ, V. E., GORDON, W. A. & GROUP, T. C. 2016. The first NINDS/NIBIB consensus meeting to define neuropathological criteria for the diagnosis of chronic traumatic encephalopathy. *Acta Neuropathol,* 131**,** 75-86.

MCKEE, A. C., STERN, R. A., NOWINSKI, C. J., STEIN, T. D., ALVAREZ, V. E., DANESHVAR, D. H., LEE, H. S., WOJTOWICZ, S. M., HALL, G., BAUGH, C. M., RILEY, D. O., KUBILUS, C. A., CORMIER, K. A., JACOBS, M. A., MARTIN, B. R., ABRAHAM, C. R., IKEZU, T., REICHARD, R. R., WOLOZIN, B. L., BUDSON, A. E., GOLDSTEIN, L. E., KOWALL, N. W. & CANTU, R. C. 2013. The spectrum of disease in chronic traumatic encephalopathy. *Brain,* 136**,** 43-64.

MCKHANN, G., DRACHMAN, D., FOLSTEIN, M., KATZMAN, R., PRICE, D. & STADLAN, E. M. 1984. Clinical diagnosis of Alzheimer's disease: report of the NINCDS-ADRDA Work Group under the auspices of Department of Health and Human Services Task Force on Alzheimer's Disease. *Neurology,* 34**,** 939-44.

MENON, D. K., SCHWAB, K., WRIGHT, D. W. & MAAS, A. I. 2010. Position statement: definition of traumatic brain injury. *Arch Phys Med Rehabil,* 91**,** 1637-40.

MORTIMER, J. A., VAN DUIJN, C. M., CHANDRA, V., FRATIGLIONI, L., GRAVES, A. B., HEYMAN, A., JORM, A. F., KOKMEN, E., KONDO, K. & ROCCA, W. A. 1991. Head trauma as a risk factor for Alzheimer's disease: a collaborative re-analysis of case-control studies. EURODEM Risk Factors Research Group. *International journal of epidemiology,* 20 Suppl 2**,** S28-35.

NAGAMOTO-COMBS, K., MCNEAL, D. W., MORECRAFT, R. J. & COMBS, C. K. 2007. Prolonged microgliosis in the rhesus monkey central nervous system after traumatic brain injury. *J Neurotrauma,* 24**,** 1719-42.

NAKAMURA, K., GREENWOOD, A., BINDER, L., BIGIO, E. H., DENIAL, S., NICHOLSON, L., ZHOU, X. Z. & LU, K. P. 2012. Proline isomer-specific antibodies reveal the early pathogenic tau conformation in Alzheimer's disease. *Cell,* 149**,** 232-44.

NARAYAN, R. K., MICHEL, M. E., ANSELL, B., BAETHMANN, A., BIEGON, A., BRACKEN, M. B., BULLOCK, M. R., CHOI, S. C., CLIFTON, G. L., CONTANT, C. F., COPLIN, W. M., DIETRICH, W. D., GHAJAR, J., GRADY, S. M., GROSSMAN, R. G., HALL, E. D., HEETDERKS, W., HOVDA, D. A., JALLO, J., KATZ, R. L., KNOLLER, N., KOCHANEK, P. M., MAAS, A. I., MAJDE, J., MARION, D. W., MARMAROU, A., MARSHALL, L. F., MCINTOSH, T. K., MILLER, E., MOHBERG, N., MUIZELAAR, J. P., PITTS, L. H., QUINN, P., RIESENFELD, G., ROBERTSON, C. S., STRAUSS, K. I., TEASDALE, G., TEMKIN, N., TUMA, R., WADE, C., WALKER, M. D., WEINRICH, M., WHYTE, J., WILBERGER, J., YOUNG, A. B. & YURKEWICZ, L. 2002. Clinical trials in head injury. *J Neurotrauma,* 19**,** 503-57.

NELSON, P. T., TROJANOWSKI, J. Q., ABNER, E. L., AL-JANABI, O. M., JICHA, G. A., SCHMITT, F. A., SMITH, C. D., FARDO, D. W., WANG, W.-X., KRYSCIO, R. J., NELTNER, J. H., KUKULL, W. A., CYKOWSKI, M. D., VAN ELDIK, L. J. & IGHODARO, E. T. 2016. "New Old Pathologies": AD, PART, and Cerebral Age-Related TDP-43 With Sclerosis (CARTS). *Journal of Neuropathology & Experimental Neurology,* 75**,** 482-498.

NESELIUS, S., BRISBY, H., THEODORSSON, A., BLENNOW, K., ZETTERBERG, H. & MARCUSSON, J. 2012. CSF-biomarkers in Olympic boxing: diagnosis and effects of repetitive head trauma. *PLoS One,* 7**,** e33606.

NESELIUS, S., ZETTERBERG, H., BLENNOW, K., RANDALL, J., WILSON, D., MARCUSSON, J. & BRISBY, H. 2013. Olympic boxing is associated with elevated levels of the neuronal protein tau in plasma. *Brain Inj,* 27**,** 425-33.

NORDSTROM, A. & NORDSTROM, P. 2018. Traumatic brain injury and the risk of dementia diagnosis: A nationwide cohort study. *PLoS Med,* 15**,** e1002496.

ODDO, M. & HUTCHINSON, P. J. 2018. Understanding and monitoring brain injury: the role of cerebral microdialysis. *Intensive Care Med,* 44**,** 1945-1948.

OMALU, B., SMALL, G. W., BAILES, J., ERCOLI, L. M., MERRILL, D. A., WONG, K. P., HUANG, S. C., SATYAMURTHY, N., HAMMERS, J. L., LEE, J., FITZSIMMONS, R. P. & BARRIO, J. R. 2018. Postmortem Autopsy-Confirmation of Antemortem [F-18]FDDNP-PET Scans in a Football Player With Chronic Traumatic Encephalopathy. *Neurosurgery,* 82**,** 237-246.

OWEN, D. R., GUO, Q., KALK, N. J., COLASANTI, A., KALOGIANNOPOULOU, D., DIMBER, R., LEWIS, Y. L., LIBRI, V., BARLETTA, J., RAMADA-MAGALHAES, J., KAMALAKARAN, A., NUTT, D. J., PASSCHIER, J., MATTHEWS, P. M., GUNN, R. N. & RABINER, E. A. 2014. Determination of [11C]PBR28 Binding Potential in vivo: A First Human TSPO Blocking Study. *Journal of Cerebral Blood Flow & Metabolism,* 34**,** 989-994.

PALACIOS, E. M., MARTIN, A. J., BOSS, M. A., EZEKIEL, F., CHANG, Y. S., YUH, E. L., VASSAR, M. J., SCHNYER, D. M., MACDONALD, C. L., CRAWFORD, K. L., IRIMIA, A., TOGA, A. W. & MUKHERJEE, P. 2017. Toward Precision and Reproducibility of Diffusion Tensor Imaging: A Multicenter Diffusion Phantom and Traveling Volunteer Study. *AJNR Am J Neuroradiol,* 38**,** 537-545.

PERRY, D. C., STURM, V. E., PETERSON, M. J., PIEPER, C. F., BULLOCK, T., BOEVE, B. F., MILLER, B. L., GUSKIEWICZ, K. M., BERGER, M. S., KRAMER, J. H. & WELSH-BOHMER, K. A. 2016. Association of traumatic brain injury with subsequent neurological and psychiatric disease: a meta-analysis. *J Neurosurg,* 124**,** 511-26.

PICHET BINETTE, A., GONNEAUD, J., VOGEL, J. W., LA JOIE, R., ROSA-NETO, P., COLLINS, D. L., POIRIER, J., BREITNER, J. C. S., VILLENEUVE, S., VACHON-PRESSEAU, E., INITIATIVE, F. T. A. S. D. N. & GROUP, T. P.-A. R. 2020. Morphometric network differences in ageing versus Alzheimer's disease dementia. *Brain,* 143**,** 635-649.

PREISCHE, O., SCHULTZ, S. A., APEL, A., KUHLE, J., KAESER, S. A., BARRO, C., GRÄBER, S., KUDER-BULETTA, E., LAFOUGERE, C., LASKE, C., VÖGLEIN, J., LEVIN, J., MASTERS, C. L., MARTINS, R., SCHOFIELD, P. R., ROSSOR, M. N., GRAFF-RADFORD, N. R., SALLOWAY, S., GHETTI, B., RINGMAN, J. M., NOBLE, J. M., CHHATWAL, J., GOATE, A. M., BENZINGER, T. L. S., MORRIS, J. C., BATEMAN, R. J., WANG, G., FAGAN, A. M., MCDADE, E. M., GORDON, B. A., JUCKER, M., ALLEGRI, R., AMTASHAR, F., BATEMAN, R., BENZINGER, T., BERMAN, S., BODGE, C., BRANDON, S., BROOKS, W., BUCK, J., BUCKLES, V., CHEA, S., CHHATWAL, J., CHREM, P., CHUI, H., CINCO, J., CLIFFORD, J., CRUCHAGA, C., D'MELLO, M., DONAHUE, T., DOUGLAS, J., EDIGO, N., EREKIN-TANER, N., FAGAN, A., FARLOW, M., FARRAR, A., FELDMAN, H., FLYNN, G., FOX, N., FRANKLIN,

E., FUJII, H., GANT, C., GARDENER, S., GHETTI, B., GOATE, A., GOLDMAN, J., GORDON, B., GRAFF-RADFORD, N., GRAY, J., GURNEY, J., HASSENSTAB, J., HIROHARA, M., HOLTZMAN, D., HORNBECK, R., DIBARI, S. H., IKEUCHI, T., IKONOMOVIC, S., JEROME, G., JUCKER, M., KARCH, C., KASUGA, K., KAWARABAYASHI, T., KLUNK, W., KOEPPE, R., KUDER-BULETTA, E., LASKE, C., LEE, J.-H., LEVIN, J., MARCUS, D., MARTINS, R., MASON, N. S., MASTERS, C., MAUE-DREYFUS, D., MCDADE, E., MONTOYA, L., MORI, H., MORRIS, J., NAGAMATSU, A., NEIMEYER, K., NOBLE, J., et al. 2019. Serum neurofilament dynamics predicts neurodegeneration and clinical progression in presymptomatic Alzheimer's disease. *Nature Medicine,* 25**,** 277-283.

QUIGLEY, H., COLLOBY, S. J. & O'BRIEN, J. T. 2011. PET imaging of brain amyloid in dementia: a review. *Int J Geriatr Psychiatry,* 26**,** 991-9.

RAFII, M. S. & AISEN, P. S. 2019. Alzheimer's Disease Clinical Trials: Moving Toward Successful Prevention. *CNS Drugs,* 33**,** 99-106.

RAJ, R., KAPRIO, J., KORJA, M., MIKKONEN, E. D., JOUSILAHTI, P. & SIIRONEN, J. 2017. Risk of hospitalization with neurodegenerative disease after moderate-to-severe traumatic brain injury in the working-age population: A retrospective cohort study using the Finnish national health registries. *PLoS Med,* 14**,** e1002316.

RAMLACKHANSINGH, A. F., BROOKS, D. J., GREENWOOD, R. J., BOSE, S. K., TURKHEIMER, F. E., KINNUNEN, K. M., GENTLEMAN, S., HECKEMANN, R. A., GUNANAYAGAM, K., GELOSA, G. & SHARP, D. J. 2011. Inflammation after trauma: microglial activation and traumatic brain injury. *Ann Neurol,* 70**,** 374-83.

RANSOHOFF, R. M. 2016. A polarizing question: do M1 and M2 microglia exist? *Nat Neurosci,* 19**,** 987-91.

REUTER, M., TISDALL, M. D., QURESHI, A., BUCKNER, R. L., VAN DER KOUWE, A. J. W. & FISCHL, B. 2015. Head motion during MRI acquisition reduces gray matter volume and thickness estimates. *Neuroimage,* 107**,** 107-115.

ROHRER, J. D., WOOLLACOTT, I. O., DICK, K. M., BROTHERHOOD, E., GORDON, E., FELLOWS, A., TOOMBS, J., DRUYEH, R., CARDOSO, M. J., OURSELIN, S., NICHOLAS, J. M., NORGREN, N., MEAD, S., ANDREASSON, U., BLENNOW, K., SCHOTT, J. M., FOX, N. C., WARREN, J. D. & ZETTERBERG, H. 2016. Serum neurofilament light chain protein is a measure of disease intensity in frontotemporal dementia. *Neurology,* 87**,** 1329-36.

ROSS, D. E., OCHS, A. L., SEABAUGH, J. M., DEMARK, M. F., SHRADER, C. R., MARWITZ, J. H. & HAVRANEK, M. D. 2012. Progressive brain atrophy in patients with chronic neuropsychiatric symptoms after mild traumatic brain injury: a preliminary study. *Brain Inj,* 26**,** 1500-9.

ROSSO, S. M., LANDWEER, E. J., HOUTERMAN, M., DONKER KAAT, L., VAN DUIJN, C. M. & VAN SWIETEN, J. C. 2003. Medical and environmental risk factors for sporadic frontotemporal dementia: a retrospective case-control study. *J Neurol Neurosurg Psychiatry,* 74**,** 1574-6.

ROWE, C. C., NG, S., ACKERMANN, U., GONG, S. J., PIKE, K., SAVAGE, G., COWIE, T. F., DICKINSON, K. L., MARUFF, P., DARBY, D., SMITH, C., WOODWARD, M., MERORY, J., TOCHON-DANGUY, H., O'KEEFE, G., KLUNK, W. E., MATHIS, C. A., PRICE, J. C., MASTERS, C. L. & VILLEMAGNE, V. L. 2007. Imaging beta-amyloid burden in aging and dementia. *Neurology,* 68**,** 1718-25.

SANDELIUS, Å., ZETTERBERG, H., BLENNOW, K., ADIUTORI, R., MALASPINA, A., LAURA, M., REILLY, M. M. & ROSSOR, A. M. 2018. Plasma neurofilament light chain concentration in the inherited peripheral neuropathies. *Neurology,* 90**,** e518-e524.

SAVICA, R., PARISI, J. E., WOLD, L. E., JOSEPHS, K. A. & AHLSKOG, J. E. 2012. High school football and risk of neurodegeneration: a community-based study. *Mayo Clin Proc,* 87**,** 335-40.

SCAHILL, R. I., SCHOTT, J. M., STEVENS, J. M., ROSSOR, M. N. & FOX, N. C. 2002. Mapping the evolution of regional atrophy in Alzheimer's disease: Unbiased analysis of fluid-registered serial MRI. *Proceedings of the National Academy of Sciences,* 99**,** 4703-4707.

SCHAFFERT, J., LOBUE, C., WHITE, C. L., CHIANG, H. S., DIDEHBANI, N., LACRITZ, L., ROSSETTI, H., DIEPPA, M., HART, J. & CULLUM, C. M. 2018. Traumatic brain injury history is associated with an earlier age of dementia onset in autopsy-confirmed Alzheimer's disease. *Neuropsychology,* 32**,** 410-416.

SCHEID, R., PREUL, C., GRUBER, O., WIGGINS, C. & VON CRAMON, D. Y. 2003. Diffuse axonal injury associated with chronic traumatic brain injury: evidence from T2*-weighted gradient-echo imaging at 3 T. *AJNR Am J Neuroradiol,* 24**,** 1049-56.

SCHLAEPFER, W. W. & LYNCH, R. G. 1977. Immunofluorescence studies of neurofilaments in the rat and human peripheral and central nervous system. *J Cell Biol,* 74**,** 241-50.

SCHMIDT, M. L., ZHUKAREVA, V., NEWELL, K. L., LEE, V. M. & TROJANOWSKI, J. Q. 2001. Tau isoform profile and phosphorylation state in dementia pugilistica recapitulate Alzheimer's disease. *Acta Neuropathol,* 101**,** 518-24.

SCHOTT, J. M., BARTLETT, J. W., BARNES, J., LEUNG, K. K., OURSELIN, S., FOX, N. C. & ALZHEIMER'S DISEASE NEUROIMAGING INITIATIVE, I. 2010. Reduced sample sizes for atrophy outcomes in Alzheimer's disease trials: baseline adjustment. *Neurobiol Aging,* 31**,** 1452-62, 1462 e1-2.

SCOTT, G., RAMLACKHANSINGH, A. F., EDISON, P., HELLYER, P., COLE, J., VERONESE, M., LEECH, R., GREENWOOD, R. J., TURKHEIMER, F. E., GENTLEMAN, S. M., HECKEMANN, R. A., MATTHEWS, P. M., BROOKS, D. J. & SHARP, D. J. 2016. Amyloid pathology and axonal injury after brain trauma. *Neurology,* 86**,** 821-8.

SCOTT, G., ZETTERBERG, H., JOLLY, A., COLE, J. H., DE SIMONI, S., JENKINS, P. O., FEENEY, C., OWEN, D. R., LINGFORD-HUGHES, A., HOWES, O., PATEL, M. C., GOLDSTONE, A. P., GUNN, R. N., BLENNOW, K., MATTHEWS, P. M. & SHARP, D. J. 2018. Minocycline reduces chronic microglial activation after brain trauma but increases neurodegeneration. *Brain,* 141**,** 459-471.

SHAHIM, P., GREN, M., LIMAN, V., ANDREASSON, U., NORGREN, N., TEGNER, Y., MATTSSON, N., ANDREASEN, N., OST, M., ZETTERBERG, H., NELLGARD, B. & BLENNOW, K. 2016a. Serum neurofilament light protein predicts clinical outcome in traumatic brain injury. *Sci Rep,* 6**,** 36791.

SHAHIM, P., POLITIS, A., VAN DER MERWE, A., MOORE, B., CHOU, Y.-Y., PHAM, D. L., BUTMAN, J. A., DIAZ-ARRASTIA, R., GILL, J. M., BRODY, D. L., ZETTERBERG, H., BLENNOW, K. & CHAN, L. 2020a. Neurofilament light as a biomarker in traumatic brain injury. *Neurology,* 95**,** e610-e622.

SHAHIM, P., POLITIS, A., VAN DER MERWE, A., MOORE, B., EKANAYAKE, V., LIPPA, S. M., CHOU, Y.-Y., PHAM, D. L., BUTMAN, J. A., DIAZ-ARRASTIA, R., ZETTERBERG, H., BLENNOW, K., GILL, J. M., BRODY, D. L. & CHAN, L. 2020b. Time course and diagnostic utility of NfL, tau, GFAP, and UCH-L1 in subacute and chronic TBI. *Neurology,* 95**,** e623-e636.

SHAHIM, P., TEGNER, Y., GUSTAFSSON, B., GREN, M., ÄRLIG, J., OLSSON, M., LEHTO, N., ENGSTRÖM, Å., HÖGLUND, K., PORTELIUS, E., ZETTERBERG, H. & BLENNOW, K. 2016b.

Neurochemical Aftermath of Repetitive Mild Traumatic Brain Injury. *JAMA Neurology,* 73**,** 1308-1315.

SHAHIM, P., TEGNER, Y., MARKLUND, N., BLENNOW, K. & ZETTERBERG, H. 2018. Neurofilament light and tau as blood biomarkers for sports-related concussion. *Neurology,* 90**,** e1780-e1788.

SHAHIM, P., ZETTERBERG, H., TEGNER, Y. & BLENNOW, K. 2017. Serum neurofilament light as a biomarker for mild traumatic brain injury in contact sports. *Neurology,* 88**,** 1788-1794.

SHAPIRA, Y., SETTON, D., ARTRU, A. A. & SHOHAMI, E. 1993. Blood-brain barrier permeability, cerebral edema, and neurologic function after closed head injury in rats. *Anesth Analg,* 77**,** 141-8.

SHARP, D. J. & JENKINS, P. O. 2015. Concussion is confusing us all. *Pract Neurol,* 15**,** 172-86.

SIDAROS, A., ENGBERG, A. W., SIDAROS, K., LIPTROT, M. G., HERNING, M., PETERSEN, P., PAULSON, O. B., JERNIGAN, T. L. & ROSTRUP, E. 2008. Diffusion tensor imaging during recovery from severe traumatic brain injury and relation to clinical outcome: a longitudinal study. *Brain,* 131**,** 559-72.

SIDAROS, A., SKIMMINGE, A., LIPTROT, M. G., SIDAROS, K., ENGBERG, A. W., HERNING, M., PAULSON, O. B., JERNIGAN, T. L. & ROSTRUP, E. 2009. Long-term global and regional brain volume changes following severe traumatic brain injury: a longitudinal study with clinical correlates. *Neuroimage,* 44**,** 1-8.

SIMON, D. W., MCGEACHY, M. J., BAYIR, H., CLARK, R. S. B., LOANE, D. J. & KOCHANEK, P. M. 2017. The far-reaching scope of neuroinflammation after traumatic brain injury. *Nature Reviews Neurology,* 13**,** 171-191.

SMALL, G. W., KEPE, V., SIDDARTH, P., ERCOLI, L. M., MERRILL, D. A., DONOGHUE, N., BOOKHEIMER, S. Y., MARTINEZ, J., OMALU, B., BAILES, J. & BARRIO, J. R. 2013. PET scanning of brain tau in retired national football league players: preliminary findings. *Am J Geriatr Psychiatry,* 21**,** 138-44.

SMITH, D. H., CHEN, X. H., PIERCE, J. E., WOLF, J. A., TROJANOWSKI, J. Q., GRAHAM, D. I. & MCINTOSH, T. K. 1997. Progressive atrophy and neuron death for one year following brain trauma in the rat. *J Neurotrauma,* 14**,** 715-27.

SMITH, D. H., JOHNSON, V. E. & STEWART, W. 2013. Chronic neuropathologies of single and repetitive TBI: substrates of dementia? *Nat Rev Neurol,* 9**,** 211-21.

SMITH, D. H., MEANEY, D. F. & SHULL, W. H. 2003. Diffuse axonal injury in head trauma. *J Head Trauma Rehabil,* 18**,** 307-16.

SMITH, S. M., JENKINSON, M., JOHANSEN-BERG, H., RUECKERT, D., NICHOLS, T. E., MACKAY, C. E., WATKINS, K. E., CICCARELLI, O., CADER, M. Z., MATTHEWS, P. M. & BEHRENS, T. E. 2006. Tract-based spatial statistics: voxelwise analysis of multi-subject diffusion data. *Neuroimage,* 31**,** 1487-505.

SMITH, S. M., RAO, A., DE STEFANO, N., JENKINSON, M., SCHOTT, J. M., MATTHEWS, P. M. & FOX, N. C. 2007. Longitudinal and cross-sectional analysis of atrophy in Alzheimer's disease: cross-validation of BSI, SIENA and SIENAX. *Neuroimage,* 36**,** 1200-6.

STERN, R. A., DANESHVAR, D. H., BAUGH, C. M., SEICHEPINE, D. R., MONTENIGRO, P. H., RILEY, D. O., FRITTS, N. G., STAMM, J. M., ROBBINS, C. A., MCHALE, L., SIMKIN, I., STEIN, T. D., ALVAREZ, V. E., GOLDSTEIN, L. E., BUDSON, A. E., KOWALL, N. W., NOWINSKI, C. J., CANTU, R. C. & MCKEE, A. C. 2013. Clinical presentation of chronic traumatic encephalopathy. *Neurology,* 81**,** 1122-9.

STRICH, S. J. 1956. Diffuse degeneration of the cerebral white matter in severe dementia following head injury. *J Neurol Neurosurg Psychiatry,* 19**,** 163-85.

TABRIZI, S. J., LEAVITT, B. R., LANDWEHRMEYER, G. B., WILD, E. J., SAFT, C., BARKER, R. A., BLAIR, N. F., CRAUFURD, D., PRILLER, J., RICKARDS, H., ROSSER, A., KORDASIEWICZ, H. B., CZECH, C., SWAYZE, E. E., NORRIS, D. A., BAUMANN, T., GERLACH, I., SCHOBEL, S. A., PAZ, E., SMITH, A. V., BENNETT, C. F. & LANE, R. M. 2019. Targeting Huntingtin Expression in Patients with Huntington's Disease. *New England Journal of Medicine,* 380**,** 2307-2316.

TAGGE, C. A., FISHER, A. M., MINAEVA, O. V., GAUDREAU-BALDERRAMA, A., MONCASTER, J. A., ZHANG, X. L., WOJNAROWICZ, M. W., CASEY, N., LU, H., KOKIKO-COCHRAN, O. N., SAMAN, S., ERICSSON, M., ONOS, K. D., VEKSLER, R., SENATOROV, V. V., JR., KONDO, A., ZHOU, X. Z., MIRY, O., VOSE, L. R., GOPAUL, K. R., UPRETI, C., NOWINSKI, C. J., CANTU, R. C., ALVAREZ, V. E., HILDEBRANDT, A. M., FRANZ, E. S., KONRAD, J., HAMILTON, J. A., HUA, N., TRIPODIS, Y., ANDERSON, A. T., HOWELL, G. R., KAUFER, D., HALL, G. F., LU, K. P., RANSOHOFF, R. M., CLEVELAND, R. O., KOWALL, N. W., STEIN, T. D., LAMB, B. T., HUBER, B. R., MOSS, W. C., FRIEDMAN, A., STANTON, P. K., MCKEE, A. C. & GOLDSTEIN, L. E. 2018. Concussion, microvascular injury, and early tauopathy in young athletes after impact head injury and an impact concussion mouse model. *Brain,* 141**,** 422-458.

TERRY, R. D., DETERESA, R. & HANSEN, L. A. 1987. Neocortical cell counts in normal human adult aging. *Ann Neurol,* 21**,** 530-9.

THELIN, E., AL NIMER, F., FROSTELL, A., ZETTERBERG, H., BLENNOW, K., NYSTRÖM, H., SVENSSON, M., BELLANDER, B. M., PIEHL, F. & NELSON, D. W. 2019. A Serum Protein Biomarker Panel Improves Outcome Prediction in Human Traumatic Brain Injury. *J Neurotrauma,* 36**,** 2850-2862.

THELIN, E. P., ZEILER, F. A., ERCOLE, A., MONDELLO, S., BUKI, A., BELLANDER, B. M., HELMY, A., MENON, D. K. & NELSON, D. W. 2017. Serial Sampling of Serum Protein Biomarkers for Monitoring Human Traumatic Brain Injury Dynamics: A Systematic Review. *Front Neurol,* 8**,** 300.

TOMAIUOLO, F., BIVONA, U., LERCH, J. P., DI PAOLA, M., CARLESIMO, G. A., CIURLI, P., MATTEIS, M., CECCHETTI, L., FORCINA, A., SILVESTRO, D., AZICNUDA, E., SABATINI, U., DI GIACOMO, D., CALTAGIRONE, C., PETRIDES, M. & FORMISANO, R. 2012. Memory and anatomical change in severe non missile traumatic brain injury: approximately 1 vs. approximately 8 years follow-up. *Brain Res Bull,* 87**,** 373-82.

TRABZUNI, D., WRAY, S., VANDROVCOVA, J., RAMASAMY, A., WALKER, R., SMITH, C., LUK, C., GIBBS, J. R., DILLMAN, A., HERNANDEZ, D. G., AREPALLI, S., SINGLETON, A. B., COOKSON, M. R., PITTMAN, A. M., DE SILVA, R., WEALE, M. E., HARDY, J. & RYTEN, M. 2012. MAPT expression and splicing is differentially regulated by brain region: relation to genotype and implication for tauopathies. *Hum Mol Genet,* 21**,** 4094-103.

TRIVEDI, M. A., WARD, M. A., HESS, T. M., GALE, S. D., DEMPSEY, R. J., ROWLEY, H. A. & JOHNSON, S. C. 2007. Longitudinal changes in global brain volume between 79 and 409 days after traumatic brain injury: relationship with duration of coma. *J Neurotrauma,* 24**,** 766-71.

URYU, K., CHEN, X. H., MARTINEZ, D., BROWNE, K. D., JOHNSON, V. E., GRAHAM, D. I., LEE, V. M., TROJANOWSKI, J. Q. & SMITH, D. H. 2007. Multiple proteins implicated in neurodegenerative diseases accumulate in axons after brain trauma in humans. *Exp Neurol,* 208**,** 185-92.

US FOOD AND DRUG ADMINISTRATION 2018. Early Alzheimer's Disease: Developing Drugs for Treatment Guidance for Industry (draft guidance).
VARATHARAJ, A., LILJEROTH, M., DAREKAR, A., LARSSON, H. B. W., GALEA, I. & CRAMER, S. P. 2019. Blood-brain barrier permeability measured using dynamic contrast-enhanced magnetic resonance imaging: a validation study. *J Physiol,* 597**,** 699-709.
VARGAS, M. E. & BARRES, B. A. 2007. Why is Wallerian degeneration in the CNS so slow? *Annu Rev Neurosci,* 30**,** 153-79.
WANG, H. K., LEE, Y. C., HUANG, C. Y., LILIANG, P. C., LU, K., CHEN, H. J., LI, Y. C. & TSAI, K. J. 2015. Traumatic brain injury causes frontotemporal dementia and TDP-43 proteolysis. *Neuroscience,* 300**,** 94-103.
WANG, J. T., MEDRESS, Z. A. & BARRES, B. A. 2012. Axon degeneration: molecular mechanisms of a self-destruction pathway. *J Cell Biol,* 196**,** 7-18.
WARNER, M. A., MARQUEZ DE LA PLATA, C., SPENCE, J., WANG, J. Y., HARPER, C., MOORE, C., DEVOUS, M. & DIAZ-ARRASTIA, R. 2010. Assessing spatial relationships between axonal integrity, regional brain volumes, and neuropsychological outcomes after traumatic axonal injury. *J Neurotrauma,* 27**,** 2121-30.
WARREN, JASON D., ROHRER, JONATHAN D. & HARDY, J. 2012. Disintegrating Brain Networks: from Syndromes to Molecular Nexopathies. *Neuron,* 73**,** 1060-1062.
WATANABE, Y. & WATANABE, T. 2017. Meta-analytic evaluation of the association between head injury and risk of amyotrophic lateral sclerosis. *Eur J Epidemiol,* 32**,** 867-879.
WHITTALL, K. P., MACKAY, A. L., GRAEB, D. A., NUGENT, R. A., LI, D. K. & PATY, D. W. 1997. In vivo measurement of T2 distributions and water contents in normal human brain. *Magn Reson Med,* 37**,** 34-43.
WILKINSON, K. D., LEE, K. M., DESHPANDE, S., DUERKSEN-HUGHES, P., BOSS, J. M. & POHL, J. 1989. The neuron-specific protein PGP 9.5 is a ubiquitin carboxyl-terminal hydrolase. *Science,* 246**,** 670-3.
WILSON, J. T., PETTIGREW, L. E. & TEASDALE, G. M. 1998. Structured interviews for the Glasgow Outcome Scale and the extended Glasgow Outcome Scale: guidelines for their use. *J Neurotrauma,* 15**,** 573-85.
WILSON, L., HORTON, L., KUNZMANN, K., SAHAKIAN, B. J., NEWCOMBE, V. F., STAMATAKIS, E. A., VON STEINBUECHEL, N., CUNITZ, K., COVIC, A., MAAS, A., VAN PRAAG, D. & MENON, D. 2020. Understanding the relationship between cognitive performance and function in daily life after traumatic brain injury. *J Neurol Neurosurg Psychiatry*.
WINKLER, A. M., RIDGWAY, G. R., WEBSTER, M. A., SMITH, S. M. & NICHOLS, T. E. 2014. Permutation inference for the general linear model. *Neuroimage,* 92**,** 381-97.
WOODS, A. H. 1911. Trauma as a Cause of Amyotrophic Lateral Sclerosis. *Journal of the American Medical Association,* LVI**,** 1876-1876.
WORKER, A., DIMA, D., COMBES, A., CRUM, W. R., STREFFER, J., EINSTEIN, S., MEHTA, M. A., BARKER, G. J., S, C. R. W. & O'DALY, O. 2018. Test-retest reliability and longitudinal analysis of automated hippocampal subregion volumes in healthy ageing and Alzheimer's disease populations. *Hum Brain Mapp,* 39**,** 1743-1754.
WORLD HEALTH ORGANISATION 2018. International Classification of Diseases. 11th Revision ed.
WYSS-CORAY, T. 2016. Ageing, neurodegeneration and brain rejuvenation. *Nature,* 539**,** 180-186.

YEH, F.-C., ZAYDAN, I. M., SUSKI, V. R., LACOMIS, D., RICHARDSON, R. M., MAROON, J. C. & BARRIOS-MARTINEZ, J. 2019. Differential tractography as a track-based biomarker for neuronal injury. *NeuroImage,* 202**,** 116131.

YU, T., HSU, Y. J., FAIN, K. M., BOYD, C. M., HOLBROOK, J. T. & PUHAN, M. A. 2015. Use of surrogate outcomes in US FDA drug approvals, 2003-2012: a survey. *BMJ Open,* 5**,** e007960.

ZANIER, E. R., BERTANI, I., SAMMALI, E., PISCHIUTTA, F., CHIARAVALLOTI, M. A., VEGLIANTE, G., MASONE, A., CORBELLI, A., SMITH, D. H., MENON, D. K., STOCCHETTI, N., FIORDALISO, F., DE SIMONI, M. G., STEWART, W. & CHIESA, R. 2018. Induction of a transmissible tau pathology by traumatic brain injury. *Brain,* 141**,** 2685-2699.

ZAROW, C., VINTERS, H. V., ELLIS, W. G., WEINER, M. W., MUNGAS, D., WHITE, L. & CHUI, H. C. 2005. Correlates of hippocampal neuron number in Alzheimer's disease and ischemic vascular dementia. *Ann Neurol,* 57**,** 896-903.

ZETTERBERG, H., HIETALA, M. A., JONSSON, M., ANDREASEN, N., STYRUD, E., KARLSSON, I., EDMAN, A., POPA, C., RASULZADA, A., WAHLUND, L. O., MEHTA, P. D., ROSENGREN, L., BLENNOW, K. & WALLIN, A. 2006. Neurochemical aftermath of amateur boxing. *Arch Neurol,* 63**,** 1277-80.

ZETTERBERG, H., SMITH, D. H. & BLENNOW, K. 2013. Biomarkers of mild traumatic brain injury in cerebrospinal fluid and blood. *Nat Rev Neurol,* 9**,** 201-10.

ZHANG, H., AVANTS, B. B., YUSHKEVICH, P. A., WOO, J. H., WANG, S., MCCLUSKEY, L. F., ELMAN, L. B., MELHEM, E. R. & GEE, J. C. 2007. High-dimensional spatial normalization of diffusion tensor images improves the detection of white matter differences: an example study using amyotrophic lateral sclerosis. *IEEE Trans Med Imaging,* 26**,** 1585-97.

ZHANG, H., SCHNEIDER, T., WHEELER-KINGSHOTT, C. A. & ALEXANDER, D. C. 2012. NODDI: practical in vivo neurite orientation dispersion and density imaging of the human brain. *Neuroimage,* 61**,** 1000-16.

ZHOU, Y., KIERANS, A., KENUL, D., GE, Y., RATH, J., REAUME, J., GROSSMAN, R. I. & LUI, Y. W. 2013. Mild traumatic brain injury: longitudinal regional brain volume changes. *Radiology,* 267**,** 880-90.

9 Appendix

9.1 Permissions for content reproduction from published papers

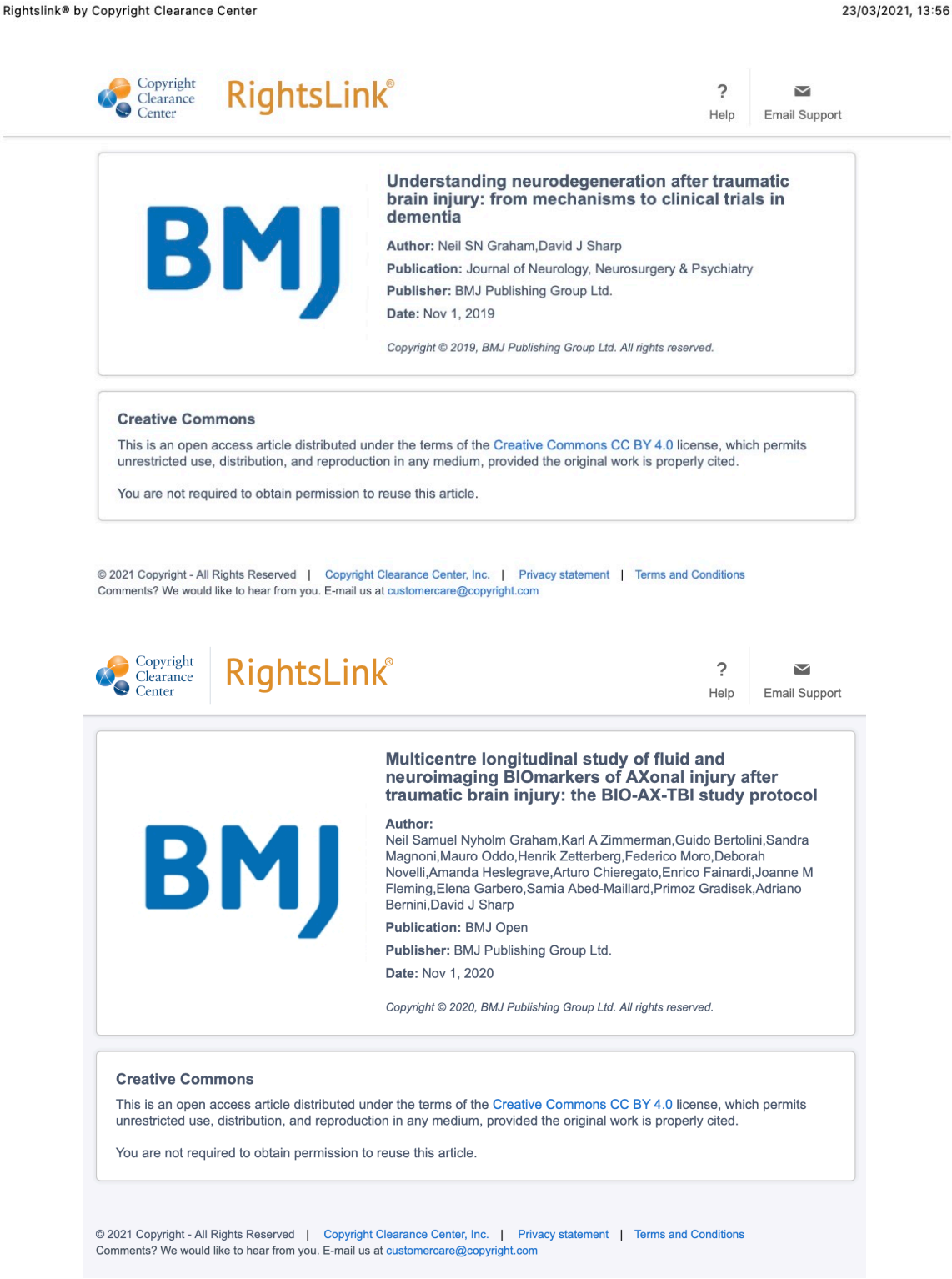

Rightslink® by Copyright Clearance Center 23/03/2021, 13:56

Copyright Clearance Center RightsLink® Help Email Support

Understanding neurodegeneration after traumatic brain injury: from mechanisms to clinical trials in dementia

Author: Neil SN Graham,David J Sharp

Publication: Journal of Neurology, Neurosurgery & Psychiatry

Publisher: BMJ Publishing Group Ltd.

Date: Nov 1, 2019

Copyright © 2019, BMJ Publishing Group Ltd. All rights reserved.

Creative Commons

This is an open access article distributed under the terms of the Creative Commons CC BY 4.0 license, which permits unrestricted use, distribution, and reproduction in any medium, provided the original work is properly cited.

You are not required to obtain permission to reuse this article.

© 2021 Copyright - All Rights Reserved | Copyright Clearance Center, Inc. | Privacy statement | Terms and Conditions
Comments? We would like to hear from you. E-mail us at customercare@copyright.com

Copyright Clearance Center RightsLink® Help Email Support

Multicentre longitudinal study of fluid and neuroimaging BIOmarkers of AXonal injury after traumatic brain injury: the BIO-AX-TBI study protocol

Author:
Neil Samuel Nyholm Graham,Karl A Zimmerman,Guido Bertolini,Sandra Magnoni,Mauro Oddo,Henrik Zetterberg,Federico Moro,Deborah Novelli,Amanda Heslegrave,Arturo Chieregato,Enrico Fainardi,Joanne M Fleming,Elena Garbero,Samia Abed-Maillard,Primoz Gradisek,Adriano Bernini,David J Sharp

Publication: BMJ Open

Publisher: BMJ Publishing Group Ltd.

Date: Nov 1, 2020

Copyright © 2020, BMJ Publishing Group Ltd. All rights reserved.

Creative Commons

This is an open access article distributed under the terms of the Creative Commons CC BY 4.0 license, which permits unrestricted use, distribution, and reproduction in any medium, provided the original work is properly cited.

You are not required to obtain permission to reuse this article.

© 2021 Copyright - All Rights Reserved | Copyright Clearance Center, Inc. | Privacy statement | Terms and Conditions
Comments? We would like to hear from you. E-mail us at customercare@copyright.com

OXFORD UNIVERSITY PRESS LICENSE
TERMS AND CONDITIONS

Mar 23, 2021

This Agreement between Dr. Neil Graham ("You") and Oxford University Press ("Oxford University Press") consists of your license details and the terms and conditions provided by Oxford University Press and Copyright Clearance Center.

License Number	5034810076117
License date	Mar 23, 2021
Licensed content publisher	Oxford University Press
Licensed content publication	Brain
Licensed content title	Diffuse axonal injury predicts neurodegeneration after moderate–severe traumatic brain injury
Licensed content author	Graham, Neil S N; Jolly, Amy
Licensed content date	Oct 25, 2020
Type of Use	Thesis/Dissertation
Institution name	
Title of your work	PhD Thesis
Publisher of your work	Imperial College London
Expected publication date	Apr 2021
Permissions cost	0.00 GBP
Value added tax	0.00 GBP
Total	0.00 GBP
Title	PhD Thesis
Institution name	Imperial College London
Expected presentation date	Apr 2021
Portions	Figures 1-6; Tables 1-2
Requestor Location	Dr. Neil Graham C3NL lab 3rd Flr Burlington Danes Hammersmith Hosp. Du Cane Rd. London, W12 0NN United Kingdom Attn: Dr. Neil Graham
Publisher Tax ID	GB125506730
Total	0.00 GBP

OXFORD UNIVERSITY PRESS LICENSE
TERMS AND CONDITIONS

Apr 10, 2021

This Agreement between Dr. Neil Graham ("You") and Oxford University Press ("Oxford University Press") consists of your license details and the terms and conditions provided by Oxford University Press and Copyright Clearance Center.

License Number	5045570134822
License date	Apr 10, 2021
Licensed content publisher	Oxford University Press
Licensed content publication	Brain
Licensed content title	Diffuse axonal injury predicts neurodegeneration after moderate–severe traumatic brain injury
Licensed content author	Graham, Neil S N; Jolly, Amy
Licensed content date	Oct 25, 2020
Type of Use	Thesis/Dissertation
Institution name	
Title of your work	PhD Thesis
Publisher of your work	Imperial College London
Expected publication date	Apr 2021
Permissions cost	0.00 USD
Value added tax	0.00 USD
Total	0.00 USD
Title	PhD Thesis
Institution name	Imperial College London
Expected presentation date	Apr 2021
Portions	Selected article text, pp3685-3698.
Requestor Location	Dr. Neil Graham C3NL lab 3rd Flr Burlington Danes Hammersmith Hosp. Du Cane Rd. London, W12 0NN United Kingdom Attn: Dr. Neil Graham
Publisher Tax ID	GB125506730
Total	0.00 USD